AD A040870



NW



MISCELLANEOUS PAPER S-73-1

STATE-OF-THE-ART FOR ASSESSING EARTHQUAKE HAZARDS IN THE UNITED STATES

Report 6

FAULTS AND EARTHQUAKE MAGNITUDE

by

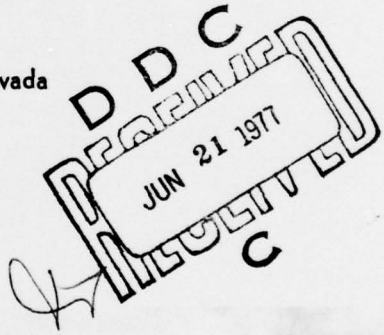
David B. Slemmons

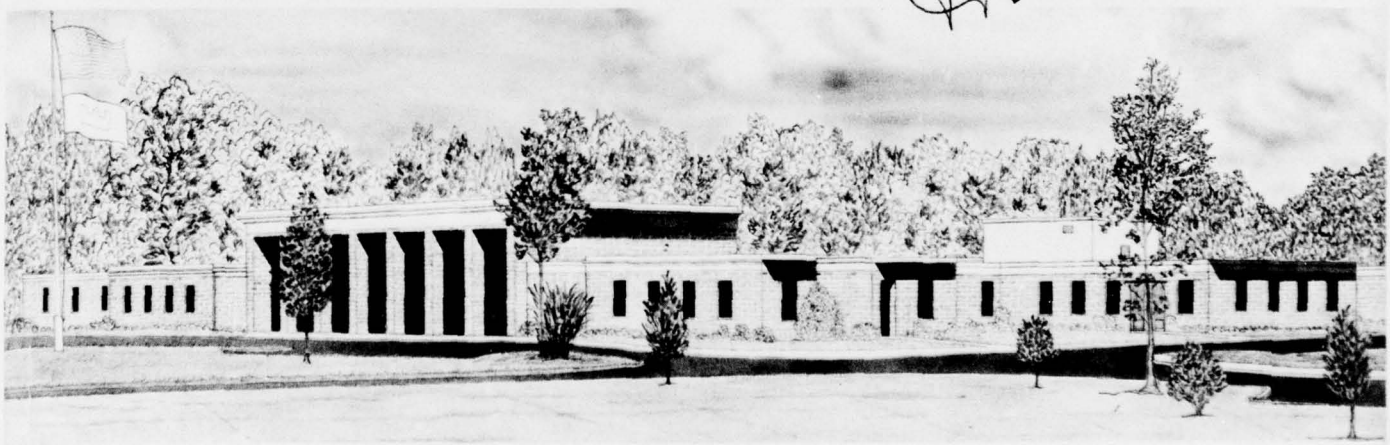
Mackay School of Mines, University of Nevada
Reno, Nevada 89507

May 1977

Report 6 of a Series

Approved For Public Release; Distribution Unlimited





AD No.
DDC FILE COPY

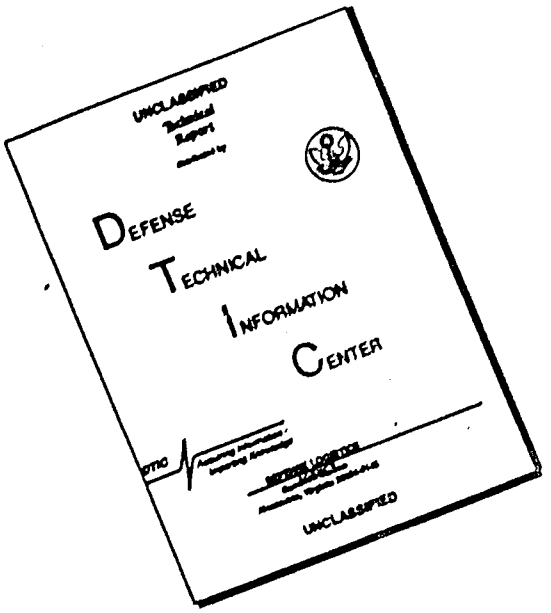
Prepared for Office, Chief of Engineers, U. S. Army
Washington, D. C. 20314

Under Contract No. DACW39-76-C-0009

Monitored by U. S. Army Engineer Waterways Experiment Station
Soils and Pavements Laboratory
P. O. Box 631, Vicksburg, Miss. 39180

Destroy this report when no longer needed. Do not return
it to the originator.

DISCLAIMER NOTICE



THIS DOCUMENT IS BEST QUALITY AVAILABLE. THE COPY FURNISHED TO DTIC CONTAINED A SIGNIFICANT NUMBER OF PAGES WHICH DO NOT REPRODUCE LEGIBLY.

(15) WES

(19) MP-S-73-1

Unclassified

SECURITY CLASSIFICATION OF THIS PAGE (When Data Entered)

REPORT DOCUMENTATION PAGE

READ INSTRUCTIONS BEFORE COMPLETING FORM

1. REPORT NUMBER: Miscellaneous Paper S-73-1	2. GOVT ACCESSION NO.
3. RECIPIENT'S CATALOG NUMBER	
4. TITLE (and Subtitle): STATE-OF-THE-ART FOR ASSESSING EARTHQUAKE HAZARDS IN THE UNITED STATES; Report 6, FAULTS AND EARTHQUAKE MAGNITUDE.	5. TYPE OF REPORT & PERIOD COVERED: Report 6 of a series
	6. PERFORMING ORG. REPORT NUMBER
7. AUTHOR(s): David B. Slemmons	8. CONTRACT OR GRANT NUMBER(s): Contract No. DACW 39-76-C-0009 (15) 0009 new
9. PERFORMING ORGANIZATION NAME AND ADDRESS: Mackay School of Mines, University of Nevada, Reno, Nevada 89507	10. PROGRAM ELEMENT, PROJECT, TASK AREA & WORK UNIT NUMBERS
11. CONTROLLING OFFICE NAME AND ADDRESS: Office, Chief of Engineers, U. S. Army, Washington, D. C. 20314	12. REPORT DATE: May 1977
	13. NUMBER OF PAGES: ~~166~~ 170 pp.
14. MONITORING AGENCY NAME & ADDRESS (if different from Controlling Office): U. S. Army Engineer Waterways Experiment Station, Soils and Pavements Laboratory, P. O. Box 631, Vicksburg, Miss. 39180	15. SECURITY CLASS. (of this report): Unclassified
	15a. DECLASSIFICATION/DOWNGRADING SCHEDULE

16. DISTRIBUTION STATEMENT (of this Report)

Approved for public release; distribution unlimited.

17. DISTRIBUTION STATEMENT (of the abstract entered in Block 20, if different from Report)

18. SUPPLEMENTARY NOTES

19. KEY WORDS (Continue on reverse side if necessary and identify by block number)

Earthquake engineering
Earthquake hazards
Earthquake resistant structures
Earthquakes
Faults and faulting (Geology)
Fractures and fracturing (Geology)
State-of-the-art studies

20. ABSTRACT (Continue on reverse side if necessary and identify by block number)

The short seismologic and historic records, in combination with the long recurrence intervals between potentially damaging earthquakes, create a need for developing geologic methods as alternatives or supplements to seismologic methods of establishing design earthquakes. The main goal of this report is to review geologic methods of determining the maximum probable earthquakes for active faults based on empirical relationships between magnitude, length of surface faulting, maximum fault displacement, and combinations of fault length and maximum displacement.

(Continued)

DD FORM 1 JAN 73 1473 EDITION OF 1 NOV 65 IS OBSOLETE

Unclassified

SECURITY CLASSIFICATION OF THIS PAGE (When Data Entered)

214070

20. ABSTRACT (Continued).

Empirical studies have developed and refined the formulations and graphs relating earthquake magnitude to surface faulting. The present study updates the most recent studies of this type on the basis of data that have become available over the past six years.

The application of the method requires the careful determination of fault activity or nonactivity, or rate of activity, and an integrated program of historic, seismologic, geologic, geomorphic, and geophysical studies. The criteria for activity are summarized and methods of resolving questions of activity are provided. The geomorphic evidence for activity and type of fault is summarized in terms of complex, branching, conjugate, and distributed fracture patterns that require a regional and integrated geological and geophysical approach.

The relationship of fracture patterns is presented in terms of plate tectonic environments and conjugate deformation by faulting, folding, and warping. The complex pattern analysis required for distributed fracture systems is considered for each fault type--strike-slip, normal-slip, reverse-slip, and oblique-slip--with examples and source literature provided for each type. Case histories are given for the selection of design values.

PREFACE

This report was prepared by Prof. David B. Slemmons of the Mackay School of Mines, University of Nevada in Reno, as part of ongoing work at the U. S. Army Engineer Waterways Experiment Station (WES) in Civil Works Investigation Studies, "Methodologies for Selecting Design Earthquakes," sponsored by the Office, Chief of Engineers, U. S. Army. This is the sixth of a series of state-of-the-art reports on methodologies for determining the severity of bedrock motion during earthquakes.

Preparation of the report was under the direction of Dr. Ellis L. Krinitzsky, Chief, Engineering Geology Research Facility, WES. General direction was by Mr. James P. Sale, Chief, Soils and Pavements Laboratory, and Mr. Don C. Banks, Chief, Engineering Geology and Rock Mechanics Division. The author wishes to express his appreciation for many helpful editorial and technical suggestions from Mrs. Ruth Slemmons, Drs. John E. Allen and Ansel G. Johnson of Portland State University, Messrs. Manuel G. Bonilla and Carl Wentworth of the U. S. Geological Survey, Mr. George E. Brogan of Woodward-Clyde Consultants at Orange, California, and Mr. Richard F. Hardyman of Mackay School of Mines, University of Nevada in Reno, who reviewed a draft of the report.

COL G. H. Hilt, CE, and COL J. L. Cannon, CE, were Directors of WES during the period of this study. Mr. F. R. Brown was Technical Director.



CONTENTS

	Page
PREFACE	1
LIST OF TABLES	4
LIST OF FIGURES	5
CONVERSION FACTORS, U. S. CUSTOMARY TO METRIC (SI) UNITS OF MEASUREMENT	9
PART I: INTRODUCTION	10
Need for Length of Fault and Maximum Displacement	10
General Relation of Earthquake Magnitude to Fault Length and Maximum Fault Displacement	11
Terminology	13
Relation Between Earthquake Deformation and Surface Faulting	21
Difficulty in Determination of Fault Length	28
Design Earthquakes from Fault Length and Maximum Displacement Data	29
PART II: DETAILED RELATION OF EARTHQUAKE MAGNITUDE TO FAULT LENGTH AND MAXIMUM DISPLACEMENT	32
General Statement	32
Empirical Relation of Logarithm of Maximum Displacement (Log D) to Magnitude (M)	33
Empirical Relation of Logarithm of Fault Length (Log L) to Logarithm of Maximum Fault Displacement (Log D)	34
Empirical Relation of Logarithm of Fault Length (Log L) to Magnitude (M)	35
Empirical Relation of Logarithm of Fault Length (L) Times Maximum Displacement (D) to Magnitude (M)	36
Empirical Relation of Logarithm of Fault Length Times the Square of Displacement (Log LD^2) to Magnitude (M)	37
PART III: RELATION BETWEEN PLATE TECTONICS, FAULT TYPE, MAXIMUM FAULT DISPLACEMENT, FAULT LENGTH, AND EARTHQUAKE MAGNITUDE	38
Introduction	38
Faults of Megathrust Zones	40
Faults of Rises and Rift Zones	42
Faults of Cordillera Mountain Zones	43
PART IV: METHODS OF DETERMINING FAULT ACTIVITY OR NONACTIVITY	49
Introduction	49
Historical Criteria for Activity	50
Seismologic Methods	53
Geologic Methods	56
Geodetic Methods	62
Trenching Methods	63

CONTENTS

	Page
Absolute and Relative Rates of Fault Activity	64
Classification of Rates of Displacement	65
PART V: METHODS OF DETERMINING TOTAL FAULT LENGTH	69
Introduction	69
Geologic Evaluation	69
Geophysical Analysis	77
PART VI: NEW DETERMINATIONS OF RELATIONS OF EARTHQUAKE MAGNITUDE TO MAXIMUM FAULT DISPLACEMENT AND LENGTH OF SURFACE FAULTING	86
Earthquake Magnitudes	87
Revision of Fault Length and Displacement Data	87
Results of Compilation	88
Reliability of Results	88
Method of Statistical Analysis	99
Data Selected for This Report	99
PART VII: FAULT RUPTURE PATTERNS	101
Introduction	101
Types of Distributed and Branching Faults	101
PART VIII: SIZE AND SHAPE OF AREA TO BE EVALUATED	106
General Comments	106
Megathrust Fault Zones	106
Strike-Slip Fault Zones	107
Normal-Slip Fault Zones	108
Reverse-Slip Fault Zones	109
Summary	109
PART IX: DETERMINATION OF FAULT LENGTH AND EARTHQUAKE MAGNITUDE FOR EN ECHELON AND CONJUGATE FAULT SYSTEMS	111
PART X: METHODS OF APPLYING FAULT LENGTH TO DETERMINE DESIGN EARTHQUAKE PARAMETERS	115
PART XI: METHODS OF DETERMINING OR USING MAXIMUM FAULT DISPLACEMENT	117
REFERENCES	118
APPENDIX A: GEOMORPHIC FEATURES OF ACTIVE FAULT ZONES	A1
Introduction	A1
Minor Geomorphic Features of Active Strike-Slip Faults	A1
Major Geomorphic Features of Strike-Slip Faults	A13
Geomorphic Features of Normal-Slip Faults	A17
Geomorphic Features of Reverse-Slip Faults	A33

LIST OF TABLES

No.	Title	Page
1	Directly and Indirectly Determined Relations Between Earthquake Magnitude and Design Parameters	31
2	Relation of Earthquake Magnitude (M) to Logarithm of Maximum Displacement (Log D): M = a + b Log D	34
3	Relation of Logarithm of Maximum Displacement (Log D) to Logarithm of Fault Length (Log L): Log D = a + b Log L . .	34
4	Relation of Earthquake Magnitude (M) to Logarithm of Fault Length (Log L): M = a + b Log L	35
5	Relation of Magnitude (M) to Logarithm of Fault Length (L) Times Displacement (D): M = a + b Log LD	37
6	Relation of Earthquake Magnitude (M) to Logarithm of Fault Length (L) Times Displacement (D) Squared: M = a + b Log LD^2	37
7	Criteria Used for Recognition of Active Faults	49
8	Classification of Fault Activity Based on Available Data . . .	51
9	Elements of Displacement Vectors of the Atera Fault, Japan . .	61
10	Estimates of Earthquake Magnitude for the Palo Colorado-San Gregorio Fault Zone	80
11	Equations of Best Straight-Line Fit for Magnitude Versus Log Displacement: M = a + b Log D	94
12	Equations of Best Straight-Line Fit for Log Displacement Versus Log Length: Log D = a + b Log L	95
13	Equations of Best Straight-Line Fit for Magnitude Versus Log Fault Length: M = a + b Log L	96
14	Equations of Best Straight-Line Fit for Magnitude Versus Log Length Times Displacement: M = a + b Log LD	97
15	Equations of Best Straight-Line Fit for Magnitude Versus Log Length Times Square of Displacement: M = a + b Log LD^2 . .	98
16	Relationships of Earthquake Magnitude, Fault Type, Length of Fault Rupture (in Metres), Maximum Surface Fault Displacement (in Metres), Date of Main Earthquake, Locality, and Name of Fault(s) with Associated Surface Faulting	100
17	Estimates of Earthquake Magnitude for the San Andreas, Calaveras, and Hayward Fault Zones, California	112
A1	Relative Abundance of Geomorphological Features Observed Along Strike-Slip Faults in California	A18

LIST OF FIGURES

No.	Title	Page
1	Relation of earthquake magnitude to length of the zone of surface faulting	12
2	Relation between time or recurrence interval (in years), strain rates across fault zones (in cm/yr), and earthquake magnitude, using data from Table 11 and Figure 25 and using methods based on Wallace[30]	15
3	Surface effects of faulting on strike-slip, normal-slip, and reverse-slip faults before, during, and after displacement	17
4	Fault types defined by slip direction in the fault plane	18
5	Schematic map of deformation and surface faulting on an active fault with a total shift accommodated by 70% slip and 30% distortion (drag)	20
6	Discontinuous and irregular surface fault displacements along the three main segments of the Coyote Creek fault from the Borrego Mountain earthquake of April 9, 1968	21
7	En echelon pattern of rupture on four separate, but related surface faults from the 1915 Pleasant Valley, Nevada, earthquake	24
8	Discontinuous normal-slip and normal-oblique-slip surface faulting from the 1954 sequence of four earthquakes in central Nevada, the July 5, 1954, southern Rainbow Mountain faulting, the August 23, 1954, reactivation of the Rainbow Mountain fault zone, the December 16, 1954, Fairview Peak system of faulting, and the Dixie Valley system of faults of December 1954	25
9	Discontinuous reverse-slip and reverse-oblique-slip faulting, geodetic deformation, and aftershock earthquakes from the February 1971 San Fernando, California, earthquake	26
10	Discontinuous zone of surface faulting along the north, central, and south breaks from the Borrego Mountain earthquake of April 9, 1968	27
11	Observed fault displacements on the San Andreas fault from the 1906 earthquake	28
12	Relation of earthquake magnitude to length of associated surface faulting or long axis of aftershock area	36
13	Major tectonic plates	39
14	The Sierra Nevada-Great Valley-Klamath Mountains region of low regional seismicity and the conjugate right-slip faults of northwest trend and left-slip faults of east-west to northeast trend	44

LIST OF FIGURES (CONTINUED)

No.	Title	Page
15	Four systems of faults in southwest Japan	47
16	Aftershocks and surface faulting from the Parkfield-Cholame earthquake zone of 1966	54
17	Map of the Borrego Mountain region showing location of seismographic stations (triangles), epicenter of main shock, aftershock epicenters (crosses), and active faults	55
18	Estimated average apparent slip rate along the San Andreas fault zone in California	58
19	South wall of trench 1 showing progressively greater offset of older strata and bending of strata (drag) across the branching break of the 1968 event	60
20	Block diagrams of the Atera fault, Japan, offsets of geomorphic features, river terraces, and terrace faces	61
21	Denali fault system in central Alaska Range	72
22	Seismic profile and geologic cross section interpreted from the profile N-N' across the Palo Colorado-San Gregorio fault zone, California	81
23	Generalized cross section showing the types of fault offsets shown by seismic reflection surveys in Monterey Bay	82
24	Map showing faults along the floor of Monterey Bay	83
25	Maximum surface fault displacement on main fault as related to earthquake magnitude	89
26	Maximum surface displacement on main fault as related to length of associated surface rupture zone	90
27	Relation of earthquake magnitude to length of zone of surface rupture along the main fault zone	91
28	Relation of earthquake magnitude to surface faulting length times maximum surface fault displacement	92
29	Relation of earthquake magnitude to surface faulting length times square of maximum surface fault displacement	93
30	Diagram showing (I) main fault zone; (II) branch fault; and (III) secondary faults	102
31	Antithetic faults of the Carson Range-Truckee Meadows area . .	104
32	Models of three fundamental structures of basement due to horizontal compression	105
A1	Ridge trace on the 1906 San Andreas fault zone 1 mile northwest of Bolinas Lagoon; view to southwest	A3

LIST OF FIGURES (CONTINUED)

No.	Title	Page
A2	Diagram of, and sequence of structures in, the Riedel experiment	A4
A3	Comparisons of peak and postpeak structures in shear zones of different magnitudes	A5
A4	Sketch map of the detailed relations between right-slip en echelon fractures, accompanying mounds or pressure ridges, which together make up mole tracks on the San Andreas fault zone and depressions or trench traces, Parkfield-Cholame earthquake area of June-August, 1966	A7
A5	Trench trace or trench phase trace of Gilbert	A8
A6	Fracture with en echelon appearance on the Anatolian fault zone near the Varto, Turkey, earthquake area of 1966	A9
A7	En echelon fractures in asphalt from the 1966 Parkfield-Cholame area	A10
A8	Fault map of a section of the Dasht-e Bayaz earthquake zone, Iran, of 1966	A12
A9	Block diagram showing landforms produced along active strike-slip faults in areas with steep topography	A14
A10	Block diagram showing geomorphic features developed along active strike-slip faults in area with moderately steep topography	A15
A11	Oblique aerial view of the San Andreas fault, Carrizo Plains, California	A16
A12	Types of fault scarps and fault traces for normal-slip faults	A21
A13	Striations on the 1954 Fairview Peak fault	A22
A14	The 1915 Pleasant Valley, Nevada, fault scarp with an irregular trace at or near the bedrock-alluvium contact	A23
A15	The 1915 Pleasant Valley, Nevada, fault scarp with a "zigzag" trace at the bedrock-alluvium contact	A24
A16	Fault-trace fissure on the 1915 Pleasant Valley fault which exposed the bedrock fault with vertical component of offset of 3.78 m on a fault plane of 54° W dip; the striations have an angle of pitch of 85° N, indicating a right-slip of about 30 cm	A26
A17	Graben trace along 1954 Dixie Valley fault zone along west side of Dixie Valley	A27
A18	Simple fault scarp near Genoa, Carson Valley, Nevada	A30

LIST OF FIGURES (CONTINUED)

No.	Title	Page
A19	Three stages of mountain and valley development by block faulting	A31
A20	Block-fault mountain and valley terrain with rotated and tilted fault blocks	A32
A21	Distributed fault pattern for reverse-slip and normal-slip faults	A34
A22	Patton Bay reverse-slip fault, Montague Island, from the 1964 Alaska earthquake	A35
A23	Examples of microscopically deformed rock with faulted drape folds	A37

CONVERSION FACTORS, U. S. CUSTOMARY TO METRIC (SI)
UNITS OF MEASUREMENT

U. S. customary units of measurement used in this report can be converted to metric (SI) units as follows:

Multiply	By	To Obtain
inches	25.4	millimetres
feet	0.3048	metres
miles (U. S. statute)	1.609344	kilometres
miles (U. S. nautical)	1.852	kilometres
degrees (angular)	0.01745329	radians

STATE-OF-THE-ART FOR ASSESSING EARTHQUAKE HAZARDS IN THE UNITED STATES

FAULTS AND EARTHQUAKE MAGNITUDE

PART I: INTRODUCTION

Need for Length of Fault and Maximum Displacement

1. Modern engineering practice includes design of structures to accommodate strong earthquake motion. Most active faults have, by man's time framework, very long intervals between the shallow-focus faulting events which are associated with most damaging earthquakes. The recurrence intervals or time gaps for these events are measured in hundreds, thousands, tens of thousands, or even hundreds of thousands of years. These long time intervals, in combination with the short and often nonrepresentative nature of the historic and seismologic records, require that geologic methods be used as alternatives or supplements to historic methods of establishing design events.

2. The geologic method of determining design earthquakes is based on the well-established correlation between size, usually designated by magnitude, of earthquakes and size of the epicentral region as shown by the activated fault length and maximum fault displacement (Bonilla and Buchanan[1]). These relationships are shown in approximately 150 historic earthquake examples of surface faulting, with all major types of faults and tectonic provinces represented.

3. Geologic methods of determining design earthquakes are essential for: (a) faults with very low to moderate rates of activity, (b) faults with high rates of activity that are historically aseismic or have activity rates that are nonrepresentative of their long-term or average activity, and (c) faults in regions where the historic record is short or the seismologic data are obtained from poorly located, distant, or low-gain seismological stations. The geologic method also provides an independent measure of predicted size and frequency of

earthquakes for regions with historically high seismic activity and adequate seismographic station coverage and study. When both geologic and seismologic methods of determining design earthquakes are used, the results are generally similar or compatible. If the results are not compatible, the source data and assumptions used for the two determinations should be evaluated before selecting a design earthquake.

General Relation of Earthquake Magnitude to Fault Length and Maximum Fault Displacement

4. The general relation between magnitude of shallow-focus earthquakes and size or volume of the deformed region and the length and amount of displacement on activated surface faults was recognized at least two decades ago (Tsuboi,[2] Richter[3]). Tocher[4] noted that displacement along faults during large earthquakes is hazardous to the works of man and he developed, for surface faulting in the western United States, the relation of magnitude to fault length and to the product of fault length and maximum displacement. Many subsequent refinements, shown in Figure 1, have been formulated by adding additional data points (Iida[5,6]), applying the method to specific areas, as for southern California (Albee and Smith[7]), and by refining the source data as for the western United States (Bonilla,[8,9] Bonilla and Buchanan[1]) and the world (Ambraseys and Tchalenko,[10] Bonilla and Buchanan[1]). Various dislocation models have been proposed by seismologists (Aki,[11] Brune,[12] Chinnery,[13] King and Knopoff,[14,15] Press,[16] and Wyss and Brune[17]) to relate magnitude (M), fault length (L), displacement (D), and width or depth (W). Chinnery[13] noted that these lead to possible linear relations between the magnitude and the log L (at least for $M > 6.5$ or 7), log LD, log LD^2, log D, and log LDW. The data of Bonilla and Buchanan[1] do not resolve whether the correct model involves a linearity with log D or log D^2.

5. Current engineering applications calculate design earthquakes from relations between magnitude and log L and log D. The correlation of magnitude to fault length and to maximum displacement has high correlation coefficients and has led to widespread use in estimating design earthquakes. The source mechanism studies of Chinnery,[13] King

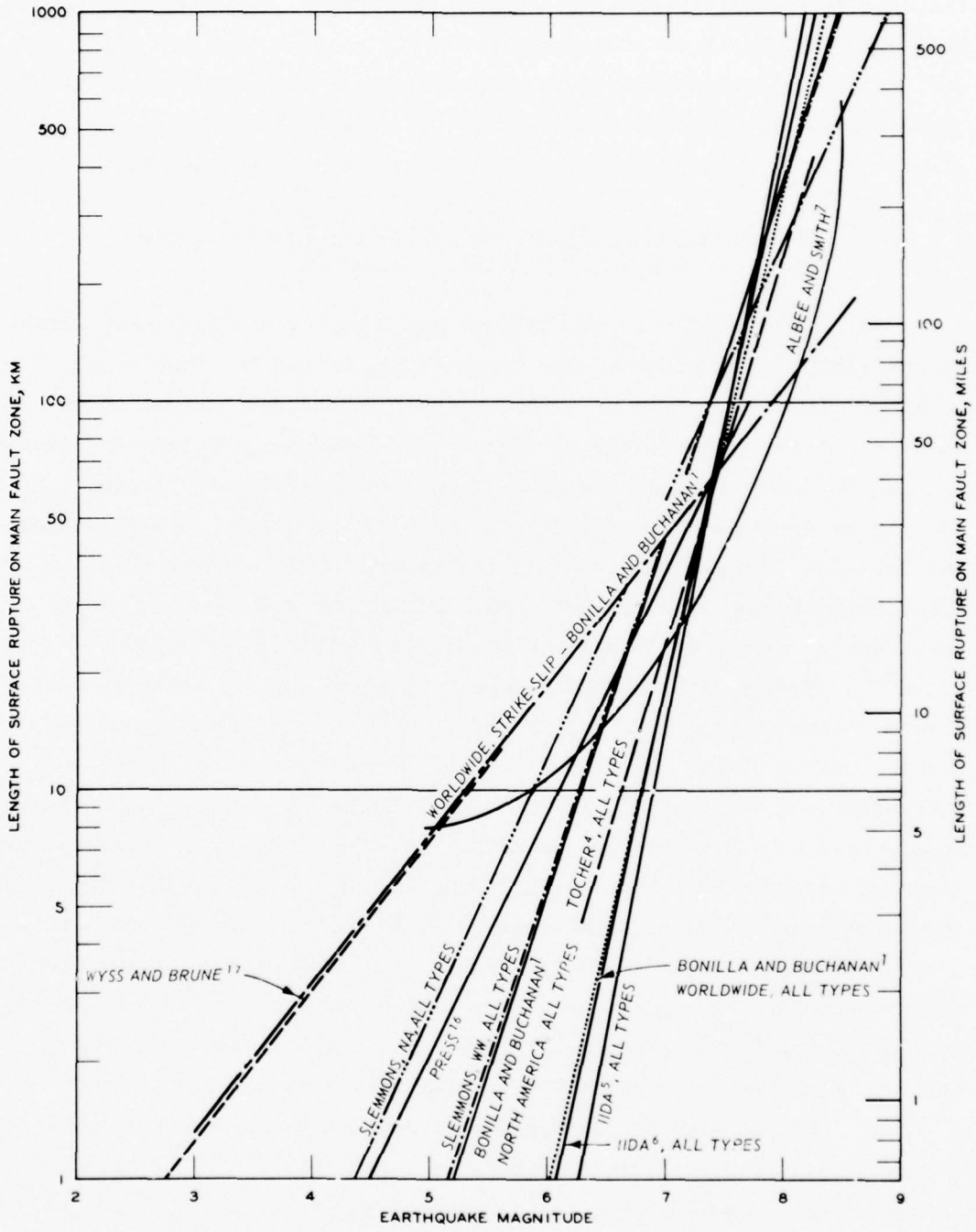


Figure 1. Relation of earthquake magnitude to length of the zone of surface faulting

and Knopoff,[14] and Liebermann and Pomeroy,[18] along with the good to excellent correlation coefficients determined by Bonilla and Buchanan,[1] suggest that magnitude versus log LD or log LD^2 will also be useful in engineering application where both L and D are known. The magnitude versus log LD and log LD^2 correlations both appear to be linear on the plots that follow in a later section of this report, although as noted by Chinnery,[13] both cannot be linear.

Terminology

Definitions of fault activity and nonactivity

6. Definitions of the term "active fault" will be reviewed by Slemmons and McKinney (in press). Currently there are no universally accepted definitions for active and inactive faults. The wide range in definitions for active faults varies from those based on very low rates of fault activity or recurrence as used for siting of nuclear reactors and other vital structures, to practical definitions that apply to faults with higher rates of activity near less important structures. The most widely used definitions follow the general philosophy expressed by Louderback,[19] Allen et al.,[20] Albee and Smith,[7] Wentworth et al.,[21] the International Atomic Energy Agency,[22] the United States Atomic Energy Commission,[23] and Sherard et al.[24] Although definitions of active faults vary widely, the following elements appear in most definitions: (a) Active faults contrast with "dead" faults in that they have the potential for reactivation from current tectonic processes and are likely to produce damaging earthquakes at some time in the future. (b) Evidence for activity can be provided by historic documentation of fault displacement, or geologic evidence of activity in the recent geologic history, generally defined as activity in the Holocene or some part of the Quaternary. (c) Seismologic or other geophysical evidence of current tectonic deformation at the fault.

7. The earlier definitions of active faults (Willis,[25] Louderback[19]) classified faults as either "active," with the potential for future reactivation, or "dead" and no longer likely to have renewed

activity. Some define "active" to be essentially synonymous with "historic." In view of the demonstrated inadequacy of the historic and seismologic periods of observation (Ambraseys[26]), and the much longer term nature of geologic evidence, most workers prefer definitions similar to the following:

a. Active fault: An active fault is a fault that has slipped in historic or recent geologic time, and is likely to have renewed displacements in the future. The fault activity is indicated by historic, geologic, or geophysical evidence and may occur at rates that vary from very low, with long recurrence intervals, to very high, with very short recurrence intervals. Fault activity is similar to that of active volcanoes, which either may show current or historical activity or be dormant, with the potential for, or probability of, future activity.

b. Dead fault: A dead fault is a fault that was active during an earlier orogenic period, but is not active within the present tectonic setting. Some ancient faults do not offset late Cenozoic deposits. The northern part of the White Wolf fault zone, California, which is marked by a remarkably linear segment of the Kern River, does not offset a high terrace level basaltic flow of Pliocene age (Sharp[27]). This fault is classified as "dead," and high magnitude earthquakes are not expected along this fault segment. Some faults of this type, with very low rates of regional deformation, may generate low magnitude earthquakes of similar character and size to the regional earthquakes that are the low "background noise" of seismic activity that occurs within a seismotectonic province. These low magnitude earthquakes are sometimes referred to as "floating" earthquakes, or dispersed patterns of low seismicity in which the earthquakes cannot be correlated with faults or other geologic structures.

c. Capable faults: The definition for capable or active faults as used for siting nuclear reactors and other vital structures is specified by the United States Atomic Energy Commission (now designated the Energy Research and Development Agency, ERDA)[23,28] and the International Atomic Energy Agency.[22] Their definitions are summarized on page 7 of Krinitzsky.[29]

These definitions use time or rates of recurrence that imply rates of deformation on faults as shown in Figure 2. In essence, active or "capable" faults have been displaced during the last 35,000 years, or have had more than one displacement during the last 500,000 years.

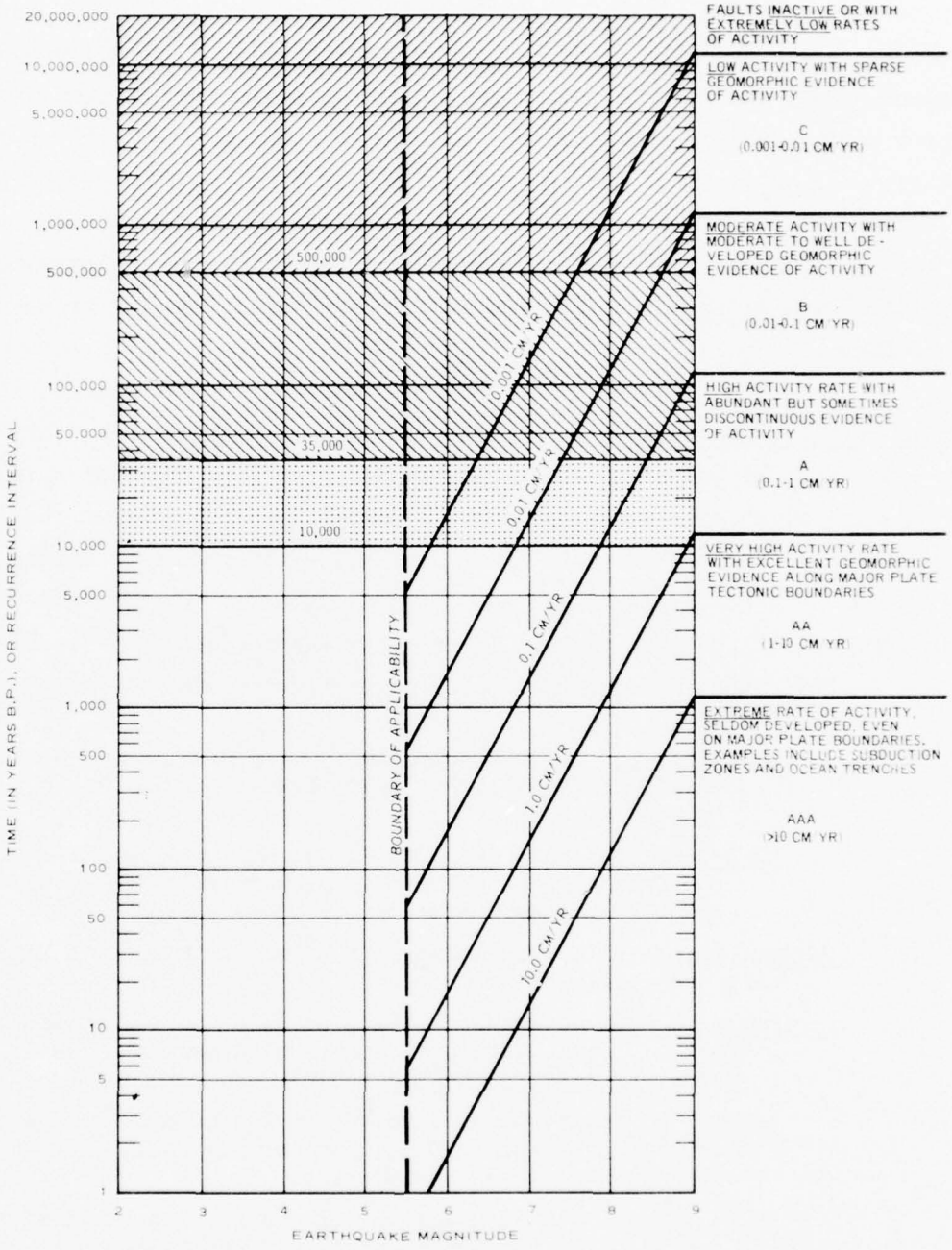


Figure 2. Relation between time or recurrence interval (in years), strain rates across fault zones (in cm/yr), and earthquake magnitude, using data from Table 11 and Figure 25 and using methods based on Wallace.[30] Matsuda[57] classified the rates shown by letters on the right side of the diagram

8. In normal engineering practice, the most widely accepted definition of active fault is based on faults that are affected by current tectonic forces and have evidence of displacement during the Holocene (approximately the last 10,000 years). Dead faults are those that were active during earlier tectonic episodes, but are not active in the present tectonic environment and accordingly do not offset Holocene deposits or surfaces. Some faults that are dead according to this definition may be active with longer periods of measurement, or may become reactivated, sometimes with different slip-types of faulting, with changing tectonic environment.

Classification of
faults by slip direction

9. Slip is the relative displacement of formerly adjacent points on opposite sites of a fault, measured along the fault surface. The slip direction defines the main types of faults--strike-slip, normal-slip, reverse(thrust)-slip (Figure 3), and a number of intermediate combinations or oblique-slip types. These types are defined as follows:

Dip-slip: The component of slip parallel to the dip of a fault.

Normal-slip: Slip parallel to the dip of a fault, where the overlying side has moved downward relative to the underlying side.

Reverse-slip: Slip parallel to the dip of a fault, where the overlying side has moved upward relative to the underlying side. Also called thrust-slip.

Oblique-slip: Slip intermediate in orientation between dip-slip and strike-slip.

Strike-slip: The component of slip parallel to the strike of a fault. A fault with pure strike-slip and no dip-slip is termed a strike-slip fault.

Left-slip: Slip parallel to the strike of a fault where the block on the opposite side of the fault from an observer has moved to the left.

Right-slip: Slip parallel to the strike of a fault where the block on the opposite side of the fault from an observer has moved to the right.

Slip vector: A directed line segment with magnitude and orientation equivalent to the slip; sense is undefined because fault displacement is relative.

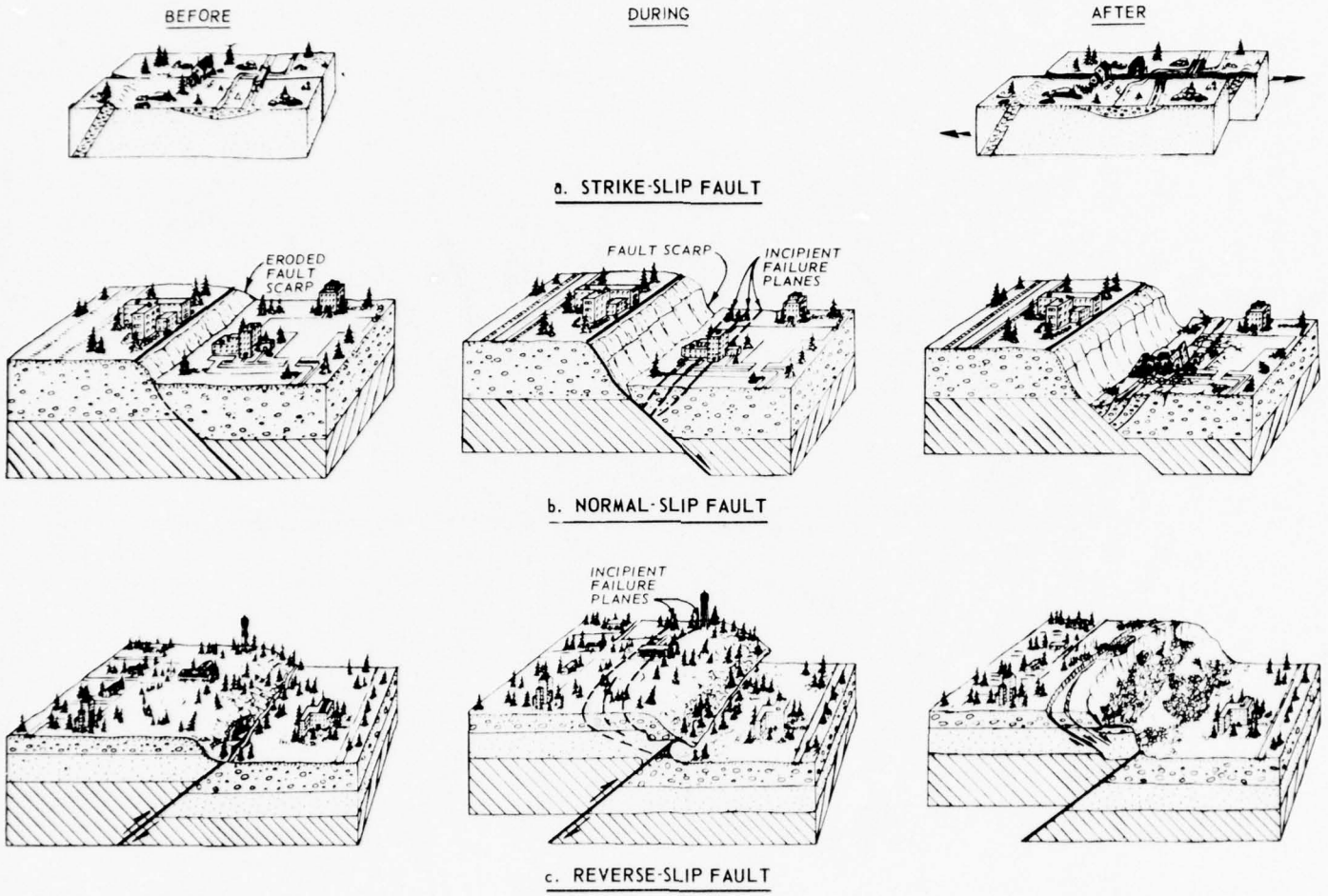


Figure 3. Surface effects of faulting on strike-slip, normal-slip, and reverse-slip faults before, during, and after displacement (after Cluff et al.[31]). Oblique-slip faults combine strike-slip and normal-slip or reverse-slip components to form normal-oblique-slip or reverse-oblique-slip faults

10. Bonilla and Buchanan[1] classify faults into five main types by slip direction. They represent the directions by means of a circle on the fault plane as viewed from the side dipping toward the observer (Figure 4). The five principal types are denoted by the letters A through E. If a point on the far side of the fault plane is displaced by faulting to the rim of the circle, the indicated type of fault would be produced. This displacement produces a radial line on the projection circle that makes an angle in the fault plane with the horizontal line

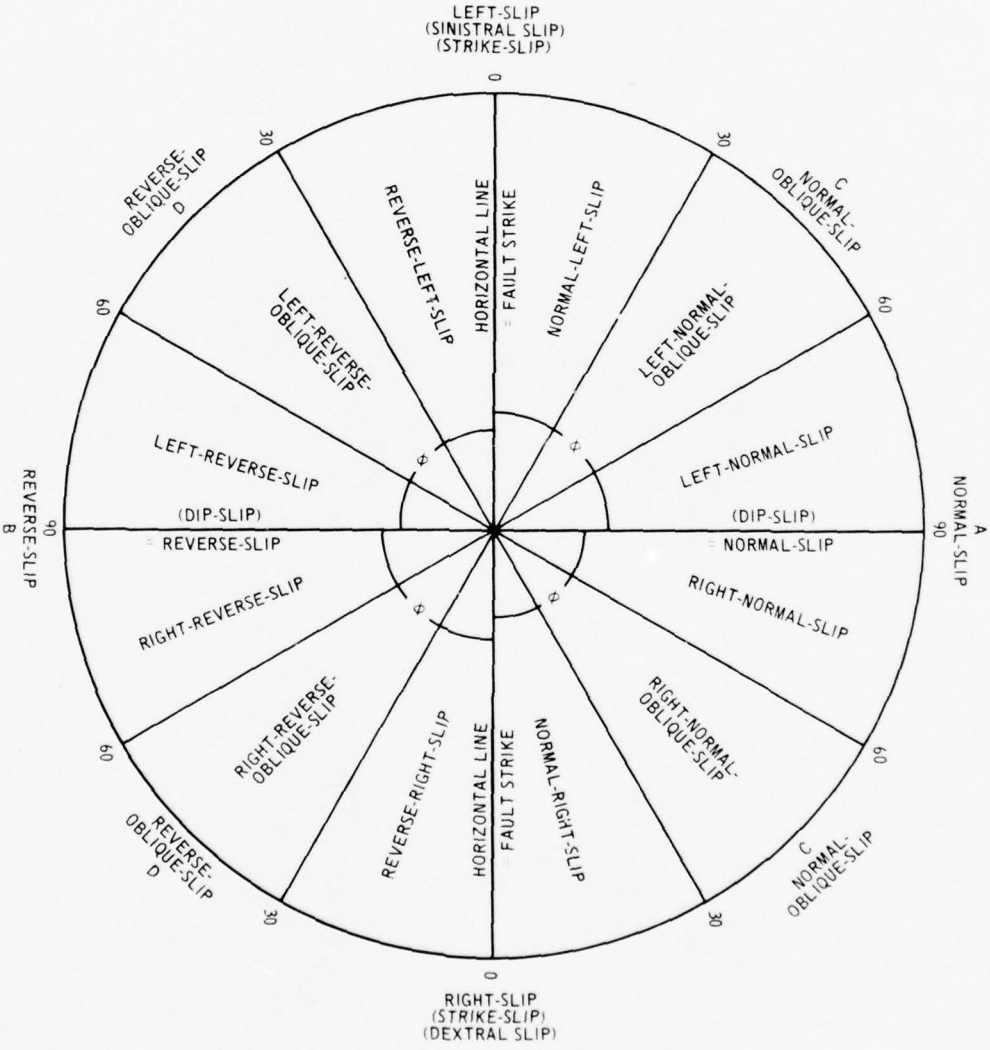


Figure 4. Fault types defined by slip direction in the fault plane (after Bonilla and Buchanan[1])

which represents the strike of the fault; this angle is called $\emptyset$ and also can be measured from striations or slickensides in the fault surface. This angle can be calculated from the relative values of the strike-slip (SS) and dip-slip (DS) by the function:

$$\text{cotangent } \emptyset = SS/DS$$

Fault slip and distortion

11. The amount of slip as measured by displacement of linear geologic, geodetic, or cultural features across the fault zone commonly is affected by deformation near the fault plane. The total regional deformation (Figure 5) can be depicted by viewing a linear feature such as a straight stream segment, a pipeline, or a highway crossing the fault plane. The total regional displacement near the fault is termed shift, the displacement on the fault plane as slip, and the displacement by folding, warping, or drag as distortion. Distortion is a common type of local deformation near faults and partly accounts for variability of historic surface fault displacement measurements and the observation that the length of the zone of surface faulting is shorter than the length of the aftershock zone or the zone of geodetic deformation. Measurements of fault shift are generally more consistent than fault slip.

12. Similar deformation can develop in the vertical plane and the surface faulting may have displacements that are less than the true displacement at depth, or may have irregular displacements along the fault trace (Figure 6).

Classification by
complexity of fracturing

13. Historic surface faulting varies greatly in pattern of fracturing. The resulting fracture zones may be single, simple, narrow surface faults, or branching patterns, or distributed patterns which may include secondary faults at some distance from the main fault (Bonilla[8]). Simple fault zones usually have single, narrow, and steeply dipping fault traces.

14. Grouped or branching patterns are more common than simple

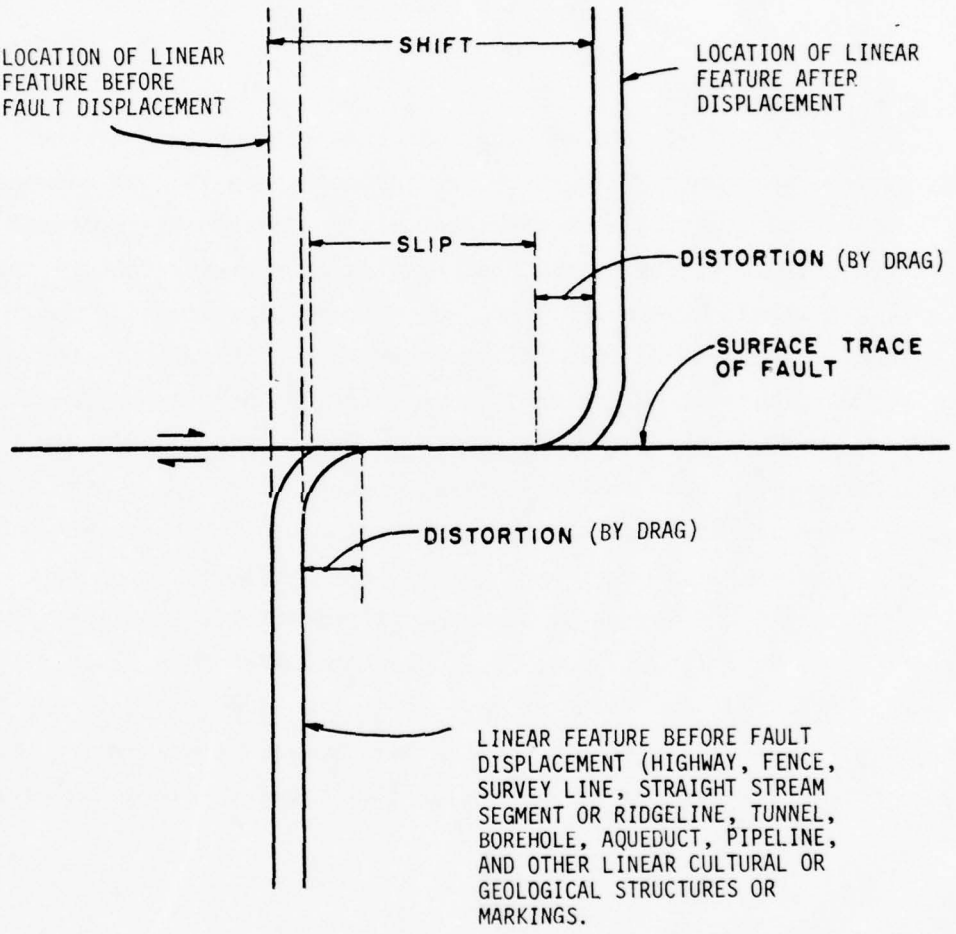


Figure 5. Schematic map of deformation and surface faulting on an active fault with a total shift accommodated by 70% slip and 30% distortion (drag)

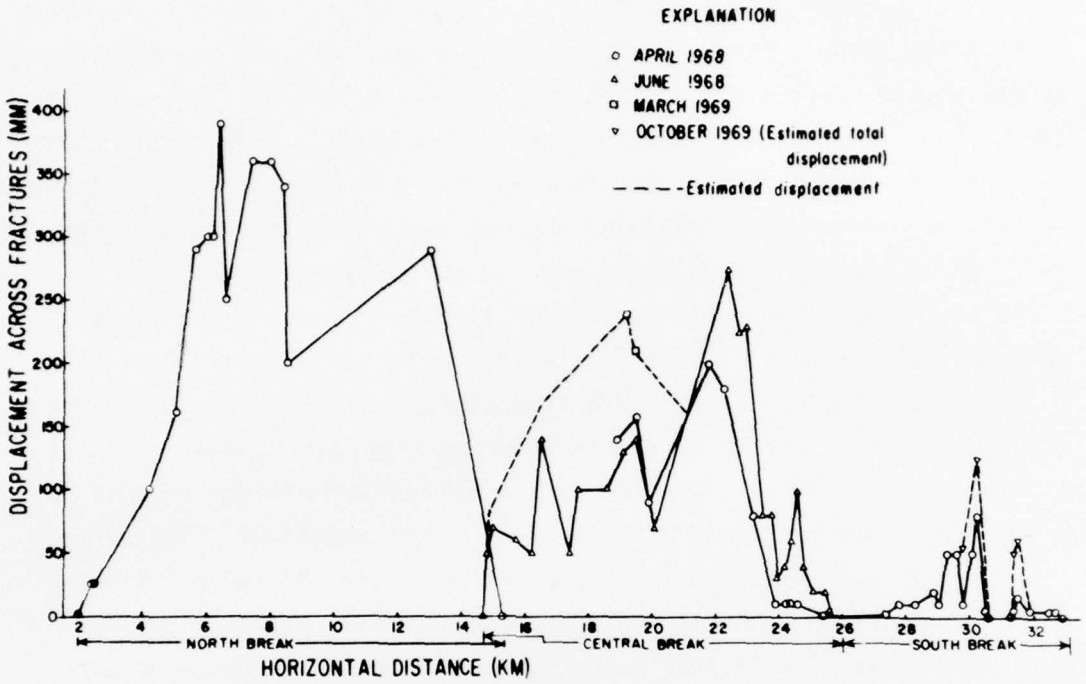


Figure 6. Discontinuous and irregular surface fault displacements along the three main segments of the Coyote Creek fault from the Borrego Mountain earthquake of April 9, 1968 (from Clark[32])

faults. These groupings are commonly expressed as patterns or irregularities of major topographic features of the region: mountain blocks, valley blocks, or groups of mountains and intervening valleys. The active faulting of these distributed fault patterns during major earthquakes may produce faulting along either separate or connected faults, sometimes with different types of faulting in conjugate systems. The evaluation of faults in this type of region is a difficult problem, and involves a careful regional approach with detailed mapping and analysis of the faults and folds as will be discussed in a later section of this report.

Relation Between Earthquake Deformation and Surface Faulting

15. Surface faulting is a surface expression of deformation

within the earth. The rupturing generally occurs suddenly during earthquakes, although for a few faults, slow creeping displacements may occur without the abrupt release of the elastic strain that has accumulated. At the higher temperature and pressure that exists deeper in the earth's crust or upper mantle, failure may take place more or less continuously by plastic deformation without accompanying earthquakes. The overlying, more brittle crustal materials accumulate strain and episodically release it by surface displacement and seismic energy release.

16. The surface deformation may include widespread uplift, subsidence, or horizontal distortion, which can be detected and delineated by geodetic methods. Surface faulting commonly develops along the central part of the zone of deformation during large earthquakes of magnitude 6 or 7 and higher. The length and maximum and average amounts of displacement are proportional to the earthquake magnitude. The aftershocks generally are strongly aligned along the faults and are broadly distributed through the epicentral region, or region of deformation. Subsequent migration of strain may provide aftershocks, and additional surface or subsurface faulting extending into adjoining regions.

17. The depth of the zone of earthquake faulting and elastic release of seismic energy is poorly known. For the megathrusts of major subduction zones, the main fault zone and earthquake activity can extend to depths of several hundred kilometres (Benioff[33] zones). Such zones have very high rates (up to 10 or 15 cm/yr average rate) of deformation (Oliver[34]). Many faults above the Benioff zone, and the faults of most other regions have earthquakes that are limited to the uppermost few tens of kilometres. Kasahara[35] and Chinnery[36] estimate from dislocation theory that the faulting associated with the Tango, Japan, earthquake of 1927 extended to depths of about 10 to 15 km. The Tanna faulting during the North Idu, Japan, earthquake of 1930 extended to depths of about 8 to 12 km. Kasahara estimated that the strike-slip San Andreas faulting of 1906 extended to depths of about 2 to 6 km. Thatcher[37] reanalyzed geodetic data from the 1906 earthquake and noted that the seismic (earthquake-causing) slip was limited to approximately the upper 10 km, although the faulting may have had deeper, aseismic extensions. Most

of the main earthquakes and aftershocks of surface faulting events in the western United States during the past 20 years have been well studied seismologically and geologically. All major types of faulting are represented--strike-slip, normal-slip, reverse-slip, and oblique-slip; nearly all have earthquake foci that are less than 15 km deep and some zones (as shown by the aftershocks along the San Andreas fault near Parkfield-Cholame in 1966) have foci that are mainly in the upper 6 km (Eaton et al.[38]).

18. Surface faulting is commonly distributed along branching faults or separate faults, in a zone that may be approximately oval in form (see United States Department of Commerce[39] for reports on geodetic measurements of crustal movement, 1906-71). Plastic deformation or folding in surficial soil, sediments, and bedrock may cause irregularities of displacements or gaps along main structural trends. The complex fracture patterns that form on different slip types of faults are shown in the following examples:

a. Normal-slip faults: 1915 Pleasant Valley, Nevada, earthquake zone with four separate en echelon normal-slip faults (Figure 7).

b. Normal-, normal-oblique-, and strike-slip faults: 1954 earthquake sequence in central Nevada with at least six separate north-south trending faults in a zone 58 miles long and 29 miles wide (Figure 8).

c. Reverse-slip and reverse-oblique-slip faults: 1971 San Fernando, California, zone of discontinuous faulting (Figure 9).

d. Strike-slip faults: 1968 Borrego Mountain, California, zone of irregular surface faulting along three segments of the Coyote Creek fault zone (Figure 10).

19. Normal-slip, reverse-slip, and oblique-slip faults generally have scarp heights and fault displacements that vary from zero at each end to maximum offset in the central section (bilateral symmetry), but uneven propagation of the fault to the surface may lead to a sawtooth fault pattern. Some faults have maximum displacements near one end of the fault (unilateral symmetry). Although strike-slip faults tend to have more consistent amount of displacement along the fault, the measured displacements may be irregular, as in the case of the 1968

BEST AVAILABLE COPY



Figure 7. En echelon pattern of rupture on four separate, but related surface faults from the 1915 Pleasant Valley, Nevada, earthquake. The four faults are normal faults with mainly dip-slip displacement, although minor right-slip components are present in parts of the Pearce scarp. The en echelon pattern is suggestive of deep left-slip deformation on the northeast trending zone (unpublished studies of Wallace and Slemmons)

BEST AVAILABLE COPY





Figure 8. Discontinuous normal-slip and normal-oblique-slip surface faulting from the 1954 sequence of four earthquakes in central Nevada, the July 5, 1954, southern Rainbow Mountain faulting, the August 23, 1954, reactivation of the Rainbow Mountain fault zone, the December 16, 1954, Fairview Peak system of faulting, and the Dixie Valley system of faults of December 1954. The region of deformation forms a zone of 58 miles (93 km) length and 29 miles (47 km) width

BEST AVAILABLE COPY

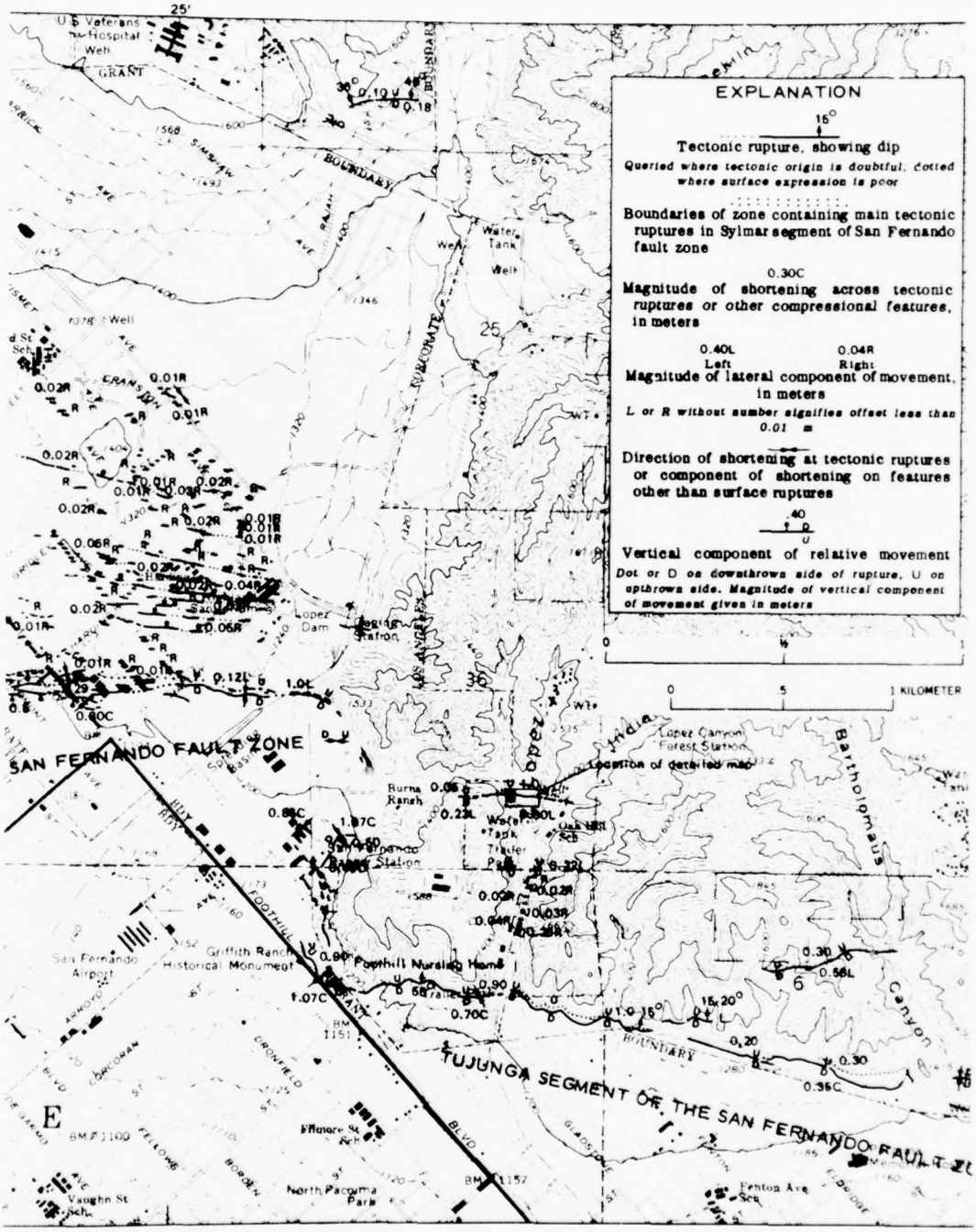


Figure 9. Discontinuous reverse-slip and reverse-oblique-slip faulting, geodetic deformation, and aftershock earthquakes from the February 1971 San Fernando, California, earthquake. Note complex shatter pattern of faulting that is generalized on this map

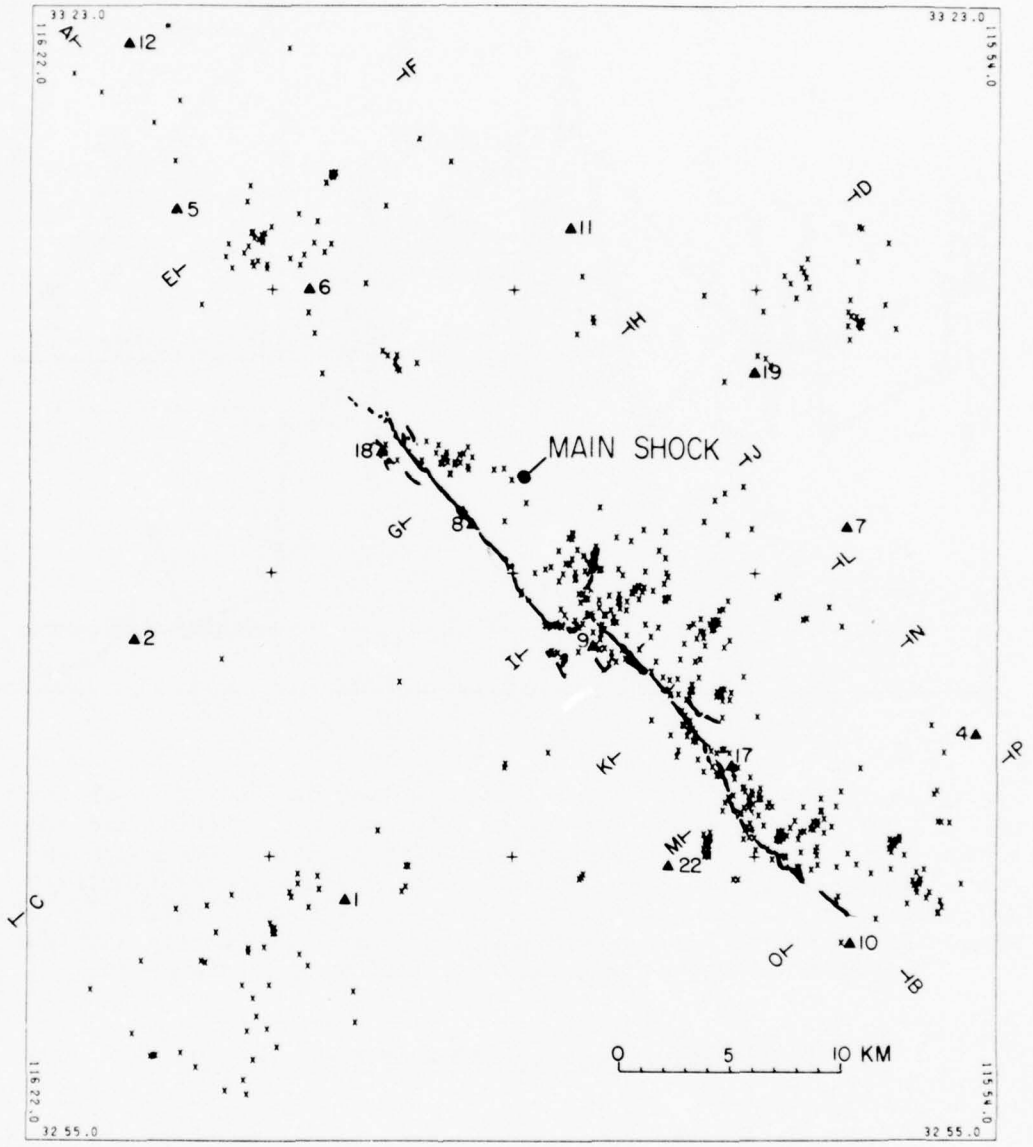


Figure 10. Discontinuous zone of surface faulting along the north, central, and south breaks from the Borrego Mountain earthquake of April 9, 1968 (from Clark[32])

Borrego Mountain earthquake (Figure 6). The surface displacement may be reduced by distortion or folding (Figures 5 and 11).

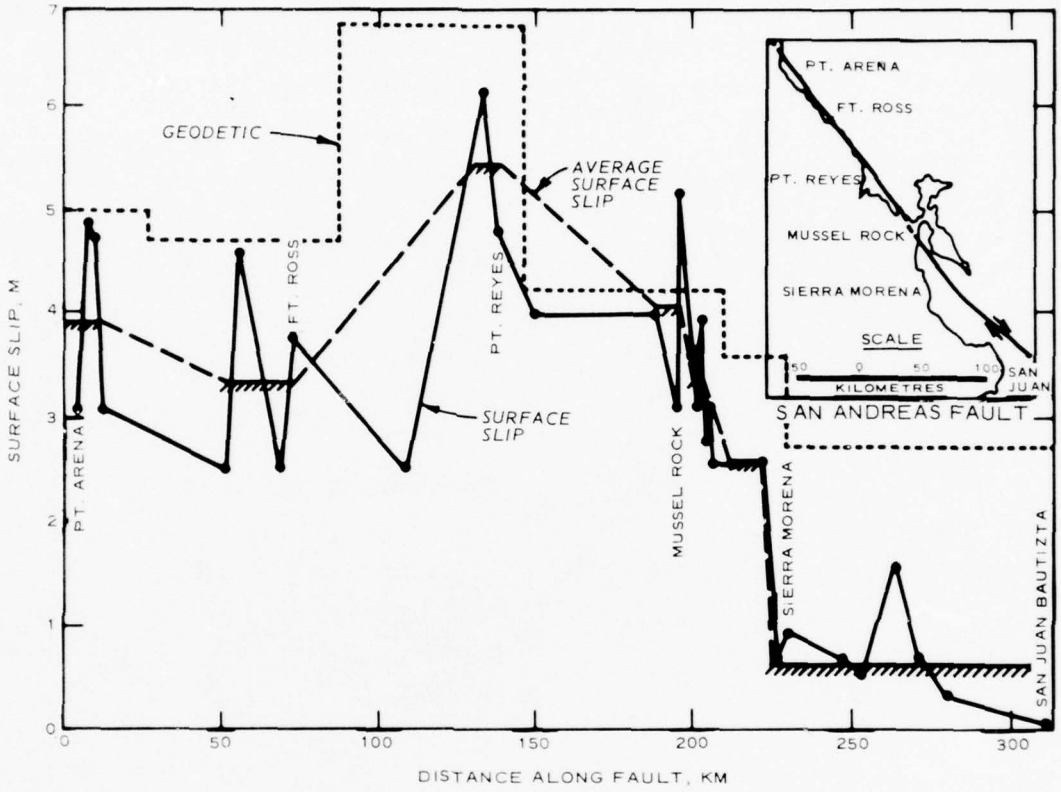


Figure 11. Observed fault displacements on the San Andreas fault from the 1906 earthquake. Dots are actual observations; hatched line connected by dashes shows a rough average of these data. Bar graph is based on 6 geodetic profiles across the fault zone and the faulting model based on slip on segments of a 10-km-deep fault (Thatcher[37,40]). Many of the measured field observations appear to be smaller than the geodetic values as the result of local drag or distortion

Difficulty in Determination of Fault Length

20. Several factors make the determination of fault length difficult. These problems arise mainly from the complexities of interpretation of branching or distributed patterns of faulting, and concealment of all or part of many fault zones. This results in part from the fact that for earthquakes of less than about 7 magnitude, most of the

activated fault plane may be concealed in the lithospheric plate beneath the earth's surface. Difficulties in the determinative curves relating earthquake magnitude to fault length are often derived from inadequate data for many of the historic examples of surface faulting, and the variation of the proportion of total fault length activated during a given earthquake is from less than 1 percent to as much as 100 percent.

21. Factors that make the determination of the length of a given fault difficult include:

a. The fault may change from an active fault along some segments into an inactive fault along other segments.

b. Many faults are not linear, or are difficult to trace.

c. Faults may change along their length in amount of displacement or type of slip, making these characteristics difficult to recognize or evaluate.

d. The fault may belong to a complex swarm of individual ruptures, thereby making the continuity of the structure at depth difficult to distinguish.

e. Faults commonly belong to conjugate systems, with tectonically related faults of different orientations and slip types.

f. Postfaulting erosion can modify the appearance of the fault scarp, making it difficult to trace.

g. Concealment by the ocean, lakes, glaciers, streams, and geologically young sediments may cover or interrupt the outcrop of a fault.

h. The tectonic disturbance may change from fractures into warps or folds, and thereby affect the appearance of the fault.

Design Earthquakes from Fault Length and Maximum Displacement Data

22. Analysis of moderate to high magnitude earthquakes requires consideration of two types of design parameters.

a. The magnitude of earthquakes likely to be generated by future fault displacements and resulting ground motion at sites at various distances from the earthquake epicenter.

b. The extent, position, and maximum amount of displacement along surface fault ruptures.

23. To determine the anticipated earthquake ground motion at a given site, it is necessary to evaluate important active faults both near and at considerable distances from the site for which design is required. Since seismic vibrations attenuate with distance, the design earthquakes for a specific site may include a moderate magnitude earthquake from a nearby fault and/or a large earthquake from a distant major fault. When a major fault is near the site, more distant faults are generally not used for design earthquakes unless earthquake frequency or recurrence is an important consideration. Analysis of the length of the fault and the maximum displacements that have occurred on the fault leads to the design earthquake magnitude and distance of the epicenter from the site. From these parameters, Hofmann[41] and Krinitzsky and Chang[42] outline methods by which the earthquake intensity, peak acceleration, peak velocity, and peak displacement can be determined. In addition, it is possible to estimate the duration of the period of strong ground motion from the relations given in Hofmann.[41] Tabulation of these data for all significant faults for the site will assist in determination of design parameters. The tendency for active faults to show similar rates, types of slips, and amounts of displacement during repetitions of activity permits the estimate that future activity along a given fault will follow the pattern in time and space that characterized the past several events. Geomorphic and stratigraphic data commonly provide the essential information necessary for estimating future displacements at specific sites along the fault zone from this and the sizes of associated earthquakes.

24. Determination or estimation of the fault's position relative to the site, type of displacement to be expected, attitude of fault plane, length of fault zone, and maximum displacement as shown by previous events, provides a basis for determining the design earthquake. Although the earthquake may have a focus at one end (unilateral symmetry) or the middle (bilateral symmetry) of the fault zone, the main energy release is from the fault surface and adjoining rock, so the important design distance is usually the shortest distance to the activated fault. This distance from fault to site, and the earthquake magnitude, permit determination of the desired design parameters by the relations listed in Table 1.

Table 1

Directly and Indirectly Determined Relations Between Earthquake Magnitude and Design Parameters

Parameter	Figure No. in. Hofmann[41]	Krinitzsky and Chang[42]	Other Sources
Determined from Magnitude-Distance to Epicenter:			
Magnitude versus maximum acceleration	4 and 9		Gutenberg and Richter[43]
Percent maximum acceleration versus distance	24		Schnabel and Seed[44]
	10		Gutenberg and Richter[43]
	10		Benioff[45]
	10		Seed[46]
	12		Housner[47]
Magnitude-distance-maximum acceleration	13		Krishna[48]
Maximum acceleration-distance	12		Housner[47]
Distance-acceleration for strike-slip faulting	23		Hofmann[41]
Distance-acceleration for reverse-slip faulting	25		Hofmann[41]
Magnitude-shaking duration	6,9,27, and 29		Gutenberg and Richter[43]
	27 and 29		Hofmann[41]
	29		Housner[47]
Magnitude-distance-period	31		Seed[46]
Distance-attenuation	32		Benioff[45]
	17		Boore and Page[49]
Distance-predominant period	30		Gutenberg and Richter[43]
	30		Figueroa[50]
	30		Jenschke et al.[51]
	30 and 31		Seed[46]
Determined Indirectly from Magnitude-Distance-Intensity Relations:			
Distance-intensity versus acceleration		6	Neumann[52]
Intensity-acceleration by foundation types	14	7	Coulter et al.[53]
Intensity-acceleration		8	Neumann[52]
		8	Gutenberg and Richter[43]
		8	Hershberger[54]
		8	Medvedev et al.[55]
		8	Trifunac and Brady[55]
		9	Krinitzsky and Chang[42]
Intensity-distance-soil type		11	Neumann[52]
Intensity-acceleration-velocity-displacement (motion)		13	Trifunac and Brady[55]
Magnitude-intensity (for western United States)		14	Krinitzsky and Chang[42]
Magnitude-distance-intensity		15	Krinitzsky and Chang[42]
Intensity-peak acceleration, near and far fields		16	Krinitzsky and Chang[42]
Intensity-peak velocity, near and far fields		17	Krinitzsky and Chang[42]
Intensity-peak displacement, near and far fields		18	Krinitzsky and Chang[42]

PART II: DETAILED RELATION OF EARTHQUAKE MAGNITUDE TO FAULT LENGTH AND MAXIMUM DISPLACEMENT

General Statement

25. Two methods have been used to determine the relation between earthquake magnitude and fault length: (a) empirical studies based on field observations of surface faulting from earthquakes (Tocher,[4] Iida,[5,6] Albee and Smith,[7] Bonilla,[8,9] and Bonilla and Buchanan[1]) and (b) focal mechanism studies of dislocations based on seismologic and elasticity theory that relates seismic energy release, focal mechanisms, and source parameters. Several studies of source mechanisms have discussed the disagreement in relations obtained from the earlier fault compilations (Press,[16] Brune and Allen,[56] King and Knopoff,[14] and Chinnery[13]). However, the more recent empirical curves of Bonilla[8,9] and Bonilla and Buchanan[1] closely approximate the seismological dislocation models of Chinnery[13] and Wyss and Brune.[17]

26. The source mechanism studies for a wide range of earthquake magnitudes suggest that for large earthquakes where the length (L) of the source is large relative to the depth to the plastic zone, the L^2 area dependence on energy release gives good agreement with the empirical data. For smaller energy release, where the source area of deformation is above the plastic zone, an L^3 volume dependence may be more closely related to energy release. For this latter case, the source parameter data should fall more nearly on the curve of Press[16] shown in Figure 1. This source relation appears to be appropriate for explosion sources. Wyss and Brune[17] plot the relation shown in Figure 1 for fault lengths defined by earthquakes of smaller source dimensions and combined seismic wave analysis and field observation of fault displacement. The curve of Wyss and Brune[17] is in good agreement with the straight-line relation of Bonilla and Buchanan[1] data for strike-slip surface faulting.

27. In their statistical analysis, Bonilla and Buchanan[1] indicate that less than one-half of the energy contribution to magnitude is by the fault length parameter. This emphasizes the need to supplement

M versus log L determinations with M versus log D determinations. The wide variation in values a and b in the equations that follow is mainly the result of a small statistical sample. Additional scatter is introduced by variable quality of supporting field studies and magnitude determinations.

28. This section summarizes the relations obtained by previous workers for least squares fit of the equation for a straight line, $y = a + bx$. Part VI establishes new equations and charts, based on additional and more recent data. The new formulations have less scatter and have improved correlation coefficients. Workers are cautioned that, for a given data set, the linear regression analysis which leads to the solution of the equation $\log x = a + bM$ is not mathematically equivalent to the equation $M = a + b \log x$. Accordingly, the lines for the two equations are not in the same position when plotted on a graph with the same coordinates. Since the normal procedure of fault analysis is to infer from field fault parameters the magnitudes of earthquakes that are generated from a given fault length or maximum displacement, the equations and graphs of this paper are based on such formulations as $M = a + b \log D$, $M = a + b \log L$, $M = a + b \log LD$, and $M = a + b \log LD^2$. The data of Bonilla and Buchanan[1] were recalculated by linear regression analysis in order for the data to be readily compared in Tables 2 through 7 and 11 through 15, and for Figures 1 and 25 through 29.

Empirical Relation of Logarithm of Maximum Displacement (Log D) to Magnitude (M)

29. This relation provides a statistically better correlation than between fault length and magnitude and is based on the maximum surface displacement that has occurred during past earthquakes along the fault. Application of this relation may require more detailed studies of stratigraphic, soil, or geomorphic offsets than fault length. Table 2 summarizes published formulations of this relation, based on the straight-line correlation of: $M = a + b \log D$.

Table 2

Relation of Earthquake Magnitude (M) to Logarithm of Maximum Displacement (Log D): M = a + b Log D

Reference	Region	Type of Fault	No. of Events	a	b	D
Tocher[4]	Calif.-Nev.	All	9	7.012	0.720	m
Iida[6]	Worldwide	All	58	6.836	1.818	m
Bonilla and Buchanan[1]	North America	All	19	6.838	1.169	m
Bonilla and Buchanan[1]	Worldwide	All	50	6.890	1.105	m
Bonilla and Buchanan[1]	Worldwide	A normal-slip	14	6.853	0.841	m
Bonilla and Buchanan[1]	Worldwide	B reverse-slip	7	7.166	1.280	m
Bonilla and Buchanan[1]	Worldwide	C normal-oblique-slip	7	7.094	0.065	m
Bonilla and Buchanan[1]	Worldwide	D reverse-oblique-slip	5	6.928	0.067	m
Bonilla and Buchanan[1]	Worldwide	E strike-slip	17	6.881	1.332	m

Empirical Relation of Logarithm of Fault Length (Log L) to Logarithm of Maximum Fault Displacement (Log D)

30. This relation permits the estimation of maximum fault displacements along a fault of known length. The relation shows a very good statistical correlation. Table 3 summarizes published formulations of this relation, based on the straight-line correlation of: log D = a + b log L.

Table 3

Relation of Logarithm of Maximum Displacement (Log D) to Logarithm of Fault Length (Log L): Log D = a + b Log L

Reference	Region	Type of Fault	No. of Events	a	b	D	L
Tocher[4]	Calif.-Nev.	All	9	-2.809	0.664	m	m
Iida[6]	Worldwide	All	59	-3.444	1.075	m	km
Bonilla and Buchanan[1]	North America	All	19	-4.268	0.952	m	m
Bonilla and Buchanan[1]	Worldwide	All	61	-2.240	0.558	m	m
Bonilla and Buchanan[1]	Worldwide	A normal-slip	20	-3.136	0.775	m	m
Bonilla and Buchanan[1]	Worldwide	B reverse-slip	8	0.152	0.035	m	m
Bonilla and Buchanan[1]	Worldwide	C normal-oblique-slip	7	0.198	0.042	m	m
Bonilla and Buchanan[1]	Worldwide	D reverse-oblique-slip	5	-1.641	0.451	m	m
Bonilla and Buchanan[1]	Worldwide	E strike-slip	21	-3.273	0.752	m	m

Empirical Relation of Logarithm of Fault Length (Log L) to Magnitude (M)

31. This is the most widely used relation for estimating the magnitude of earthquakes likely to be generated by future earthquakes along faults of known length. Table 4 summarizes published formulations of this relation, based on the straight-line correlation of:
$M = a + b \log L$.

32. Albee and Smith[7] evaluated problems of earthquake risk and design for southern California. They tabulated earthquake magnitude and surface fault lengths for 19 earthquakes in California, Nevada, and Baja, California, and included also 22 earthquakes without surface faulting by use of the size (length) of the aftershock region (Figure 12).

Table 4

Relation of Earthquake Magnitude (M) to Logarithm of Fault Length (Log L): $M = a + b \text{ Log } L$

Reference	Region	Type of Fault	No. of Events	a	b	L
Tocher[4]	California-Nevada	All	10	3.415	0.825	m
Iida[5]	Worldwide	All	35	6.27	0.63	km
Iida[5]	Japan and vicinity	All	12	6.62	0.49	km
Iida[6]	Worldwide	All	54	6.07	0.76	km
Bonilla and Buchanan[1]	North America	All	14	2.008	1.075	m
Bonilla and Buchanan[1]	Worldwide	All	53	3.757	0.758	m
Bonilla and Buchanan[1]	Worldwide	A normal-slip	14	4.303	0.630	m
Bonilla and Buchanan[1]	Worldwide	B reverse-slip	7	7.497	0.047	m
Bonilla and Buchanan[1]	Worldwide	C normal-oblique-slip	7	3.828	0.751	m
Bonilla and Buchanan[1]	Worldwide	D reverse-oblique-slip	5	7.137	-0.049	m
Bonilla and Buchanan[1]	Worldwide	E strike-slip	20	1.239	1.242	m
Matsuda[57]	Japan	All	14	-4.833*	1.367*	km

* Regression analysis for $\log L = a + bM$.

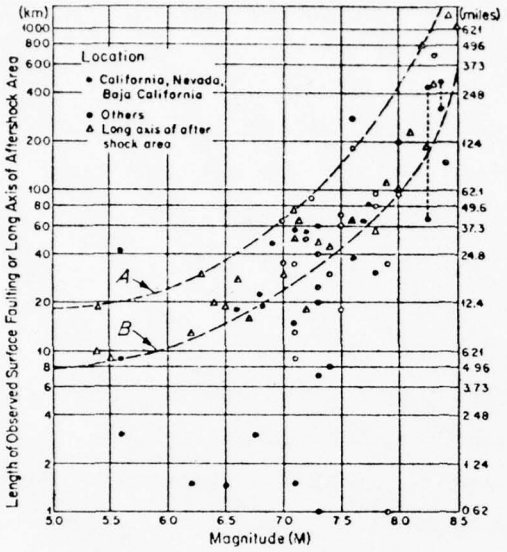


Figure 12. Relation of earthquake magnitude to length of associated surface faulting or long axis of aftershock area (from Albee and Smith[7]). Curve A is the approximate limiting curve and Curve B is a curve of best fit

Their results suggest that shallow-focus smaller earthquakes without surface faulting fall on the same curve as larger magnitude earthquakes with surface faulting. Their figure suggests that a curved relation exists between magnitude and length of associated surface faulting.

Empirical Relation of Logarithm of Fault Length (L) Times Maximum Displacement (D) to Magnitude (M)

33. This relation has been used for seismological studies, but since previous field studies have seldom resolved both fault length and maximum displacement during previous earthquakes along the fault, it has received little use in determining design earthquakes. This relation should be more representative of earthquake volume, the volume of rock with elastic seismic energy release, and it should be used whenever both fault parameters are known. The very good statistical correlation is similar to that for magnitude versus displacement correlations and is better than magnitude versus length correlations, although the standard deviation of M is much larger. Table 5 summarizes published formulations of this relation, based on the straight-line correlation of: $M = a + b \log LD$.

Empirical Relation of Logarithm of Fault Length Times the Square of Displacement (log LD^2) to Magnitude (M)

34. This relation was proposed by King and Knopoff[14] as the most representative fault parameter measure for correlation with magnitude.

Table 5

Relation of Magnitude (M) to Logarithm of Fault Length (L) Times Displacement (D): $M = a + b \log LD$

Reference	Region	Type of Fault	No. of Events	a	b	L	D
Tocher[4]	North America	All	7	4.976	0.464	m	m
Iida[5]	Japan	All	11	6.19	0.35	km	cm
Iida[5]	Worldwide	All	52	5.39	0.48	km	cm
Bonilla and Buchanan[1]	North America	All	19	3.845	0.667	m	m
Bonilla and Buchanan[1]	Worldwide	All	48	4.576	0.548	m	m
Bonilla and Buchanan[1]	Worldwide	A normal-slip	14	4.924	0.467	m	m
Bonilla and Buchanan[1]	Worldwide	B reverse-slip	6	6.200	0.314	m	m
Bonilla and Buchanan[1]	Worldwide	C normal-oblique-slip	6	5.318	0.374	m	m
Bonilla and Buchanan[1]	Worldwide	D reverse-oblique-slip	5	7.000	-0.014	m	m
Bonilla and Buchanan[1]	Worldwide	E strike-slip	17	3.797	0.722	m	m

Bonilla and Buchanan[1] compiled the relations listed in Table 6, based on the straight-line correlation of: $M = a + b \log LD^2$. The statistical correlation between magnitude and the logarithm of LD^2 is very good, although the standard deviation of the magnitude is larger than for the relation to fault length or maximum displacement.

Table 6

Relation of Earthquake Magnitude (M) to Logarithm of Fault Length (L) Times Displacement (D) Squared: $M = a + b \log LD^2$

Reference	Region	Type of Fault	No. of Events	a	b	L	D
Tocher[4]	California-Nevada	All	9	5.708	0.296	m	m
Iida[6]	Worldwide	All	52	2.980	0.408	cm	cm
King and Knopoff[14]	Worldwide	All	42	1.395*	0.526*	cm	cm
Bonilla and Buchanan[1]	North America	All	19	4.880	0.436	m	m
Bonilla and Buchanan[1]	Worldwide	All	48	5.258	0.386	m	m
Bonilla and Buchanan[1]	Worldwide	A normal-slip	14	5.567	0.310	m	m
Bonilla and Buchanan[1]	Worldwide	B reverse-slip	6	6.441	0.249	m	m
Bonilla and Buchanan[1]	Worldwide	C normal-oblique-slip	6	6.112	0.200	m	m
Bonilla and Buchanan[1]	Worldwide	D reverse-oblique-slip	5	6.955	-0.003	m	m
Bonilla and Buchanan[1]	Worldwide	E strike-slip	17	4.668	0.483	m	m

* Linear regression analysis for $\log LD^2 = a + bM$.

PART III: RELATION BETWEEN PLATE TECTONICS, FAULT TYPE, MAXIMUM FAULT DISPLACEMENT, FAULT LENGTH, AND EARTHQUAKE MAGNITUDE

Introduction

35. Review of the listings of active faults that have had historic surface faulting during earthquakes (Bonilla,[8] Bonilla and Buchanan[1]) indicates that nearly all are at or near major earth plate boundaries as defined in recent papers dealing with plate tectonics or new global tectonics (e.g. Isacks et al.,[58] Le Pichon,[59] Dewey and Bird,[60] Morgan,[61] and Oliver.[34] The slip types of faults, their focal depths and mechanisms, and sizes of the geodetic zones of deformation all suggest that they are related to strain and failure in the earth's crust, or upper mantle. The slip types accordingly are diagnostic of the major tectonic affinity of the faults, with (a) the shallow- to deep-focus megathrusts related to zones of subduction or plate convergence (Figure 13), (b) the normal faults related to extension along rises and rift zones, or as subordinate faults of other tectonically active regions, (c) the reverse-slip faults related to cordillera mountain building with compressional tectonic activity, and (d) the major strike-slip faults formed by subparallel plate movements at different rates along major plate or subplate boundaries.

36. Nearly all of the seismic energy release is distributed, along with the potential for associated surface faulting, in regions with high rates (2 or more cm/yr) of regional deformation or strain across the plate or subplate boundaries. Regions within the main plates are generally aseismic or weakly seismic, and account for a very small amount of the total seismic energy release.

37. Examination of the locations for historic examples of surface faulting listed by Bonilla[8,9] and Bonilla and Buchanan[1] indicates that nearly all of the events occurred along or near the major plate boundaries, or along tectonically conspicuous subplate boundaries. The slip types determined at the surface of nearly all events agree with their seismologically determined focal mechanisms (Smith and Sbar[62]),

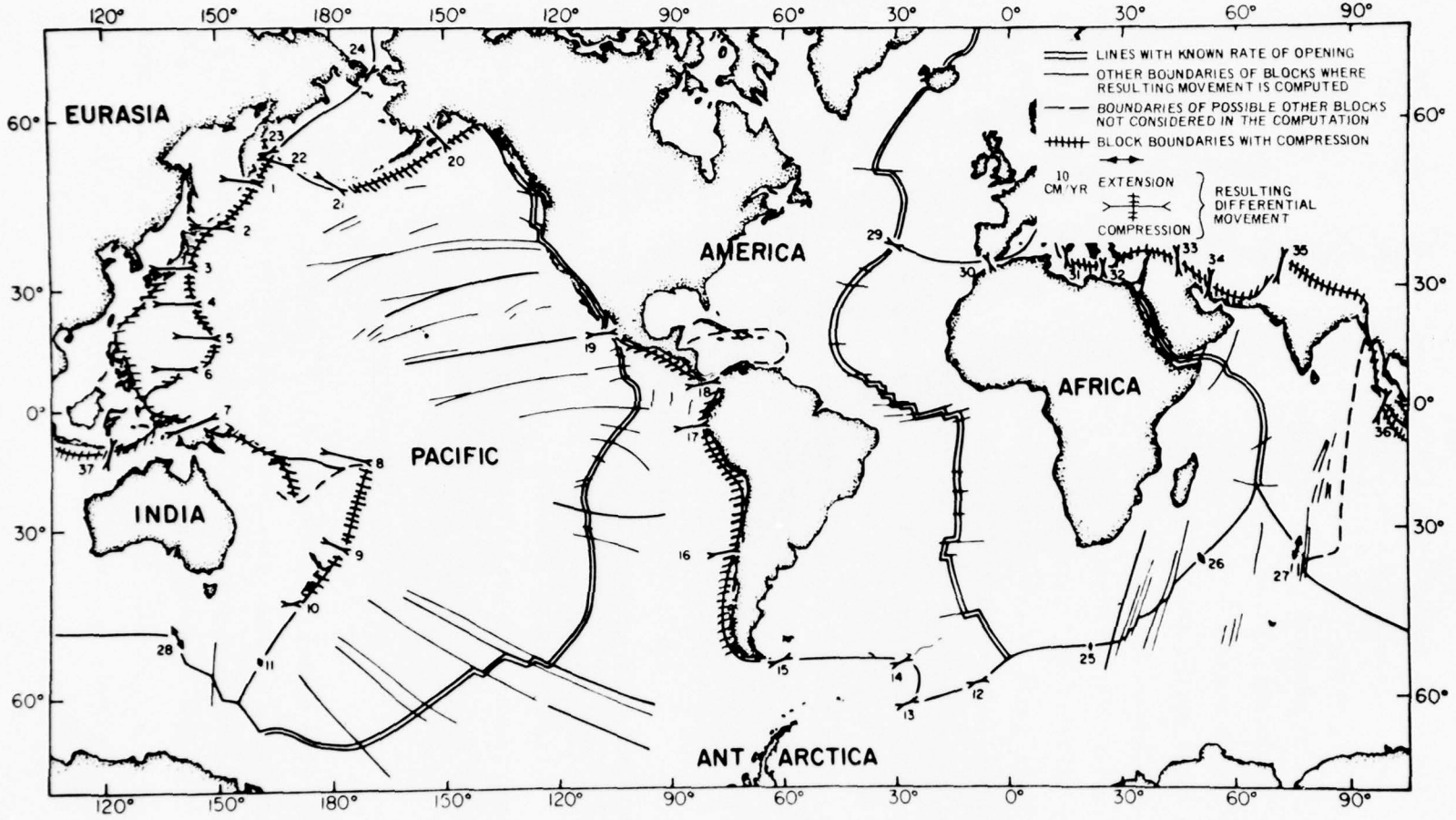


Figure 13. Major tectonic plates (after Le Pichon[59])

and with the known character of the tectonic zones to which they belong. The slip types accordingly are diagnostic of the major tectonic affinity of the faults, whether to megathrust zones, rift zones, cordillera mountain belts, or conjugate zones of complex, but genetically related, types of faulting. Subduction zones of major compressional tectonics are limited to regions adjoining oceanic trenches (Figure 13), and with maximum focal depths that become progressively deeper inland from the trench-continental shelf area. Major strike-slip faults, sometimes with great lengths, may be present in a variety of the plate and subplate boundary situations, including the lithosphere above Benioff or megathrust fault zones, where minor or local reverse-slip and normal-slip faults may also be present. The normal-slip faults are most abundant along major extensional fault systems of rises and rifts in both oceanic and continental regions, with subordinate conjugate strike-slip or local reverse-slip faults. The cordilleran mountain belts of many continental regions are marked by regions of both compressional and extensional faulting, often with patterns of strike-slip or oblique-slip conjugate faults.

38. The intraplate zones, with only a few exceptions (New Madrid earthquakes, 1811-1812; Charleston, South Carolina, 1886; etc.) are either aseismic, or are weakly active with earthquakes generally having magnitudes less than 5 or to 5.5. The methods discussed in this report may not be applicable to intraplate regions, unless active surface faults are present and their behavior can be shown to be similar to that of the faults near main plate boundaries.

Faults of Megathrust Zones

39. The megathrust, underthrust, or subduction zones were first recognized from seismic evidence by Benioff[33] for the great fault zone along the South America trench (Figure 13), a zone some 4500 km in length that dips eastward beneath the Andes and extends downward to depths of about 650 km. Other examples include parts of the Circum-Pacific Belt, including the subduction zones of New Zealand, Tonga

Trench, Japan, Kurile Islands, Kamchatka, the Aleutian arc, and the south coast of Central America. These zones represent regions of rapid (up to 13 cm/yr) collision of major earth plates and have many historic earthquakes between 8 and 8.5 magnitude. The surface expression of the megathrust fault zone is generally offshore from the continents at the ocean trenches or on the adjoining continental shelf. Focal mechanisms and focal depths show that such megathrusts vary in dip from about 10 deg for southern Alaska to about 30 deg for South America and about 60 deg in the Tonga region. The focal mechanisms for shallower earthquakes above such megathrust or Benioff fault zones may include strike-slip, dip-slip, as well as reverse-slip events.

40. The only megathrust zone that affects continental United States is in southern Alaska. There the fault plane extends from a discontinuous zone of surface faulting, mainly on offshore parts of the continental shelf, inland to depths of 170 km in the region beneath the Alaska Range. Although this subduction zone fault is reverse-slip, most of the active faults of Alaska (Brogan et al.[63]), including those that lie above this fault plane, are mainly strike-slip faults (Denali, Totschunda, and Kobuk-Alatna Hills faults), high-angle-of-dip reverse-slip faults (Hanning Bay and Patton Bay faults), or normal-slip faults (Donnelly Dome, Granite Mountain faults; the Johnstone-Icy Bay and Ragged Mountain faults), and the Castle Mountain normal-slip or oblique-slip fault. Some of these faults may change in character with change in strike; thus the Fairweather fault zone is a strike-slip fault where it is parallel to the northwestward direction of plate movement of the Pacific plate, but may change to a reverse-slip fault zone where it turns westward to parallel the megathrust belt and Aleutian Trench (Plafker,[64] and Kelleher and Savino[65]). The active faults of the hinterland may have the same aspects as the fold and fault mountain belts of the cordilleran-type regions and may have shallow-focus earthquakes and active faults.

41. Megathrust faults may have great earthquakes, as shown by the Alaska earthquake of 1964, with 8.5 magnitude, and probably develop a surface fault zone of irregular, complex surface expression and great

geodetic deformation (fault about 800 km in length, 150-250 km in width, and 9 deg in dip; Savage and Hastie,[66] and Plafker[64,67,68]). These great earthquakes have short recurrence intervals that can be determined by shoreline deformation (Plafker[64]), and the future great earthquakes of such zones will tend to fill gaps in historic activity (Kelleher and Savino[65]). The maximum earthquake for megathrust zones may exceed 8.5.

42. Estimation of design earthquakes for shallow-focus events from the many normal-slip, strike-slip, oblique-slip, and shorter reverse-slip faults above the megathrust zone should be undertaken independently of the megathrust fault. For example, design earthquakes of the main active faults in inland Alaska should be determined individually for each fault by the procedures outlined in this text, using fault length and maximum fault displacement relations to predict maximum possible earthquake magnitudes. The 1964 earthquake may not have relieved strain on these faults. The highest magnitude earthquake for faults of such fault types in megathrust regions appears to be about 8.3.

Faults of Rises and Rift Zones

43. Active oceanic rises, ridges, and rifts have dominantly extensional stress systems with faults that generally are parallel to the main structures. Conjugate oblique or cross-fracture systems and transform faults develop with oblique-slip or strike-slip faulting. The systems have continental extensions, or have analogous continental counterparts, as with the Basin and Range Province of western United States. The faults are dominantly high angle to moderate angle with a strong tendency for faults to dip at angles of about 60 deg. The faults form swarms, generally linear, but often arcuate near their terminations, with many types of grouped patterns that include step-faulted groupings, en echelon sets, orthogonal sets, rotated or tilted block mountains, and hinged faults that may reverse in the side that is up-faulted. Many of the fracture patterns resemble landslide structures and other gravity types of tensional failure. Strike-slip faults are relatively rare, or form generally short conjugate sets that trend at medium angles to the main tension and compression axes. The tension

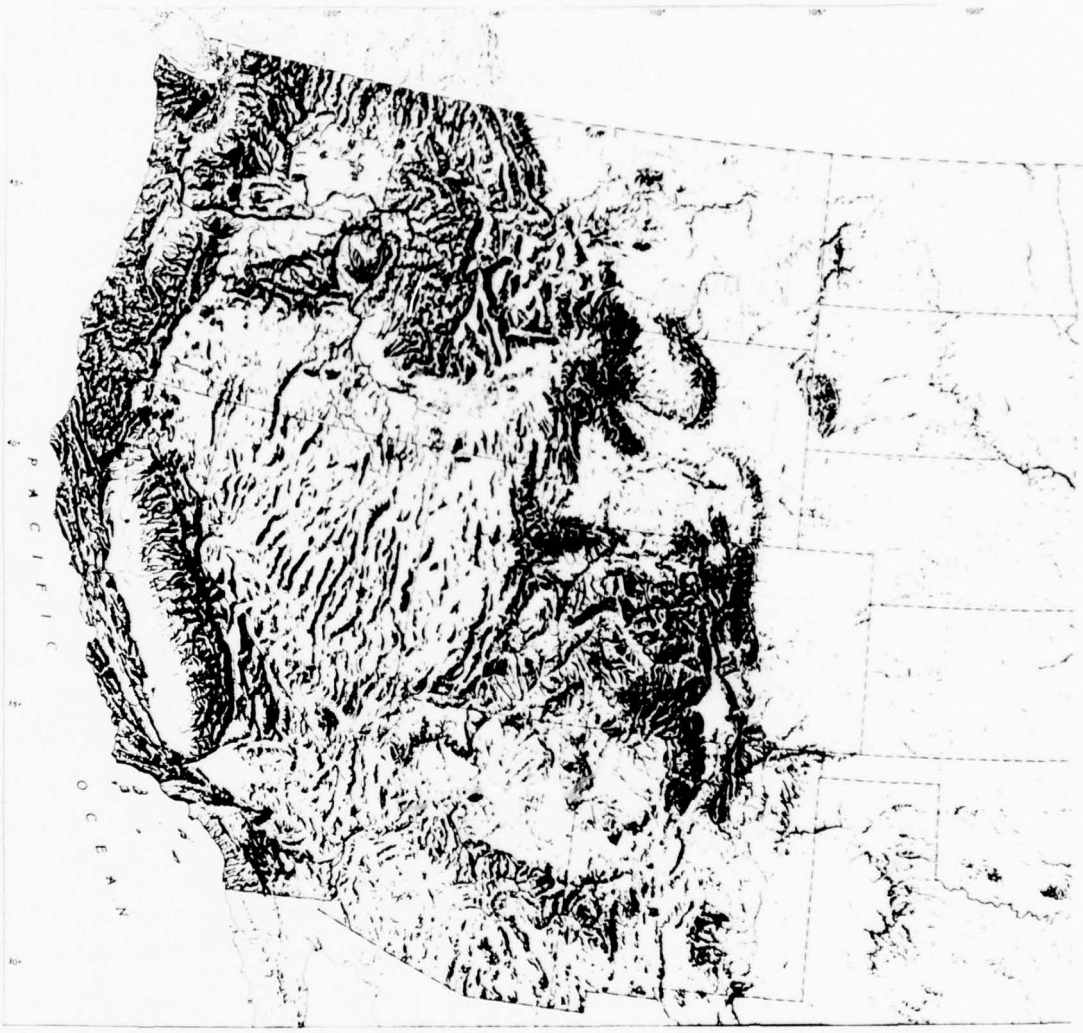
and compression axes can be defined by careful field geological studies of the faults, by focal mechanisms of earthquakes, geodetic changes before and after earthquakes, strain meter measurements, and orientation of predominant sets of igneous dikes. Examples include the faults of Iceland and African Rift systems. The similar Rio Grande Rift system and the Basin and Range Province of western United States are included in the section on faults of cordillera mountain zones.

44. The extensional fault systems and related transform faults have earthquake magnitudes of up to about 8 for the oceanic rift systems, and about 8 to 8.3 for continental zones as shown by the Owens Valley earthquake of 1872.

Faults of Cordillera Mountain Zones

45. Faults of many types are commonly developed in major orogenic belts or cordillera that are aligned along or near major plate or subplate boundaries. The faulting is commonly associated with folding, warping, and vertical ground movements. The faults, as in the complex conjugate fault patterns of central Japan, have block movements along conjugate sets of faults that involve strike-slip, reverse-slip, and local normal-slip types. The irregular mountainous terrain reflects variations in style of deformation that includes massive blocks of relatively rigid rocks, commonly granitic in composition, that may be uplifted, tilted, or downdropped with little internal seismic activity or faulting. Examples of this type of terrain include the Sierra Nevada-Great Valley rectangular block in California (see Figure 14), and some of the smaller blocks in the region north of Osaka, Japan (Figure 15), as reported by Hŭzita et al.[69]

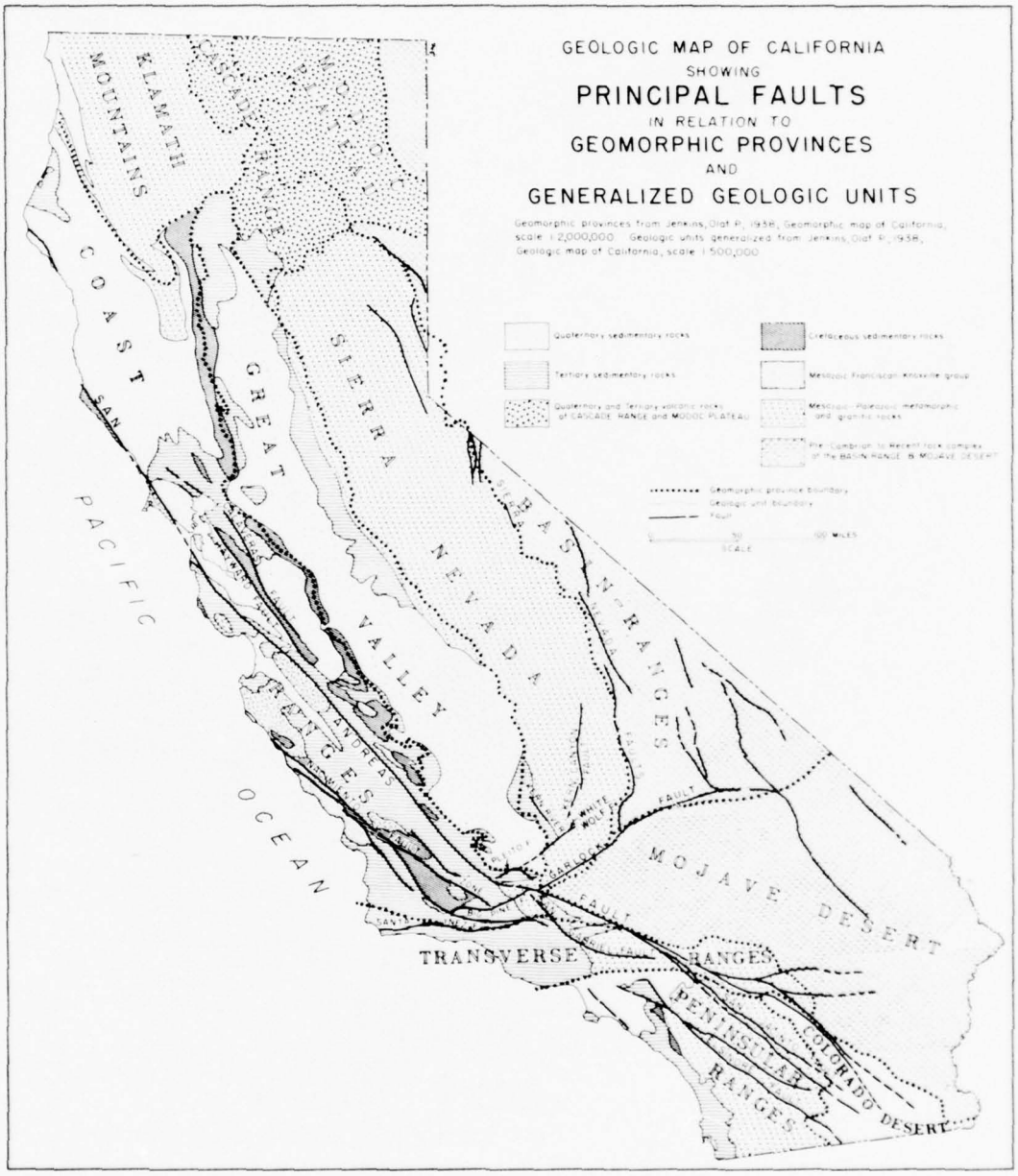
46. Faults generally include conjugate strike-slip sets like the northwest-trending left-slip faults and northeast-trending right-slip faults of Japan, or the northwest-trending right-slip faults and northeasterly trending left-slip faults of the Transverse Ranges of California (Figure 14b). The main tectonic control of the many subparallel mountain ranges or cordillera may be compressional as with the mountain



a. Shaded relief map from the U. S. National Atlas (1970). See Figure 14b for location of the Sierra Nevada-Great Valley-Klamath Mountain area

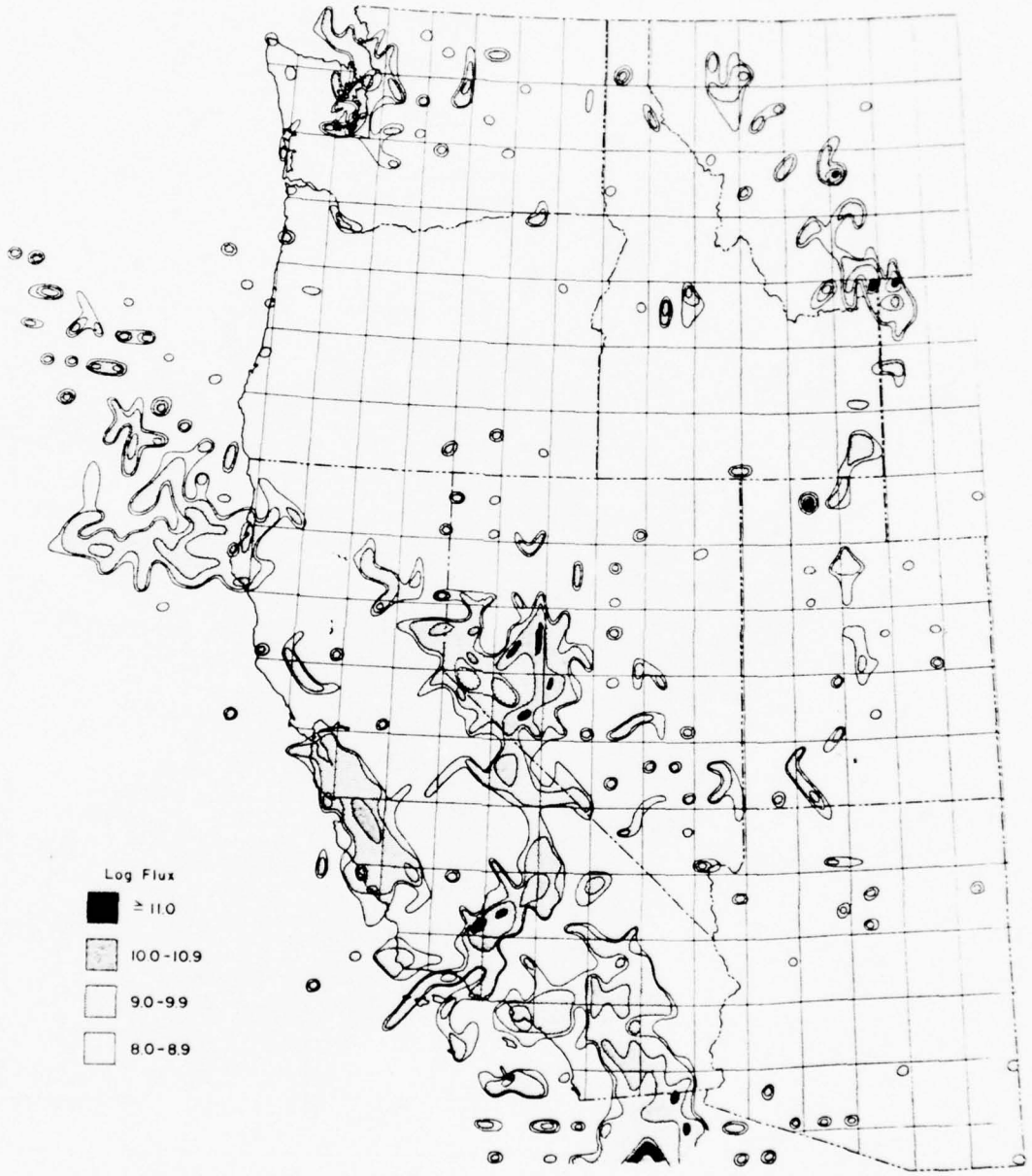
Figure 14. The Sierra Nevada-Great Valley-Klamath Mountains region of low regional seismicity and the conjugate right-slip faults of northwest trend and left-slip faults of east-west to northeast trend (sheet 1 of 3)

BEST AVAILABLE COPY



b. Geologic map of California (after Oakeshott[70]). Note the conjugate northeast-trending Garlock, White Wolf, Big Pine, and Santa Ynez left-slip faults, and the northwest-trending San Andreas, Hayward, Calaveras, San Jacinto, and Elsinore right-slip fault systems

Figure 14 (sheet 2 of 3)



c. Earthquake energy (tectonic flux) map of southwestern United States for 1932-1961 (from Ryall et al.[71])

Figure 14 (sheet 3 of 3)

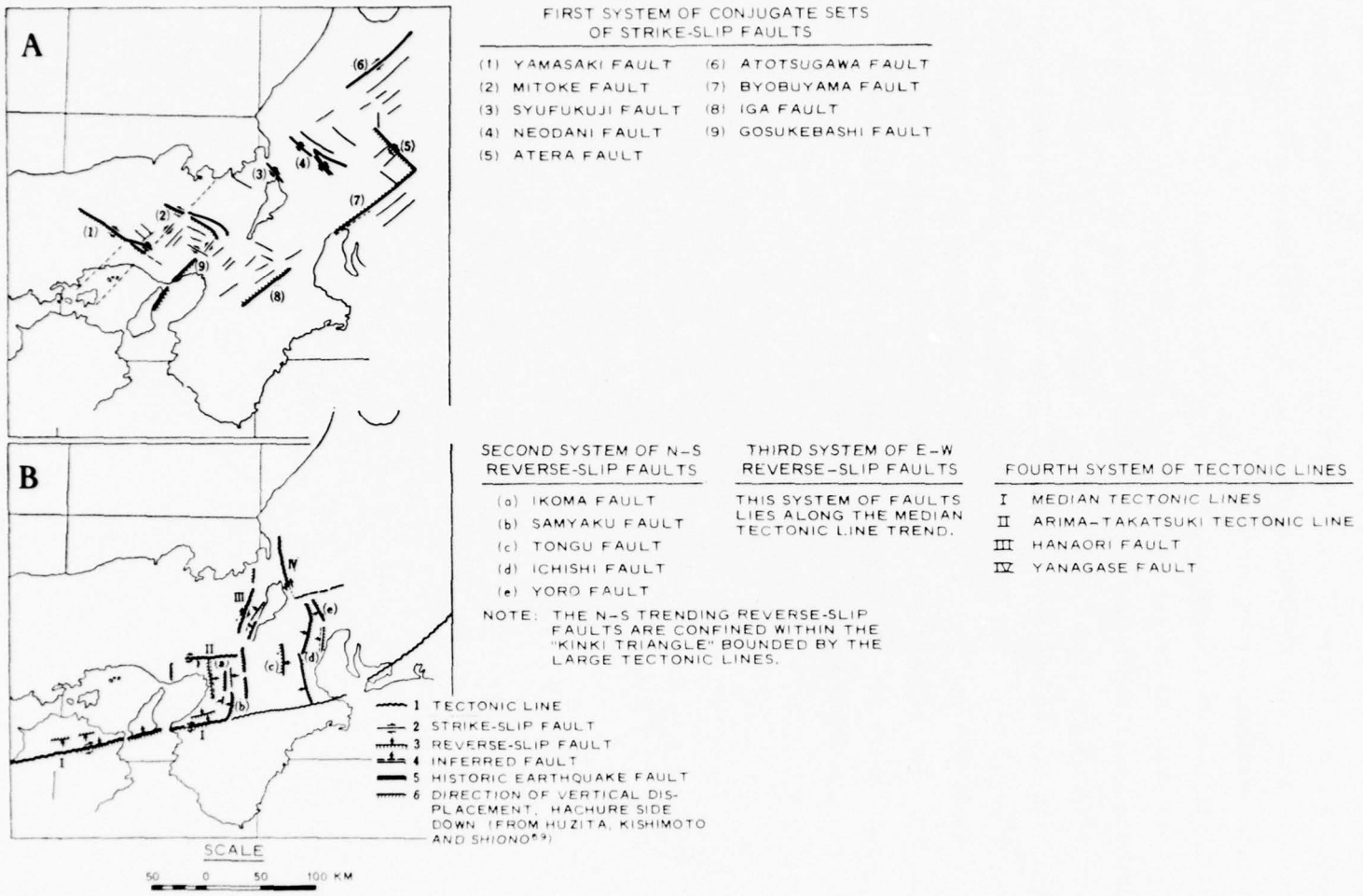


Figure 15. Four systems of faults in southwest Japan (Huzita et al.[69])

blocks of central Japan, with combinations of mainly reverse-slip and conjugate sets of strike-slip faults (central Japan), or be extensional with combinations with dominant normal-slip and conjugate sets of strike-slip faults (western United States).

47. The maximum magnitude of earthquakes of cordillera mountain zones varies with the length of the fault zones affected and the proportion of a given fault that is activated by a given event. The Neodani reverse-oblique-slip fault of Japan (fault 4 in Figure 15A) was ruptured from end to end during the 1891 Nobi or Mino Owari earthquake of about 8 magnitude. The highest magnitude for long normal-slip fault zones is about 8.3 or 8.4, with most major earthquakes falling between 7.0 and 8.0. The highest strike-slip earthquake magnitudes on the longer fault zones are about 8.3 as in the 1857 and 1906 events on the San Andreas fault system, or 8.7 as for the Mongolia earthquake of July 23, 1905.

PART IV: METHODS OF DETERMINING FAULT ACTIVITY OR NONACTIVITY

Introduction

48. To classify faults on the basis of potential activity is the goal of many fault studies, and is the first step in applying fault length and displacement to earthquake magnitude design relations. The determination of whether or not a given fault is active depends on three main kinds of criteria--historic, geologic, and seismologic (Table 7).

Table 7

Criteria Used for Recognition of Active Faults

(Modified from Cluff et al.[72])

General Criteria	
Geologic	Active fault zone indicated by such young geomorphic features as: Fault scarps, triangular facets, fault scarplets, fault rifts, fault slice ridges, shutter ridges, offset streams, enclosed depressions, sags, sag ponds and graben valleys, fault troughs, sidehill ridges, fault saddles, and such ground features as: Open fissures, mole tracks and furrows, rejuvenated streams, terrace relationships, folding or warping of young deposits, and ramps in young alluvium, en echelon faults in alluvium, and fault paths on young surfaces with groundwater barriers marked by spring alignments and vegetation contrasts. Usually combinations of above features are present. Erosional landforms are associated with many active faults but may not be diagnostic. Stratigraphic offset of late quaternary deposits by faults is indicative of activity.
Historic	Historical manuscripts, news or book accounts, personal diaries, verbal communications, and legends may describe past earthquakes, surface faulting, landsliding, fissuring, or other phenomena that may be associated with past earthquakes. Usually there are several historical accounts available. Indications of fault creep may be shown by offset fences, highways, buildings, etc., or by geodetic movements concentrated along a fault.
Seismologic	Earthquake epicentral distributions, based on instrumental methods, may delineate active faults. Lack of earthquakes does not define a fault as inactive.

The available data for each of the main criteria are generally incomplete. Even with extensive data, additional studies may be required to resolve questions of activity for specific faults. Cluff et al.[72] divided activity into four main categories: active, potentially active, activity uncertain (with subdivisions of tentatively active and tentatively inactive), and inactive (Table 8). They list additional studies needed for each of the fault activity types.

49. During the past two centuries, hundreds of faults have had surface displacements; of these, only about 150 have been noted by geologists, with less than 50 noted for North America (Bonilla[8,9]). The remoteness of many cases of surface faulting, the small surface displacement, and the short length of many surface faults (e.g. 1975 Mojave and 1966 Parkfield-Cholame earthquakes in California) make them inconspicuous and many cases of surface faulting have not been recognized or described. Accordingly, most active faults, even in densely populated and seismic parts of the U. S., still require special studies in order to provide adequate data on activity or nonactivity, rate of activity, type of fault, recurrence interval, and size of design earthquakes for future activity.

Historical Criteria for Activity

50. Historical data relating to past displacements and earthquake activity have only recently become the subject of intensive study and evaluation for design earthquakes. The source data are scattered and uncollated for most regions and most faults. Thorough analysis of historical data generally provides earthquake history and intensities for the preseismologic instrumentation period, and for determining whether there has been historic surface faulting during earthquake or creep episodes. Earthquake magnitudes can be determined from intensities. Some sources of information are summarized in Table 7. Analysis of geodetic and other leveling and triangular surveys is now providing a growing record of preearthquake, earthquake, and postearthquake ground movements related to tectonic deformation.

Table 8

Classification of Fault Activity Based on Available Data (Modified from Cluff et al.[72])

Activity Classification and Definition	Criteria			Studies to Further Define Activity
	Historic	Geologic	Seismologic	
Active - a tectonic fault with a history of strong earthquakes or surface faulting, or a fault with a short recurrence interval relative to the life of the planned project. The recurrence interval used to define activity rate may vary according to the consequence of activity	(1) Surface faulting and associated strong earthquakes (2) Tectonic fault creep, or geodetic evidence of fault displacement or deformation	(1) Geologically young deposits cut by fault (2) Youthful geomorphological features that are characteristic of geologically young displacements along the fault trace (3) Groundwater barriers in geologically young or unconsolidated deposits	Earthquake epicenters can be assigned with confidence to the fault	Additional investigation and exploration are needed to define: (1) Exact location of individual fault traces (2) Recurrence interval (3) Probable magnitude of future events (4) Type of surface deformation associated with the surface faulting (5) Probable epicenter of future earthquakes
Potentially Active - a tectonic fault without historic surface offset, but with a recurrence interval that could be sufficiently short to be significant to the particular project	No reliable report of historic surface faulting	(1) Geomorphic features that are characteristic of active faults, but with subdued, eroded, and discontinuous form (2) Faults not known to cut or displace youngest alluvial deposits, but offset older quaternary deposits (3) Water barriers in older deposits (4) Geological setting in which the geometry in relation to active or potentially active faults suggests similar degree of activity	Alignment of some earthquake epicenters along or near fault but assigned locations have low degree of confidence in location	Additional investigations are needed to resolve: (1) Time since previous activity (2) Recurrence interval (3) Location of possible fault traces. Completion of classification is less important if fault does not cross the project site and a known active fault that is capable of more frequent or higher magnitude earthquakes is closer to the site
Activity Uncertain - a fault with insufficient evidence to define past activity or recurrence interval. The following classifications can be used until the results of additional studies provide definitive evidence	Available information is insufficient to provide criteria that are sufficiently definitive to establish fault activity. This lack of information may be due to the inactivity of the fault or to lack of investigations needed to provide definitive criteria			This classification indicates that additional studies are necessary if the fault is found to be critical to the project. The importance of a fault with this classification depends upon the type of structure involved, the location of the fault in respect to the structure, and the consequences of movement

(Continued)

Table 8 (Concluded)

Activity Classification and Definition	Criteria			Studies to Further Define Activity
	Historic	Geologic	Seismologic	
Tentatively Active - predominant evidence suggests that the fault may be active even though its recurrence interval is very long or poorly defined	Available information suggests evidence of fault activity, but evidence is not definitive			
Tentatively Inactive - predominant evidence suggests that fault is not active	Available information suggests evidence of fault inactivity, but evidence is not definitive			
Inactive - A fault along which it can be demonstrated that surface faulting has not occurred in the recent past, and that the requirement interval is long enough not to be of significance to the particular project	No historic activity	Geomorphic features characteristic of active fault zones are not present and geological evidence is available to indicate that the fault has not moved in the recent past and recurrence is not likely during a time period considered significant to the site. Should indicate age of last movement: Holocene, Pleistocene, Quaternary, Tertiary, etc.	Not recognized as a source of earthquakes	No additional investigations are necessary to define activity

Indirect methods of detecting ground deformation can also be obtained by precise remeasurement of gravity stations.

51. The importance of careful historical studies is shown by the fact that in about 10 cases out of 40, historical surface faulting in western North America was recognized as the result of recent historical studies or fault evaluations. Such studies in the future are likely to further increase the number of known examples of surface faulting.

Seismologic Methods

52. Detailed study of earthquake epicentral distribution of many fault zones can indicate the activity, continuity, location, dip and strike, depth, and focal mechanism of the fault. The historic seismic activity on the San Andreas, Sargent, and Hayward fault zones (as shown in Figures 28 and 29 in Krinitzsky[29]), mainly defined by microearthquakes, clearly delineates many of the active faults in central California. Many other active faults in the same region show no microearthquake activity, and some of the microearthquakes do not appear to be related to known faults of this well-studied and well-instrumented region (U. S. Geological Survey, 1975). The aftershocks of the Parkfield earthquake zone of 1966 (Eaton et al.[38]) show a well-defined, nearly vertical segment of the San Andreas fault (Figure 16). Other parts of the San Andreas fault system have more diffuse branching, or en echelon patterns of surface faults and epicenters, as is shown on the map of the Borrego Mountain earthquakes (Figure 17). The correlation of epicenters to surface traces of faults is best for aftershock activity and for high-angle, strike-slip faults, and is more difficult in regions of reverse-slip and normal-slip faults with lower dips and more diffuse branching. Generally the aftershocks of a large earthquake clearly define the main faults. Before the main earthquake, seismicity is more dispersed and may not correlate specifically with the faults that generate the later large earthquake.

53. The main value of seismologic activity is to indicate regions in which a geological search for active faults should be conducted, or to define seismic gaps.

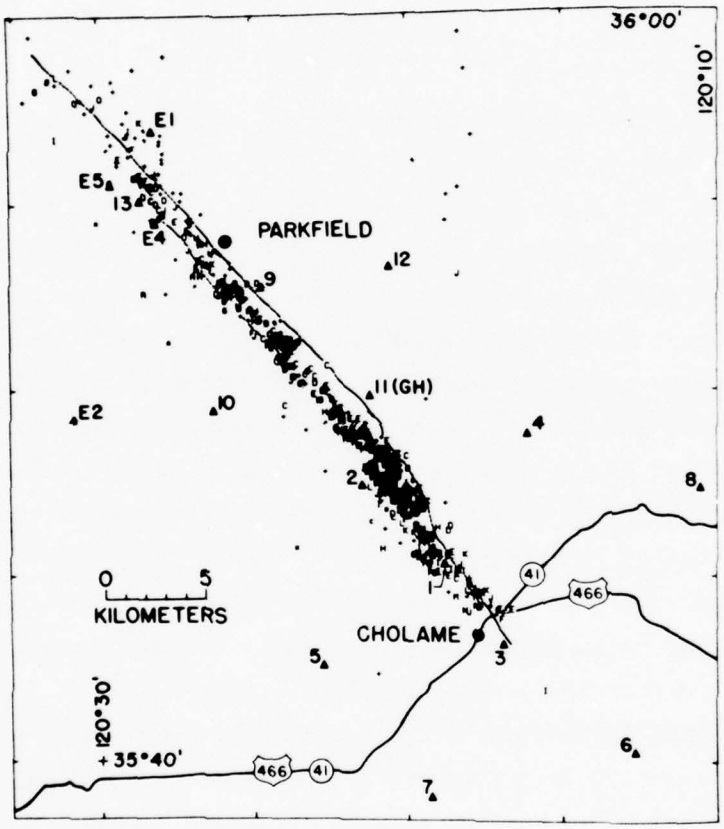


Figure 16. Aftershocks and surface faulting from the Parkfield-Cholame earthquake zone of 1966 (from Eaton et al.[38])

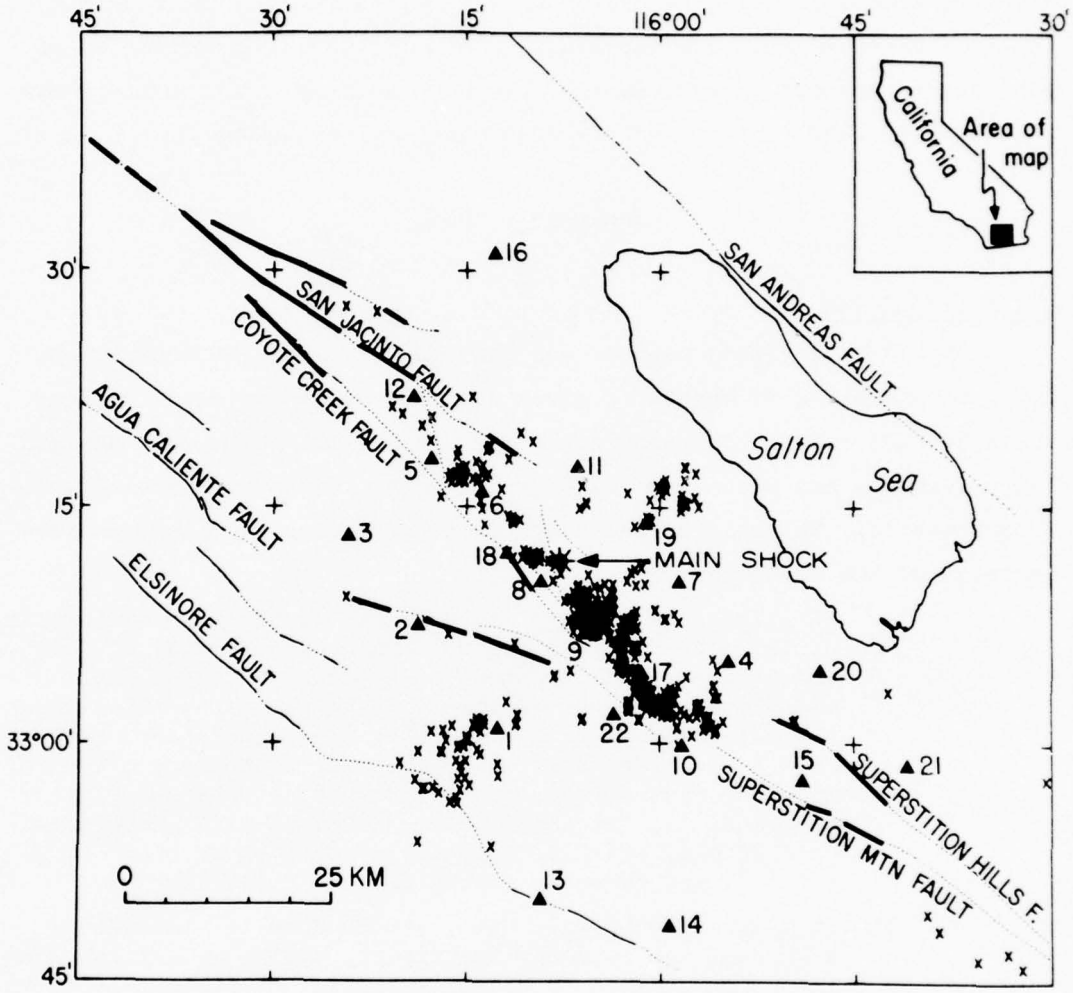


Figure 17. Map of the Borrego Mountain region showing location of seismographic stations (triangles), epicenter of main shock, aftershock epicenters (crosses), and active faults. Faults are solid where there is evidence of recent or historic surface breakage, dotted where evidence is less conclusive. Note that the dense aftershocks indicate that there is continuity between the San Jacinto and Coyote Creek faults to the north and the Superstition Mountain fault to the south. Several branching faults characterize this section of the San Jacinto fault. Compare the distributed pattern of aftershocks relative to the Parkfield-Cholame aftershocks of 1966 (Figure 16). Both aftershock sequences were recorded by the same portable field seismographs (from Hamilton[73])

54. Aftershocks in regions of historic surface faulting define the approximate limits of the zone of surface faulting. The size and shape of these regions are especially useful in defining continuity of subsurface tectonism across gaps of surface faulting, or to extrapolate the activity into regions that are inaccessible to observation.

Geologic Methods

General comments

55. Four geologic methods can provide definitive answers to the important question of whether a given fault is active or dead. All of these methods require recognition of disturbance within or on young geologic features and place increased importance on methods of dating Quaternary events. The main criteria and methods (Tables 2-7) include recognition of the following:

a. Stratigraphic offset. This method is the most definitive of the methods of evaluation and requires study of soil and stratigraphic sections to determine whether fault offsets are present or absent in young units. The search may be conducted in stream cuts, landslide scars, soil-free areas, road cuts, highway cuts, tunnel and other man-made excavations, special trenching programs (Taylor and Cluff[74]), and in direct measurement with geophysical profiling by seismic, magnetic, electric, or other methods, and borehole coring or electrical logging.

b. Structural features. The tectonic shearing associated with faulting commonly brecciates, mills, or grinds rocks into fine-grained or clayey material; or tilts, warps, or folds surrounding materials. Trenches or other exposures may reveal open fissures, clay- or sand-filled veinlets, caliche-cemented seams, or other evidence of systematic fracturing. Adjoining materials may be bent or tilted into anomalous attitudes by tectonic drag along the fault zone.

c. Geomorphic features characteristic of active surface faults. The identification, delineation, and evaluation of geomorphic features associated with active faults is the single most effective method of recognizing active faults, establishing their length, estimating their maximum earthquake fault displacements, and determining the type of faulting to be expected with future recurrence of activity. Examples of historic surface faulting

include a range in earthquake magnitude of 3.4 to about 8.5, displacements from about 1 cm to 10 to 14 m, lengths of up to about 800 to 1000 km, and development of both small-scale and large-scale topographic features. The landforms developed along the surface traces include extensive fault scarps for all fault types, as well as geomorphic forms that are restricted to or are diagnostic of particular fault types. The rupturing of basement and surficial materials results in planes or regions of weakness which over geologic time cause repetitive displacements to follow exactly or almost exactly the same surface trace for sequences of many events; commonly these have similar amounts of displacement. This repetitive character of surface displacement provides the basis for using length of fault and displacement methods of predicting design events for future surface faulting at sites on active faults, and for the magnitude of design earthquakes to be generated along the faults.

Repetitive displacements on active faults

56. Detailed studies of active faults provide many examples of repetition of offsets with similar amounts, rates, and directions of displacement in series of fault events (Clark et al.,[75] Dickinson and Grantz,[76] Slemmons,[77] Sugimura and Matsuda,[78] and Wallace[30]). The repetitive character of faulting during geologic time leads to the development of larger scale topographic features and stratigraphic offsets that normally permit the identification, characterization, and delineation of active faults, even prior to historic or future reactivation. The repetitive events may either result in features which have similar length of rupture, amount of displacement, and slip-type of movement, or these may vary according to the size of earthquake from event to event. Anomalous events with reversal of direction or type of slip have been noted in a few earthquake areas, but form a very minor part of the tectonic record. Specific examples from different types of fault zones follow.

57. Strike-slip fault zones. Dickinson and Grantz[76] show that for the San Andreas fault system, the rates of deformation have been relatively uniform for long periods of geologic time (Figure 18). Historical data for rate of deformation include surface fault geologic data, geodetic changes, and seismologic studies. The historic and

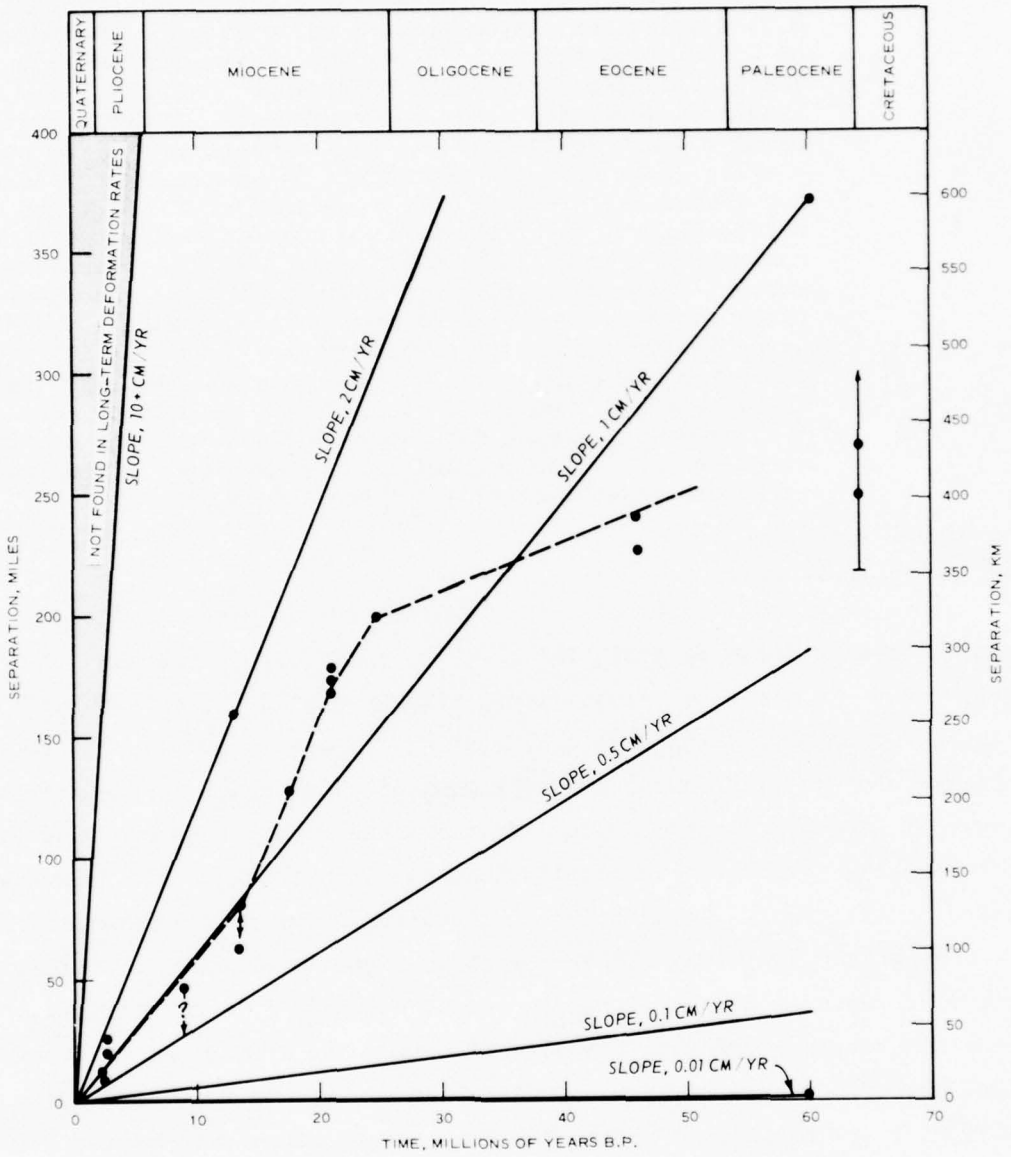


Figure 18. Estimated average apparent slip rate along the San Andreas fault zone in California (after Dickinson and Grantz[76]). Note the relatively uniform rate during the last 25,000,000 years

geologic rates for the San Andreas fault are in good agreement and indicate that the deformation was at an average rate of about 1 to 2 cm/yr from the present to about 20 or 30 million years B.P. and was about 0.7 cm/yr during the early Tertiary.

58. Clark et al[75] studied one branch of the San Andreas fault system, the Coyote Creek fault zone of the Borrego Mountain earthquake of 1968. Trenching and radiometric dating (Figure 19) show a series of vertical separations of sedimentary beds that indicate three periods of surface faulting and related drag: a period from the present to about 860 B.P., with 56-cm vertical separation and a recurrence interval for 1968 size earthquakes of 130-190 years (160-year average); a period from the present to about 1230 B.P., with 74-cm vertical separation, and a recurrence interval of about 205 years; and a period to about 3080 B.P., with 170-cm vertical separation, with a recurrence interval of about 205 years. The 1968 earthquake yielded a total vertical deformation of about 10 cm, with about 5 cm each of drag and fault slip. The field relations indicate a ratio of vertical separation to horizontal separation of about one to three or four. This suggests a Holocene fault slip rate averaging about 0.05 cm/yr vertical slip component and 0.13 to 0.046 cm/yr horizontal slip. This rate is similar to the extension of Coyote Creek fault to the north, and with the San Jacinto fault zone where the estimated average rate of deformation is about 0.25 cm/yr.

59. Conjugate reverse-slip and strike-slip fault zones. The central part of Japan provides excellent examples of long-term repetitive faulting associated with related folding and tilting of stratigraphic sections, and block faulting. The faults are conjugate faults where compressive forces developed strike-slip, reverse-slip, and oblique-slip faults. Geomorphic evidence of recurrence is clearly demonstrated by episodic displacements along the Atera fault (Sugimura and Matsuda,[78] and Sugimura[79]) with cumulative effects on a series of river terraces that vary in age from the present to 28,000 years B.P. (see Figure 20 and Table 9). The combination of strike-slip and vertical-slip components is illustrated in the block diagram that shows the maximum offset of 140 m for the 28,000-year-old terrace. The fault shows longer term topographic effects of recurrence with major drainage lines having about 8 km of horizontal separation, and a pre-Quaternary mature erosion surface with about 800 m of vertical offset. These relations indicate a 1,000,000-year date for the inception of the fault, a date that agrees

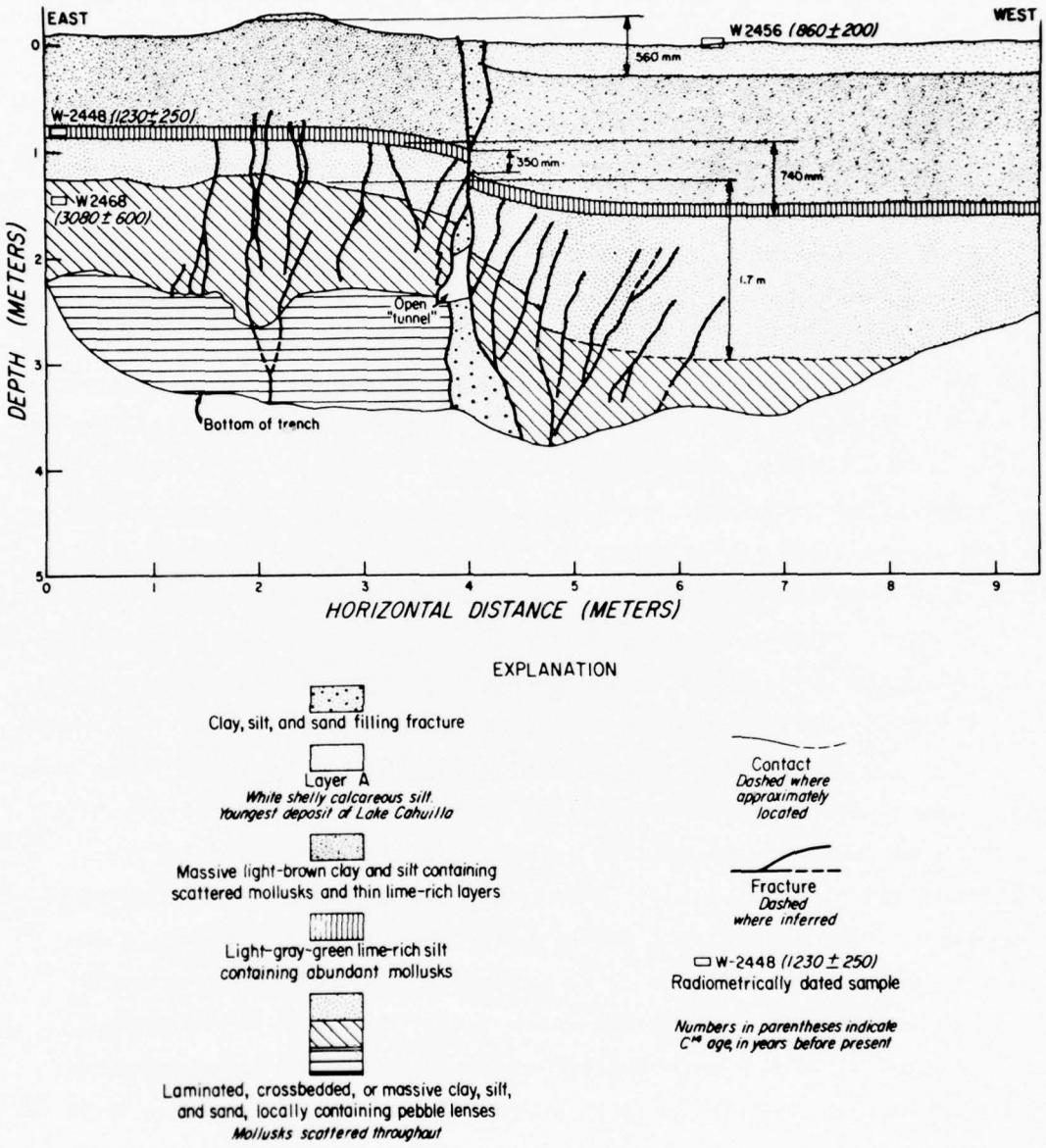


Figure 19. South wall of trench 1 showing progressively greater offset of older strata and bending of strata (drag) across the branching break of the 1968 event. All deposits appear to be lacustrine, although some are possibly fluvial or eolian. Some deposits east of the break have been removed by erosion. Surface water that entered this fracture in July 1968 eroded the tunnel and caused surface collapse along the break within 30 m of the trench. Based on sketches by M. M. Clark and R. V. Sharp (from Clark et al.[75])

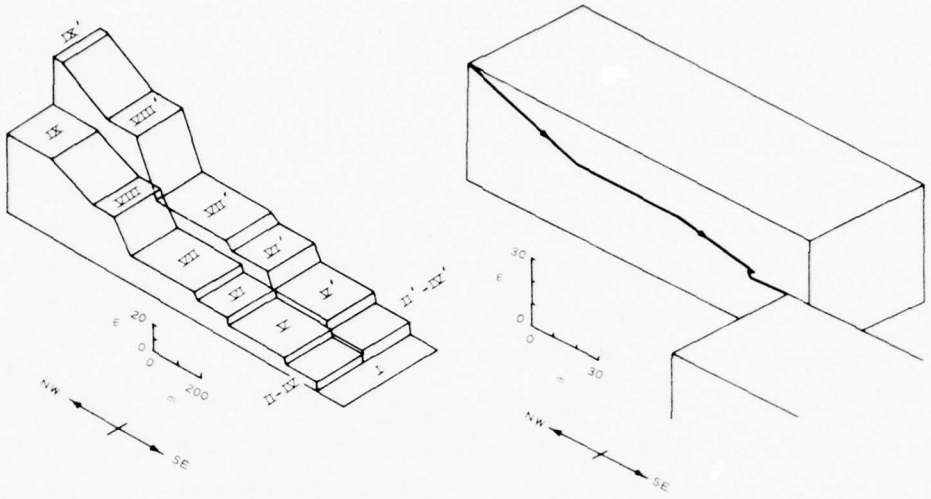


Figure 20. Block diagrams of the Atera fault, Japan, offsets of geomorphic features, river terraces, and terrace faces. The fault is a left-oblique-slip fault that offsets a series of terraces varying from youngest, I, to oldest, IX. Terrace VIII was dated at 28,000 B.P. by C^{14} radiometric dating. Primes indicate the upthrown side of fault. The cumulative horizontal offset is 140 m, the average horizontal slip rate is 0.5 cm/yr. The cumulative vertical slip is 27.5 m for an average vertical slip rate of 0.1 cm/yr (from Sugimura and Matsuda,[78] and Sugimura[79])

Table 9

Elements of Displacement Vectors of the Atera Fault, Japan

Name of Terrace	No. of Terrace	Vertical Displacement m	Horizontal Displacement m
Present floodplain	I	0	0
Saihozi	II	0.3 ± 0.1	17.0 ± 0.5
	III	1.75 ± 0.3	17.0 ± 0.5
	IV	2.45 ± 0.6	17.5 ± 0.8
Sakasitasinden	V	3.4 ± 0.6	14.0 ± 4.0
Sakasita	VI	10.0 ± 1.0	50.0 ± 7.0
	VII	10.0 ± 2.0	90.0 ± 20.0
Takabe	VIII	27.5 ± 2.0	140.0 ± 35.0
Syogenzi	IX	32.6 ± 5.0	Unknown

with an identical age determined for the regional initiation in central Honshu of subsidence, uplift, tilting folding of a synclinorium, and activation of other faults in the conjugate fault system.

60. Normal-slip fault zones. Repetitive faulting has also been shown for the Basin and Range Province (Slemmons[77]) and by an unpublished study of basin-fill sediments in the Railroad Valley graben of central Nevada by Robert Horton (personal communication, 1976). Horton analyzed drill hole data from three deep bore holes and found about 80 tilted stratigraphic units within the valley fill. The units varied in age up to about 30,000,000 years, although the tilting within the sequence may be much younger than this date. Horton found that there were episodes of tilting in a great variety of directions, so that the dip and strike of each horizon demonstrate a sequence of tilts that are similar to the fluttering down of a leaf through the air. The data suggest that events of faulting follow a pattern of similar tilt directions through several events and then a change into a new episode of different tilt direction. The repetitive effects and youthful nature of faulting in the Basin and Range region permit identification of active faults of varying degree or age of activity.

Geomorphic features of active faults

61. The geomorphic features of active faults generally express the rate of activity, the recency of last offset, and the long-term slip direction. The faults have the main, older and subdued major landforms, commonly accentuated or resharpened by each new faulting event and with a pattern of fracturing and width of fault zone that is partly a function of the fault-dip and the fault-slip type as shown in Figure 3. The recognition and interpretation of the landforms is the single most important part of the search for active faults, and the determination of total fault length and maximum fault displacement. The lack of detailed descriptions has led to the preparation of the detailed description, classification, and listing of typical examples of Appendix A.

Geodetic Methods

62. Recognition of activity along many faults is possible by

repeated geodetic surveys, either triangulation or leveling, or both (U. S. Department of Commerce,[39] and current literature cited in Thatcher[37]). Geodetic methods are capable of detecting and measuring tectonic strain of regions or across active faults. Reduction of the geodetic data permits determination of rates and directions of ground movement. The data provide another measure of fault displacement, either during earthquakes or by creeping displacements without earthquake activity, and can assist in identifying the position of branches or focus on the zone of current movement within complex zones of faulting. Precursors of surface faulting are noted in changes in rate and direction of geodetic change prior to faulting events, and periods of postearthquake creep and readjustment have also been noted (Thatcher[40]).

Trenching Methods

63. Trenching of fault zones for evidence of activity is a relatively new approach to recognition of active faults and is a technique for obtaining improved exposures of structural stratigraphic relations at selected places along the fault. Cultural and normal soil creep may remove or conceal surface indications of geologically recent offsets of the surface. In addition, faulting at a few metres depth may be expressed as a monoclinal flexure of the soil horizons, but show fault offsets of deeper layers. The trenching methods require special cleaning and dressing of the faces of the trench to reveal subtle discontinuities within unconsolidated stratigraphic units and soil (Taylor and Cluff[74]).

64. Trenches through fault zones may show the following kinds of evidence of fault displacement:

a. Offset of soils or Quaternary deposits.

b. Gouge, clay, caliche veinlets, concentration of rootlets, or staining of fissures.

c. Open fissures or pockets along fault.

d. Monoclinal flexure of young sediments.

e. Variation in water table at fault.

f. Hot spring, warm spring, or hydrothermal alteration of Quaternary deposits or soil.

g. Lithologic variation across fault.

h. Variation in thickness of stratigraphic units or soil across fault.

Absolute and Relative Rates of Fault Activity

65. Two methods of reporting rate of fault activity are in general use:

a. Average deformation rate (cm/yr) across an active fault or tectonic province as measured from seismic activity, historic or geologic displacements, and geodetic change.

b. Recurrence interval or return period between earthquake displacements.

66. The deformation rate can be expressed either quantitatively as shown in Figure 2, or in qualitative terms. If the average deformation rate is known, it is possible to infer the time interval between events of given magnitude by using the empirically derived relations between magnitude and displacement, as given in Part II of this report. Working with a specific fault to be evaluated, once the average rate of deformation across the fault is determined and the maximum magnitude earthquake is determined from length of fault or maximum displacement relations as discussed in Parts II and XI of this report, it is then possible to determine the recurrence interval for the fault for events of the assumed magnitude. Comparison of these data with the Holocene, 35,000-year, and 500,000-year dates determines the rate of activity relative to the Holocene and Nuclear Regulatory Commission scales.

67. The range in rate of activity between the six major plates of the earth as given in Figure 13 by Le Pichon[59] is between 1.4 and 11 cm/yr. For compressional interaction of these plates in subduction zones, the rates vary up to 13 cm/yr for active island arcs and ocean trenches (southern coastal Alaska, western Central America, and the western coast of South America).

68. The major faults or master faults of regions at the

boundaries between major earth plates generally release most of the world's earthquake energy (Isacks et al.[58] and Le Pichon[59]). The earthquake magnitudes appear to be related to the rates of differential movement, length of the structure, and thickness of the lithosphere. Isacks et al.[58] and Le Pichon[59] conclude that the island arc and similar compressive structures account for more than 90% of the world's seismic energy for shallow earthquakes and nearly all of the energy for deep earthquakes with rates of about 2 cm/yr and higher. Extensional or rift system zones of the ocean basins and continental areas including western United States and southeastern Alaska account for less than 9% of the earthquakes and less than 6% of the seismic energy. The largest known earthquake of the arclike structures is 8.9 in earthquake magnitude, and the largest event for ridge systems is 8.4. Nearly all of the events over 7 magnitude from ridge systems are along major transform faults. Tear faults, transform faults, and other faults may divide major plate boundaries into subprovinces. Since these faults are generally shorter than the faults at the main plate boundaries, the maximum magnitude earthquakes tend to be lower and may have characteristic, local maximums that limit each zone.

69. Rates of about 5 to 8 cm/yr are probable across the major transform faults zone of the Gulf of California, the San Andreas fault system near the north end of the Gulf of California, or the combined San Andreas fault system and Basin and Range Province opposite Northern California. Where a single fault zone is involved with such movements, the time interval between large earthquakes is short, measured in tens or hundreds of years. Where dispersed on many faults, as in the Basin and Range Province of the western United States, the faults may have shorter lengths, lower rates of deformation, and lower magnitude earthquakes.

Classification of Rates of Displacement

70. No standard or widely accepted classifications for rate of fault activity have been adopted or established. The United States Atomic Energy Commission[23] has defined a capable fault (active for

purposes of reactor siting and design) as one that has had one displacement in the past 35,000 years, or movement during the past 500,000 years. These criteria do not directly correlate with displacement rates. The International Atomic Energy Agency[22] has defined those faults with geomorphic evidence of activity and a rate of 1 m/1000 years (0.1 cm/yr) as having a high rate of activity. Matsuda[57] has divided the fault deformation rates into several types--A, B, C, and D--as shown in Figure 2.

71. An indication of the approximate limit for the definition of active faults according to the U. S. Nuclear Regulatory Commission (1973) definition of capable faults is as follows. Their fault definition includes those faults that have been subjected to displacement during the past 35,000 years, or recurring displacements during the past 500,000 years. Since most earthquakes of over 7 magnitude develop surface faulting with an average offset of about 2 m and subsurface exploration methods of detecting fault offset may be sensitive to recognition of offsets of about 1 m, this would imply a rate of activity of about 0.003 to 0.006 cm/yr. The writer has noted that faults in the arid Basin and Range Province with 6 m of offset in 50,000 years show well-developed geomorphic evidence of activity. This gives a boundary between active and practically inactive at about 0.003 to 0.006 cm/yr, a rate of activity that is about 3 orders of magnitude lower than that of the San Andreas fault system.

72. The provisional classification given in Figure 2 defines deformation rates across active faults of 1 cm/yr or more as very high; this corresponds to faults of major tectonic plates and master fault zones, where recurrence intervals between magnitude 7 events at a point on a given fault may be measured in tens or few hundreds of years, and the recurrence interval for the entire fault length is even shorter. Such very high rates provide a high probability of major activity during the life of many engineering structures.

73. The characteristics of each zone follow:

a. Very high activity (Matsuda type AA). The most active zones are those that are within about one order of magnitude of the highest rates observed along major earth plate boundaries, and major transform faults and master

fault systems, like the San Andreas fault system of California.

b. High activity (Matsuda type A). The classification for rates between 1 cm/yr and 0.1 cm/yr follows the International Atomic Energy Agency's definition of high. This range of rates characterizes many major faults of both very long to moderate lengths (see Lamar et al.,[80] and Table 9), including the San Jacinto, Big Pine, and Garlock faults of southern California, and generally is marked by many conspicuous geomorphic features that characterize active faults. The recurrence interval for magnitude 7 earthquakes at a given point along the faults is generally measured in hundreds or thousands of years, and probability of a magnitude 7 earthquake at a given point on the entire fault zone is generally measured in many tens of years to many hundreds of years. Such high rates generally should be considered for most engineering structures, even though the recurrence interval may be much longer than the expected life of the structure.

c. Moderate activity (Matsuda type B). The classification of rates between 0.1 and 0.01 cm/yr is moderate. This rate range includes faults that generally have well-developed geomorphic evidence of activity, including the Dixie Valley, Nevada, Pajarita, New Mexico, and the mid-valley fault zone of the 1872 Owens Valley earthquake. The recurrence interval for displacement along such faults and the generation of magnitude 7 or higher earthquakes is generally measured in thousands to few tens of thousands of years for a given point on the fault. This moderate rate of recurrence is much longer than the expected life for most engineering structures, but should be considered for most structures.

d. Low activity (Matsuda type C). The classification for rates between 0.01 and 0.001 cm/yr is low. Within this range of displacement rates, geomorphic evidence of activity is generally sparse, inconclusive, or lacking. The recurrence interval between magnitude 7 earthquakes or larger is generally measured in many tens of thousands of years to hundreds of thousands of years for recurrence at a given point on the fault. Engineering allowance for faults in this range of activity is generally restricted to important structures, such as nuclear reactors and dams that are vital to man's activities and safety.

e. Extremely low activity to inactive. This range of activity, taken as rates less than 0.001 cm/yr, represents rates of deformation of four or more orders of magnitude lower than that of the zones of very high activity, and includes faults that have very low rates of activity

and/or faults that are geologically inactive. It is generally difficult to evaluate the inactivity or very slow rate of physical evidence of activity, even for examples near the threshold values of activity of the U. S. Nuclear Regulatory Commission classification. Since mid to early Quaternary or late Tertiary deposits are commonly absent, the opportunity of finding direct evidence to measure or distinguish these very low rates may be lacking and the resolution of question of activity may not be possible. Faults of this type may be present in less active parts of regions of active faulting, either due to the rotation of stress fields to decrease activity on faults of certain orientations, or to development of by-passing fault systems. Faults of this type may be present in relatively inactive zones near the margins of active regions or in relatively stable provinces along the most recent areas of tectonic activity, such as the Triassic to Jurassic graben extensional faults of the eastern United States. For most engineering structures, faults of this type may be grouped as "probably (or practically) inactive," when definitive data proving an inactive status are not possible. Engineering design for fault hazards and earthquakes within this range of low activity is generally required only for major engineering structures such as nuclear reactors, large dams, and dikes that are required to protect densely populated areas, where failure could affect the safety, welfare, and vital governmental functions of large numbers of people.

PART V: METHODS OF DETERMINING TOTAL FAULT LENGTH

Introduction

74. The determination of total fault length requires that the regional as well as local tectonic setting be understood. The approach should include a thorough evaluation of all available published regional geological and geophysical literature, consultation with authorities familiar with the geology and geophysics of the area, and extensive field and photogeological study of the structures in order to establish the continuity of the faults, branches, possible conjugate sets of faults of diverse orientation and slip type, and search for evidence of continuity in areas of possible concealment.

75. The geological approach is primarily focused on determining the fault continuity and relation of folds. This requires interpolation, extrapolation, and pattern analysis. A search should be conducted for possible fault gaps or extensions across urbanized areas, geologically young formations, or bodies of water, and if special studies are needed, they should be identified and the most appropriate exploration methods determined. The geologic aspects of this phase of the work generally require matching of similar structures, stratigraphy, geomorphology, or geophysical trends, and the recognition of sheared and offset materials. This phase of the work normally requires application of photogeological and remote sensing analysis and aerial and field checking of suspect features.

Geologic Evaluation

General comments

76. Difficulty in assessing fault length varies with availability of geologic and geophysical information. Except for a few major fault zones in the western United States, the available data on length of faults and their activity are usually inadequate for most areas. For this reason, most siting studies require extensive evaluations of both

the local area and the regional setting to determine the structural continuity of active faults. The problem of determining structural continuity of faults in the area for investigation is further complicated by the fact that for most of the slip types of faults, the major structure may have branching or en echelon surface expression.

77. The difficulty encountered from distributed faults has been discussed in detail by Oakeshott.[70] The complexity of fracture pattern is minimal for major strike-slip fault zones such as the San Andreas and Garlock faults of California. Although these two faults and others in the region may show a conjugate relation to each other or may have major branches that diverge to distances of many tens of miles from the major fault zone, the faults generally show topographic, geomorphic, and stratigraphic continuity which makes the identification of the length of the structure straightforward. Any gaps in the surface expression of the faults can generally be resolved for continuity or noncontinuity by examination of available geophysical data such as magnetic surveys, gravity surveys, recent seismological plots of earthquake epicenters, and seismic refraction and reflection surveys. If the available information is inadequate to resolve the issue of continuity, either the undertaking of additional studies as shown in Table 7 or the assumption of continuity to provide a conservative approach to the evaluation is possible.

78. Historical surface fault studies of major normal-slip zones indicate a far more complex relation for regions in which normal-slip or normal-oblique-slip faults are to be expected. For example, in the six historic cases of normal-slip surface faulting with earthquakes of magnitudes of 7 or greater, all but one display primary faulting on two or more major fault zones. These fault zones may be distributed over an area up to tens of kilometres in width and may give surface faulting on the opposite sides of as many as two mountain or valley blocks.

79. Historic examples of reverse-slip faulting also show great complexity of fault pattern, and the branching character of many of the major faults makes it difficult to determine the true length and width for a given active fault zone. This relation was especially well displayed for the San Fernando earthquake area of 1971 (Wentworth and Yerkes[81]).

Structural continuity

80. Structural continuity is commonly concealed by bodies of water or geologically young surficial deposits, or not indicated because of incomplete regional geologic mapping. The geological methods that are most useful for filling the missing gaps or for determining whether separate faults may tie together include the careful determination of the strike and variation in strike of the two segments, the determination of the dip of the fault plane, the sense of displacement on the two segments to determine whether the offsets are compatible for a connection, and the determination of whether similar differences in stratigraphy or structure of the adjoining areas occur for both fault segments. The geomorphic relation, similarity or difference in topographic expression for the two faults, may resolve whether or not the two faults are likely to connect.

81. Photogeologic and remote sensing analysis of the intervening area, particularly with the aid of a variety of scales and types of photos or images and with low-sun-angle methods of analysis, will frequently reveal whether or not the fault being evaluated can extend to connect with other segments, or whether or not discordant or truncating relations preclude the extension of a known fault segment.

Similarity of history

82. Most faults have the same general history and related stratigraphy over major sections of the fault. Determination of whether faults extend or can be extrapolated to connect with other structures can sometimes be resolved by differences in degree of activity, type of activity, activity rate, or manner and amount of effect on the adjoining materials and structures. Discordant sources of data may dramatically affect correlations. An excellent example relates to the problem of whether or not the Hines Creek fault in Alaska is a branch of the very active Denali fault. Although the Hines Creek fault does not show the conspicuous landforms normally found along active faults, many geologists have argued that it must be active, since both ends of the fault appear to connect with the Denali fault (see Figure 21). Wahrhaftig et al.[82] have conclusively resolved the issue by finding a 95,000,000-year-old

BEST AVAILABLE COPY

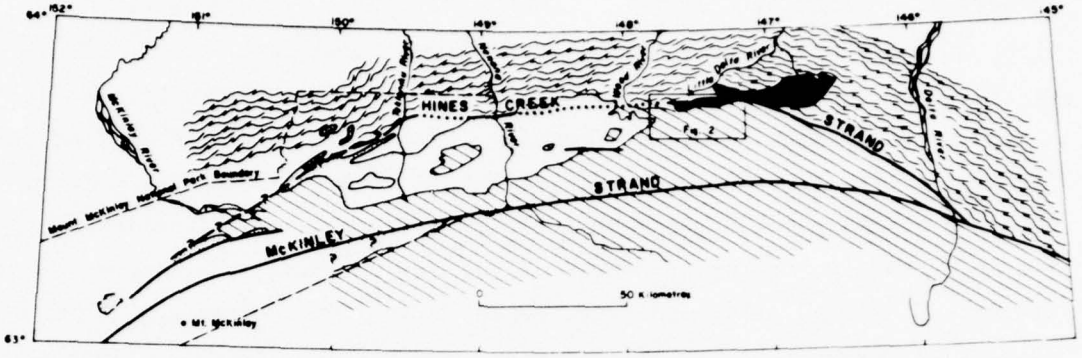


Figure 21. Denali fault system in central Alaska Range. Stipple pattern, Cantwell Formation; black, Buchanan Creek pluton (95,000,000-year cooling age); wiggles, continental tectonite terrane; diagonal lines, terrane of probable oceanic origin (from Wahrhaftig et al.[82])

intrusion that crosses the fault and is not offset by the fault.

83. The following methods can be used to determine the maximum and average amounts of displacement relative to earthquake magnitude. For geologically young offsets, geomorphic study of marine, lake, and stream terraces commonly shows episodic and cumulative offset, uplift, or tilting. With Carbon-14 or other methods of dating of these episodes, along with the amount of offset for each episode, it is possible, for a particular place along the fault, to determine recurrence interval of faulting and maximum offset-magnitude by use of equations or curves for maximum offset-magnitude, length of fault-magnitude, and recurrence interval by the Wallace[30] method. For historically active faults or for longer faults, seismologic and Wallace type analyses can determine recurrence interval for the particular place on the fault, or with the length of the entire fault known or assumed, the recurrence interval for the entire fault. Ambraseys,[83] Slemmons (unpublished data), and Allen[84] have shown that between 1 and 100% of a given fault may be activated during an earthquake. Matsuda[85] (also see Allen[84]) has described an example from Japan, where the magnitude 8 earthquake of 1891 produced nearly continuous surface faulting along the entire length of the Nobi fault system. Matsuda and Okada[86] and Allen[84] also describe the 7.1 magnitude earthquake of 1930 which produced surface faults along the

entire length (35+ km) of the segmented, partly en echelon, Tanna fault zone of Japan.

Geomorphic-topographic analysis

84. The study of landforms should be undertaken for at least two levels of detail: (a) for regional or province evaluation, and (b) for local or siting evaluation. Evaluation of the geomorphology should be based on a thorough search of literature, consultation with specialists on the geology, geomorphology, and seismology of the region, and a study of the literature and aerial photographs and imagery.

85. The evaluation of regional relations should utilize topographic maps, shaded relief maps, plastic relief maps, and aerial photographs and images at the several scales available. This phase of work should focus on identifying master and major structural trends that affect the geomorphic expression of the region to distinguish: master faults, i.e. faults that bound major tectonic plates; major faults, i.e. faults of hundreds of kilometres in length that are important on a regional or provincial scale; and local faults, i.e. faults up to a few tens of kilometres in length that are at or near the particular site.

86. Active master faults are those faults that mark the boundaries between the major plates of the earth and generally have high rates of regional deformation, measured in centimetres per year. These fault zones commonly show high seismic activity and are hundreds or thousands of kilometres in length. Magnitude-length relations show that master faults are capable of earthquakes of up to about 8.6 magnitude with associated surface faulting of hundreds of kilometres in length and maximum displacements of up to 7 to 10 m. The surface faulting for the San Andreas fault in 1857 and 1906 had earthquakes of about 8.2 or 8.3 magnitude, surface right-slip of 10 and 7 m, and displacement segments of about 200 and 270 km, or about 15 and 20% of the length of the entire San Andreas fault system. Such faults provide design earthquakes for ground motion evaluation not only near the fault but for distances up to hundreds of kilometres to either side of the fault. They also pose major design problems for structures constructed across their trace.

87. Major faulting with several tens to hundreds of kilometres of

length can produce earthquakes of somewhat greater than 8 magnitude and have associated surface faulting that is from about 30 to 100% of the total fault length, and maximum displacements of from about 1 to 7 m. Such faults generally provide the design earthquakes for sites up to 50 to 100 km from the structure and provide considerable problems for construction close to the fault.

88. Local faults have lengths of up to a few tens of kilometres. These faults generally produce maximum magnitudes of about 6.5 to 7, have associated examples of surface faulting over one-half or more of the total length of the fault, and give maximum displacements of up to about 5 m.

Photogeologic and imagery analysis

89. One of the most effective methods of detecting and delineating active faults is by photogeologic and imagery analysis. This type of analysis is most successful for determining the fault lengths of master, major, and minor faults. Small-scale or synoptic types of scales of photography and imagery (including ERTS) are best suited to detecting master and major faults, as they are sensitive to long faults that are defined by lineaments that cross many drainage lines or control long linear mountain fronts.

90. Intermediate- to large-scale photography and imagery is more applicable to shorter lengths of faults and these scales permit a better analysis of details along the fault trace. The most effective method for detailed study of faults involves use of low-sun angle photography of the type developed by Cluff and Slemmons (Slemmons,[87] Clark,[88] Cluff and Slemmons,[89] Slemmons,[90] Sherard et al.,[24] and Walker and Trexler (in press)).

91. Scales. The following comments apply to the relative value of different scales of photography and imagery that are available:

a. Synoptic (small) scales: 1/100,000 to 1/1,000,000. Scales within this range are most useful in determining or recognizing major and master faults. This scale is generally available by enlargement of ERTS imagery in a variety of spectral bands. Scales of 1/500,000 give a good balance between adequate scales for showing moderate detail and for resolution.

b. Intermediate scales: 1/20,000 to 1/100,000. Scales within this range are the scales normally available for most regional mapping and compilations. A scale of 1/60,000 is of marginal effectiveness for fault scarps of less than about 5 to 10 ft in height, even with sparse vegetation. The scales of this range are useful for master and major faults that can be traced many miles and that are likely to disturb many drainage basins. Additional photography at large scales should be obtained for suspect zones or for detailed study of active faults.

c. Detail (large) scales: 1/5,000 to 1/20,000. Scales within this range are ideal for mapping detailed relations of faults and for distinguishing and delineating faults with low scarps that are only a few feet in height.

92. Types of imagery and photography. The advantages and disadvantages of the various types of imagery (SLAR and ERTS) and photography (conventional mid-day black and white, low-sun-angle, color, infrared color, and infrared) are discussed briefly in Sherard et al.[24] For most studies, all available techniques should be used in combination, with multi-scale, multi-format study, to provide optimum results in detecting, delineating, and evaluating the character of faults. The most effective single technique is to enhance the fault scarps by either highlighting the scarps by direct low-sun-angle illumination, or with even more conspicuous results, by shading the scarp with an angle of sun illumination that grazes the fault scarp by developing extensive shading, but without casting shadows that conceal the detail of the scarp. The optimum shading effect is found when the sun shines from a direction that is perpendicular, or at least at a high angle to the trend or strike of the scarp. Examples of highlighting and shading effects are given in Appendix A, Figures A1, A14, and A17 (see also Figures 7, 8, 9, 11, 12, and 14 in Krinitzsky,[29] which illustrate fault scarps of the three main slip types). The following general comments apply to each main type.

a. Radar imagery. Radar imagery is becoming more widely available, less expensive, and of improved resolution. Side-looking-airborne-radar (SLAR) has the special advantages of being applicable to areas under unfavorable sun illumination conditions, at night, with cloud or fog cover, and with the direction and depth of shadows that can be controlled to provide maximum enhancement of the structures oriented in any desired direction. The images

are routinely mosaicked at the convenient scale of 1/250,000 for comparison with topographic maps that are generally available at the same scale. The images have excellent contrast for different types of vegetation and can reveal surface topography through dense vegetation. The imagery is of great value in detecting major, but subtle topographic trends and most master or major faults are readily distinguished on radar images. The images provide limited detail and information on degree of activity. The great number of lineaments that are normally present include a high proportion unrelated to active tectonism (Krinitzsky[29] and Gay[91]). All suspect lineaments must be checked by other types of imagery, photo interpretation, and field study.

b. Earth Resources Technology Satellite (ERTS) or Landsat imagery. ERTS imagery is available in a variety of spectral bands, and for most parts of the world. The mosaics of this imagery, or different images viewed stereographically for various lighting conditions or seasons, are very effective in detecting and delineating major and master faults and great numbers of other lineaments. As is the case with SLAR imagery, the lineaments must be checked by other methods, for most are nonactive tectonic features. Computer method of color addition or subtraction, ratioing, truncation, and linear stretching are special techniques that greatly improve the resolution and structure recognition.

c. Color aerial photography. Color aerial photography is generally more useful in fault studies than conventional black and white photography, since the color contrast of different rock types, alteration zones along faults, and the differences in vegetation are greatly enhanced. The limited exposure latitude of color films precludes the possibility of using low-sun-angle illumination.

d. Black and white aerial photography. Black and white aerial photography is the most widely used type of photography. The cost is minimal and the results are generally very satisfactory. Since some shading effects are normally present, particularly in mountainous regions, caution should be exercised when ordering aerial photographs to avoid processing with the use of an electronic dodging device. The previously mentioned low-sun-angle method is generally far more effective in enhancing irregularities of terrain, and particularly in focusing attention on fault scarps and scarplets. This method may reveal up to ten or more times as many small scarplets as would be visible on conventional photographs of the same scale, and is very effective in detecting and

delineating landslides and other types of failures in soil and rock.

e. Infrared imagery and photography. The high cost relative to conventional black and white photography and limited resolution of thermal IR make it of marginal value for most studies, although thermal IR and, to a lesser degree, color or black and white near-IR photography enhance groundwater or vegetation contrasts that are common along fault zones. The lack of ability to use color IR with low-sun-angle illumination also limits the applications of IR photography.

Geophysical Analysis

Seismologic methods

93. Seismologic methods of determining fault activity and continuity are an essential part of the geophysical analysis of faults, but may be of limited use since many faults with historic surface faulting developed in regions that were aseismic before the main earthquake, or showed activity in an adjoining area or fault segment (Kelleher and Savino,[65] and Ryall and Malone[71]). Kelleher and Savino[65] discuss examples of unilateral rupturing that starts from previously activated fault zones and extends into aseismic or weakly active fault segments. Aftershock activity, in contrast, commonly delineates faults with much greater continuity than is expressed by surface fracturing (Figures 16 and 17; see also pages 48-50 of Krinitzsky[29]).

94. The application of seismicity studies for determining fault continuity is shown by the Borrego Mountain area of the San Jacinto-Coyote Creek-Superstition Hills-Imperial fault zone in California. The pre-1968 seismicity (Hileman et al.[92]) vaguely defines the fault zone, but the post-1968 Borrego Mountain earthquake aftershock activity as shown in Figure 10 clearly indicates continuity through this zone (Thatcher et al.[93]). The increased length derived by connecting these fault segments implies, for fault length-magnitude relations, the potential for higher earthquake magnitudes than the previous fault maps suggested. An alternative interpretation is that the Coyote Creek and Superstitution Hills segment of the fault zone is characterized by more frequent, lower magnitude earthquakes. This possibility is also

suggested by the trench shown in Figure 19, which suggests frequent, small-displacement earthquakes for this area. Additional trenching, if it confirms activity by more frequent, smaller magnitude events, could invalidate the simple fault length approach to earthquake magnitude predictions for this fault. This type of approach would use Figure 2 in combination with geochronological studies and use of the magnitude-displacement relation.

Gravity methods

95. Gravity methods are a useful geophysical method for study of active fault zones (Krinitzsky[29] and Gimlett[94]). Gravity methods are most effective in regions where there is a strong density contrast between materials on either side of a fault; this is generally obtained along faults where basement rocks are displaced against unconsolidated sediments, or for faulted basement rocks where the depth of sedimentary cover is different on either side of the fault. The method is especially effective for regions of extensional faulting. Gimlett[94] demonstrated that the method provides excellent results within the Basin and Range Province for providing data on the configuration of the base and thickness of valley-fill sediments. He has also noted the advantages of the gravity method--low cost, speed and ease of application, particularly for areas with detailed topographic maps and good elevation control. The method is not only effective for boundary faults of the Basin and Range grabens, but can determine the extent and amount of tilt of louderbacks (tilted fault blocks). The method is also useful for detecting and delineating faults concealed by alluvium within the graben blocks.

Magnetic and aeromagnetic methods

96. Application of surface magnetic and aeromagnetic survey methods for evaluation of active faults is discussed in papers by Andreasen et al.,[95] Cluff et al.,[72] Krinitzsky,[29] and Sherard et al.[24] These methods can be used to detect and delineate faults concealed by recent sediments, and can provide a relatively inexpensive method of contouring the thickness of basin fill. Smith[96] located intrabasin, largely concealed, major fault grabens within the Dixie Valley graben.

Some of these graben boundary faults were also accurately delineated by the faulting of the 1954 Dixie Valley earthquake. Smith provides a detailed outline for applying the method to the Basin and Range Province with normal- and oblique-slip faults.

Seismic refraction and reflection methods (including vibroseis tr, sparker, and air gun surveys)

97. Use of these methods is generally restricted to oceanic and deep lakes. New refinements of the methods, research into special techniques, and improved data enhancement by computer analysis may expand the use of these methods and are effective also for land or shallow water areas. Major use of these rather expensive methods has been made along the Newport-Inglewood fault, some of the Channel Island faults, active faults in Monterey Bay (Greene et al.[97]), and the San Andreas fault north of Bolinas Bay, California (Curray and Nason[98]). These studies have indicated that for ocean basins and continental shelf areas, the methods can lead to rates of fault activity and recurrence intervals, as well as design earthquake values. The most recent and successful use of these methods for lakes is by Robert Smith for the Great Salt Lake. His special method of deconvoluting records has provided meaningful results even for profiling in very shallow water. The method appears to be feasible for active faults beneath other large lakes in the United States.

98. An example of an integrated geologic and geophysical study of areas covered by water is given by Greene et al.,[97] showing the total length and character of faults that crossed parts of the continental shelf as well as land areas. Application of the magnitude versus fault length relation, with allowance for predicting faulting on one-half the entire length of the fault, gives the magnitude estimates of Table 10.

99. The Monterey Bay fault and earthquake evaluation of Greene et al.[97] revealed the presence of many previously unrecognized faults. Some of these faults could be classified as active on the basis of current definitions. The seismic reflection surveys can be used to determine recurrence intervals and provide data on the time of last

Table 10

Estimates of Earthquake Magnitude for the Palo Colorado-San Gregorio Fault Zone (from Greene et al.[97])

Fault km	Earthquake Magnitude						
	Tocher[4]	Iida[6]	Albee and Smith[7]	Bonilla and Buchanan[1]	Average and Range[1]	Bonilla and Buchanan*	Slemmons (This Report)
				Half-length			
65	7.2	7.4	7.6	7.4	7.4 (7.2 to 7.6)	7.2	7.1
100	7.4	7.6	7.8	7.9	7.7 (7.4 to 7.9)	7.5-	7.4-
				Full-length			
130	7.5	7.6	8.2	8.2	7.7 (7.5 to 8.2)	7.6	7.5
200	7.7	7.8	8.3	8.7	8.3 (7.7 to 8.7)	7.8	7.6

Full length does not include an extension southward to connect with the Hoslia fault zone as proposed by some workers.
Magnitudes were established as follows:

Tocher:[4] M = 0.9 × log surface rupture length (L) in km + 5.6

Iida:[6] M = 0.76 (log L km) + 6.07

Albee and Smith:[7] Albee and Smith's Figure 4; Figure 12 of this report

Bonilla:[8] M = 1.51 (log L miles) + 5.14

Bonilla and Buchanan:[1] Read from graph of M versus L for worldwide strike-slip earthquakes

* Bonilla and Buchanan[1] 1970 data recalculated (see Table 4 herein).

displacement. The Palo Colorado-San Gregorio fault zone appears to be at least 125 miles long, and may extend northward from the faults at Half Moon Bay to join the San Andreas fault northwest of Golden Gate. A cross section and a seismic profile are shown in Figure 22, and the generalized relations are indicated in Figure 23 with symbols used to denote different ages of faulting. A detailed fault map of Monterey Bay is given in Figure 24. The great length of the main fault crossing the bay leads to estimated magnitudes of future earthquakes generated along this fault of between 7.2 and 7.9 using the magnitude versus length relations of various researchers, using the half total fault length method of plotting fault length versus magnitude (Table 10). Use of the full length

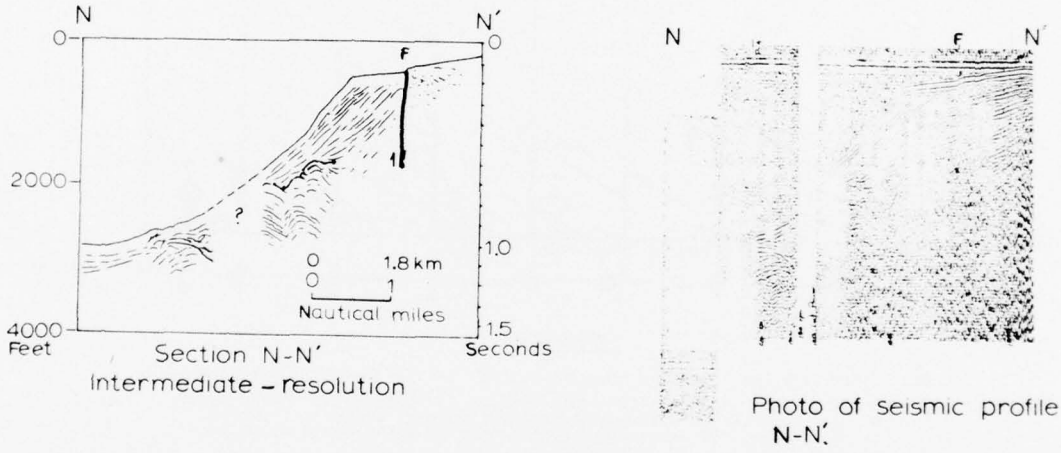
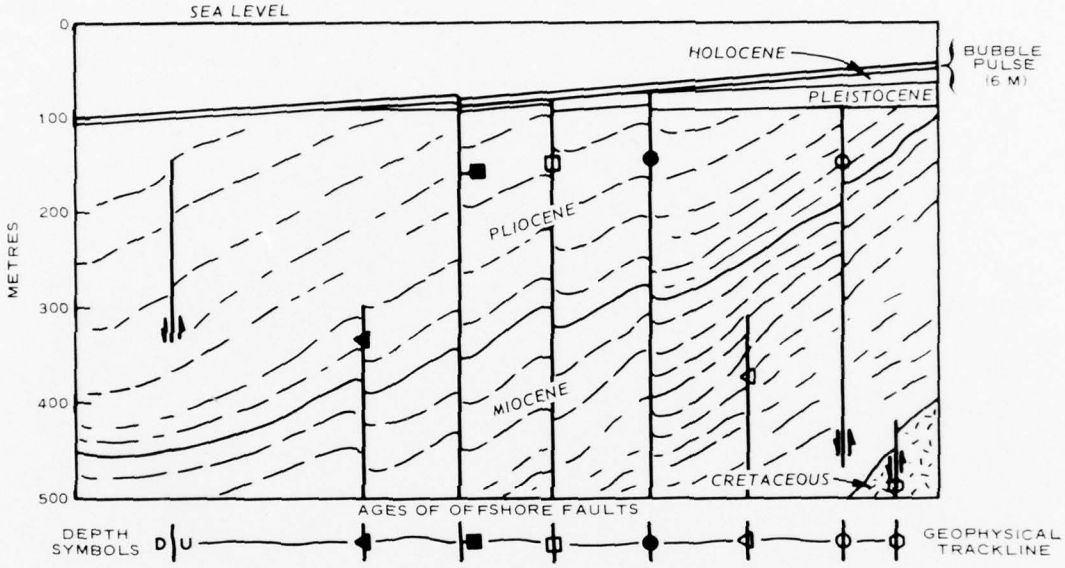


Figure 22. Seismic profile and geologic cross section interpreted from the profile N-N' across the Palo Colorado-San Gregorio fault zone, California (from Greene et al.[97])



LEGEND

- FAULTS THAT DISPLACE THE SEA FLOOR ON THE DOWNTHROWN SIDE
- FAULTS THAT EXTEND TO WITHIN 6 M (i.e., THE BASE OF THE BUBBLE PULSE) BUT DO NOT DISPLACE THE SEA FLOOR; SOME OF THESE FAULTS MAY DISPLACE HOLOCENE DEPOSITS (DEPOSITS 0 TO 10,000 YEARS OLD)
- FAULTS THAT EXTEND TO THE BASE OF, BUT NOT INTO, THE HOLOCENE DEPOSITS
- FAULTS THAT CUT MIDDLE AND LATE TERTIARY ROCKS (MIOCENE AND PLIOCENE ROCKS IN THE MONTEREY BAY AREA) AND MAY EXTEND UP TO THE BASE OF THE PLEISTOCENE DEPOSITS (DEPOSITS 10,000 TO 1.8 MILLION YEARS OLD)
- FAULTS THAT EXTEND UP INTO PLIOCENE STRATA
- FAULTS THAT EXTEND UP INTO MIOCENE STRATA
- FAULTS THAT SHOW SEPARATION IN CRETACEOUS BASEMENT ROCKS AND MAY EXTEND NO MORE THAN 100 M INTO OVERLYING STRATA OF PROBABLE EARLY TO MIDDLE TERTIARY AGE
- FAULTS THAT EXIST AT 200 TO 500 M BUT DO NOT CUT THE CRETACEOUS BASEMENT ROCKS

Figure 23. Generalized cross section showing the types of fault offsets shown by seismic reflection surveys in Monterey Bay (Greene et al.[97])

BEST AVAILABLE COPY

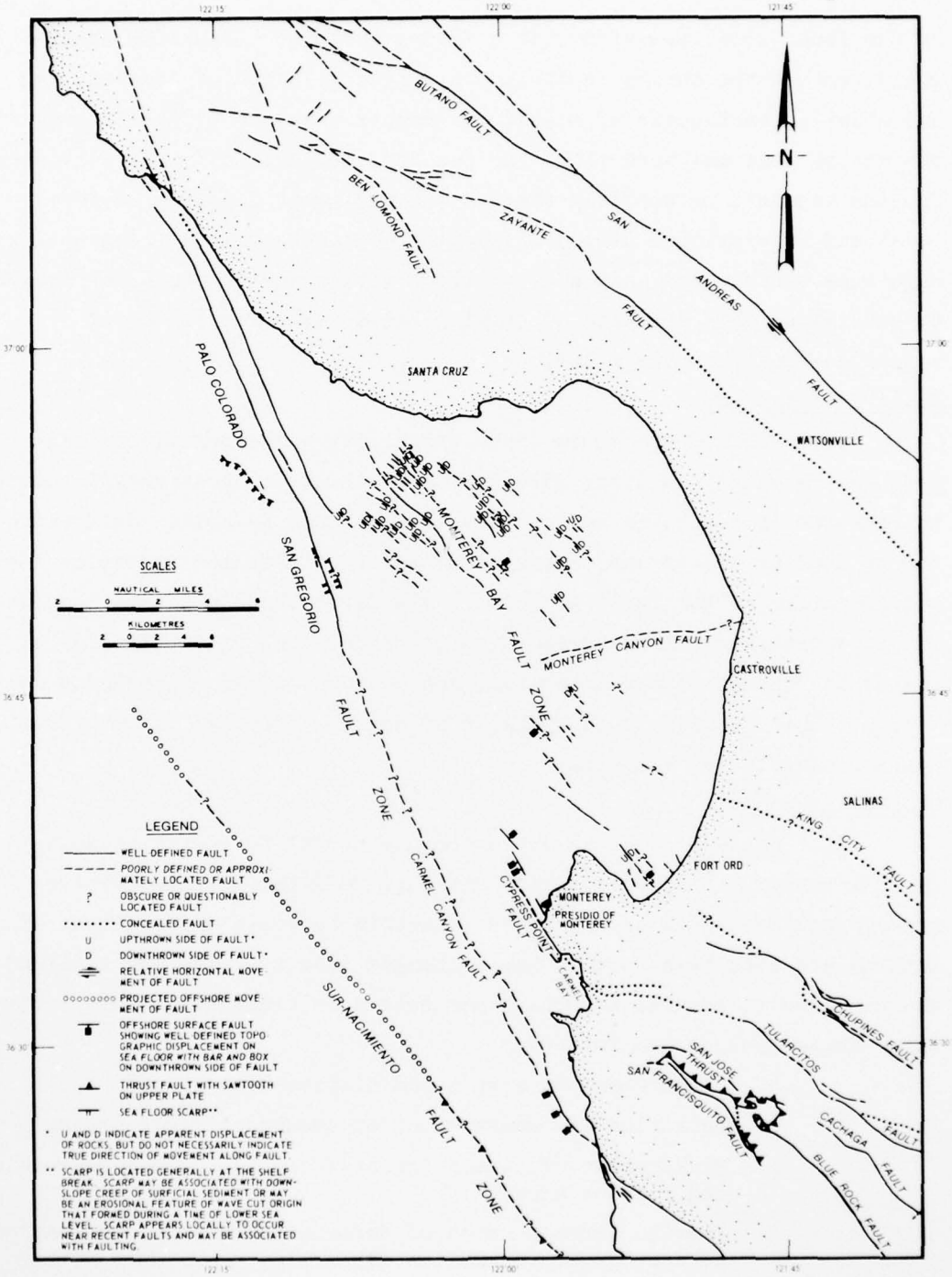


Figure 24. Map showing faults along the floor of Monterey Bay (based on Greene et al.;[97] from Jennings[99])

of the fault zone, assuming that a future earthquake faulting event would rupture the entire fault length, gives a length of over 200 km and a design earthquake of magnitude greater than 8. Detailed study of the entire zone may show (like the San Andreas fault near the Hollister-Cholame segment, or possibly the San Jacinto fault zone near Coyote Creek and Superstition Hills) disrupting segments of more frequent low-magnitude earthquakes. Such disruptions would require that some faults be subdivided into segments of varying character prior to use of magnitude-fault lengths relations.

Electrical methods

100. Surface and subsurface resistivity and other electrical methods are mainly used for identifying distinctive stratigraphic units as measured in boreholes and correlated from hole to hole. Such methods can be used to locate and determine amount of offset and determine the configuration of the fault at depth. Similar methods also are successful in determining differences in water table level on either side of faults in unconsolidated materials, and in identifying and tracing many faults. This relatively inexpensive method is effective in tracing some faults concealed by alluvium.

Geodetic methods

101. Geodetic surveys are extremely useful for defining active fault zones with high to moderate rates of deformation. Repetitive surveys are conducted across zones of active tectonic deformation. The methods are sensitive to very small changes (about 1 part per million) and can lead to several important parameters in evaluating fault activity. These include the following:

a. Measurement of strain and displacement rates.

b. Detection and measurement of amount of fault creep.

c. Measurement of strain orientation, including compression and tension axes.

d. Provide current rates of deformation for the estimation of earthquake recurrence intervals.

102. The elastic rebound theory of earthquake origin from abrupt fault displacements was proposed by Reid[100] as the result of his study

of geodetic changes in the 1906 earthquake along the San Andreas fault. Following this earthquake, most studies of geodetic changes along active fault zones in the United States, from 1906 to 1971, were conducted by the U. S. Department of Commerce, National Ocean Survey. Sixty-five of their reports have been reprinted by the U. S. Department of Commerce.[39] Other recent studies include evaluation of changes from strike-slip faulting (Hastie and Savage[101]), dip-slip faulting (Savage and Hastie[66,102]), and reverse-slip faulting (Hastie and Savage[101]).

103. Geodetic displacements are similar to observed field geologic measurements, although distortion may reduce some of the displacements that are measured in the field by geologic methods (see Figure 11, which compares field measurements of fault displacements and geodetically measured displacements on the San Andreas fault from the 1906 earthquake, after Thatcher[37]).

PART VI: NEW DETERMINATIONS OF RELATIONS OF EARTHQUAKE MAGNITUDE TO MAXIMUM FAULT DISPLACEMENT AND LENGTH OF SURFACE FAULTING

104. Since the Bonilla and Buchanan[1] compilation, several geologic, seismologic, and geodetic studies of surface faulting have become available. This section of the report responds to the need for a new surface fault compilation. This study revises the earlier values where new data are available, and adds more recent cases, but follows the general approach and method of display of data of Bonilla[8,9] and Bonilla and Buchanan.[1] Other recent compilations that were used include Ambraseys and Tchalenko,[10] Ambraseys,[103] and Matsuda.[57,85] This section retabulates historic surface faulting events and derives, by linear regression analysis, new equations and charts to relate to one another, the parameters earthquake magnitude, fault displacement, fault length, product of fault length and displacement, and product of fault length and displacement squared. The revision includes the assignment of magnitudes to several earthquakes, based on intensity data. Several new fault length and displacement values are added. Faults that are partly concealed by bodies of water are reassigned increased lengths where aftershock distributions, geodetic data, or hydrographic surveys are available. Plafker's[64,68,104] reviews of deformation of the 1960 and 1964 earthquake areas led to modification of the 1964 data and to the addition of the 1960 earthquake data to supplement the very meager data for reverse-slip faults. The closeness of fit of the length of many well-determined aftershock areas on the length of surface faulting chart suggests that future refinements of magnitude-fault length compilations should use this type of data, particularly for very large and very small earthquakes.

105. The overall effect of the above changes and additions is to increase the number of reference events from the 68 of Bonilla and Buchanan[1] to 84, an increase of 24%. About one-third of the previous magnitude, displacement, and fault length values have been revised, mostly as relatively minor changes.

Earthquake Magnitudes

106. The most appropriate measure of earthquake magnitude for engineering practice is assumed to be the local, or Richter magnitude (M). Most earlier studies used M , but some determinations of teleseismic magnitude (m) or body wave magnitude (m_b) for earthquakes of greater than magnitude 7 were not converted to M as proposed by Richter.[3] This compilation uses the revised magnitudes listed by Richter,[3] Gutenberg and Richter,[105] and Duda.[106] Duda's compilation was the basis for earthquakes of over magnitude 7 in the period 1897 to 1964. Other important sources of magnitude determinations are Matsuda[57] and Matsuzawa[107] for Japan; Karnik[108] for southern Europe and Turkey for the period to 1964; Rothe[109] for worldwide seismicity for the period 1953 to 1965; and Hileman et al.[92] for the southern California region for 1932 to 1972.

107. The four earlier earthquakes with surface faulting in California and Nevada in 1857, 1868, 1869, and 1872 are assigned magnitudes based on intensity observations based on Figure 15 of Krinitzsky and Chang[42] and Toppozada.[110] These magnitudes are 8.2 ± 0.2 for the 1857 earthquake, 6.7 ± 0.2 for the 1868 earthquake, 6.7 ± 0.2 for the 1869 earthquake, and 8.0 ± 0.2 for the 1872 earthquake. The estimated magnitudes of earthquakes of preinstrumental seismology for Europe and Japan probably have similar errors of about ±0.2, since the intensity information is similar.

Revision of Fault Length and Displacement Data

108. Measurements of many previously studied examples of historic surface faulting have been completed or are in advanced stages of restudy. After-shock studies and geodetic or hydrographic studies permit improved determination of several faults that are concealed beneath the ocean. Published accounts that provide new data are given by Ambraseys,[83,103] Hill and Beeby,[111] Bonilla,[8,9] Bonilla and Buchanan,[1] Jennings,[99] Kamb et al.,[112] Matsuda,[57,85,113] Meade and Miller,[114]

Morrison,[115] Nakamura and Tsuneishi,[116] Plafker,[64] Seih and Jahns,[117] Tasdemiroglu,[118] and Thatcher.[37,40] Measurements on faulting in the Pleasant Valley, Nevada, region are from Wallace and Slemmons (unpublished manuscript).

Results of Compilation

109. The relations between earthquake magnitude, fault displacement, fault length, the product of displacement and length, and the product of displacement squared and length are given in Figures 25 to 29 and in Tables 11 to 15. The equations for the best straight-line fit for various types of faults for North America and for worldwide earthquakes were obtained by linear regression analysis and the equations, of the form $y = a + bx$, are listed in Tables 11 to 15. The earthquake magnitudes are local or Richter magnitudes. Fault lengths, in metres, are generally determined by the zone of surface rupturing, but for zones that are partly concealed, geodetic or seismological data are used. Displacements, in metres, are the maximum resultant displacements or shifts, which include both fault slip and distortion. The listing of fault types A through E is after Bonilla and Buchanan:[1] A for normal-slip, B for reverse-slip, C for normal-oblique-slip, D for reverse-oblique-slip, and E for strike-slip. The first 28 events are North American examples of surface faulting listed in chronological order. The following 55 examples are other worldwide events listed in chronological order. Events or data items are omitted where the data are inadequate. Faults in remote areas are omitted where the length or maximum displacement values are considered to be grossly incomplete. Where two of the three data values are considered to be satisfactorily determined, the two values are used and the third is rejected by listing a deleting value of 0.

Reliability of Results

110. The careful compilation of Bonilla and Buchanan[1] forms the

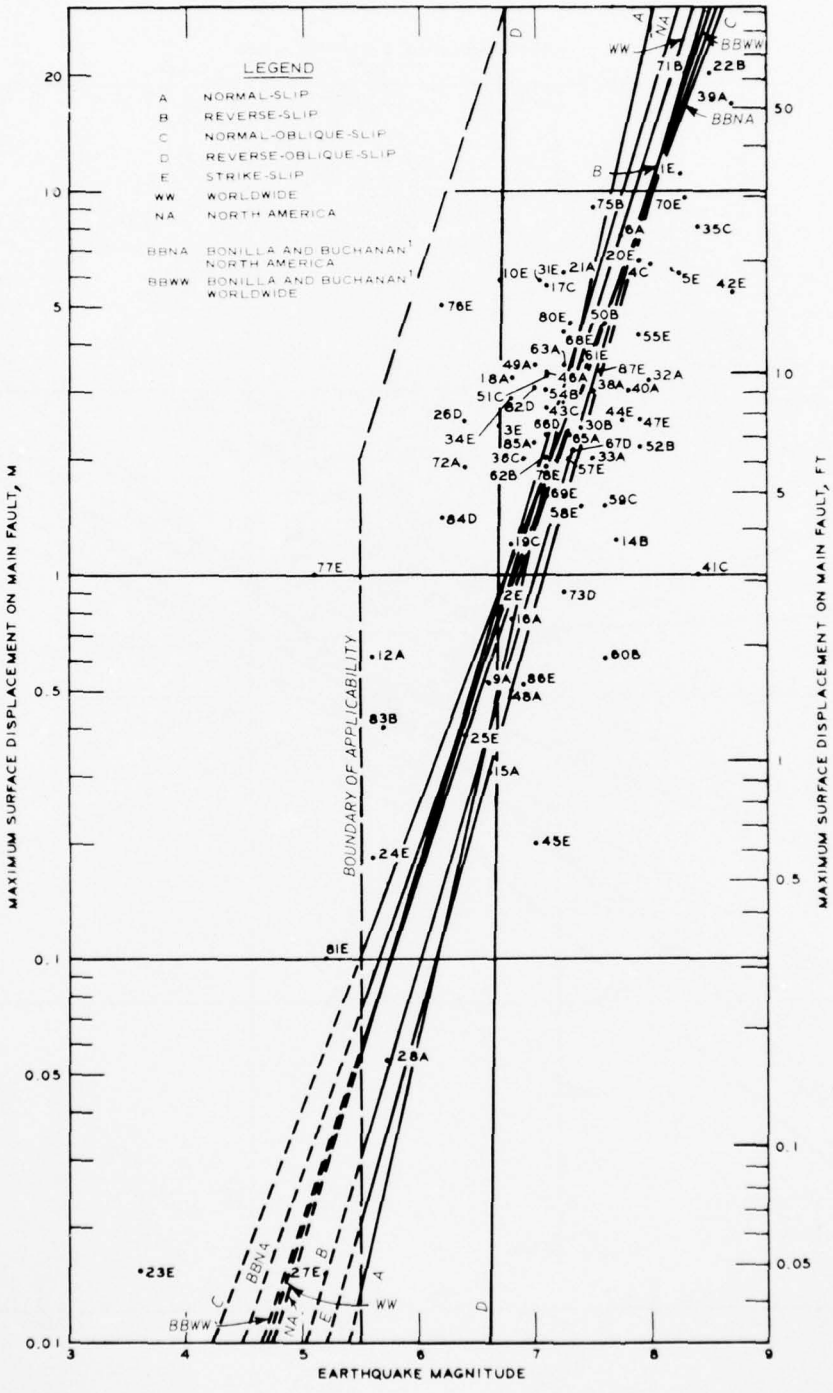


Figure 25. Maximum surface fault displacement on main fault as related to earthquake magnitude

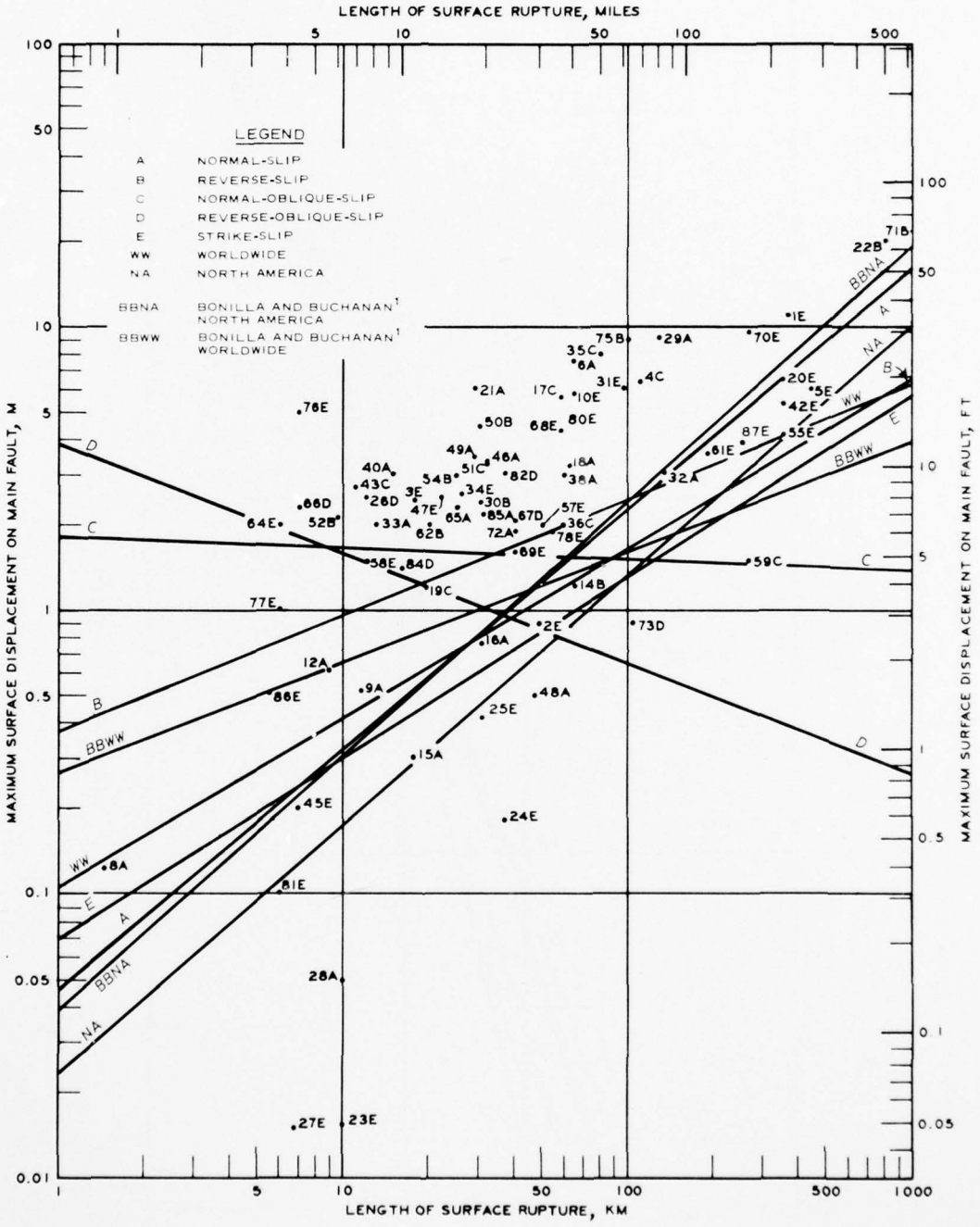


Figure 26. Maximum surface displacement on main fault as related to length of associated surface rupture zone

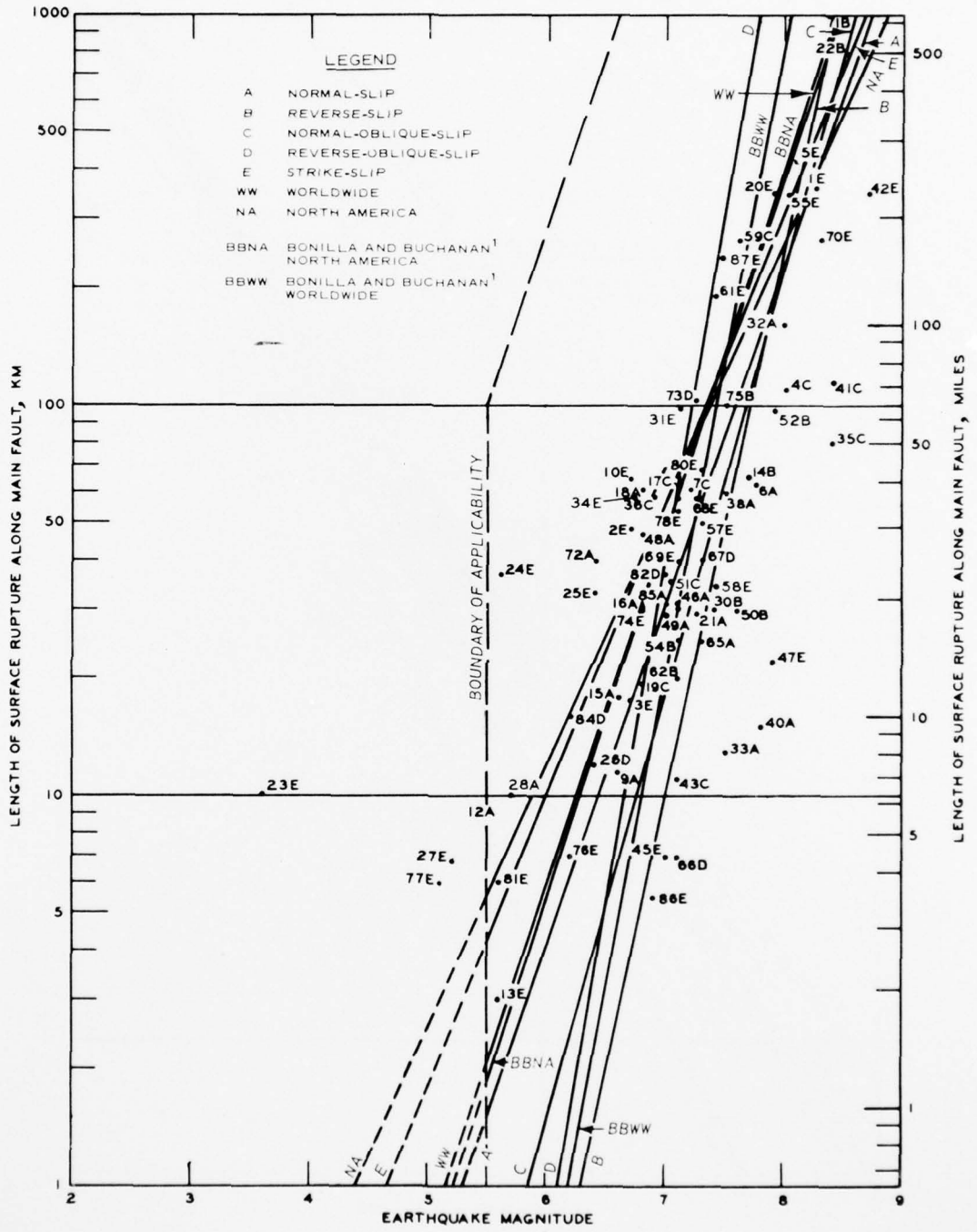


Figure 27. Relation of earthquake magnitude to length of zone of surface rupture along the main fault zone

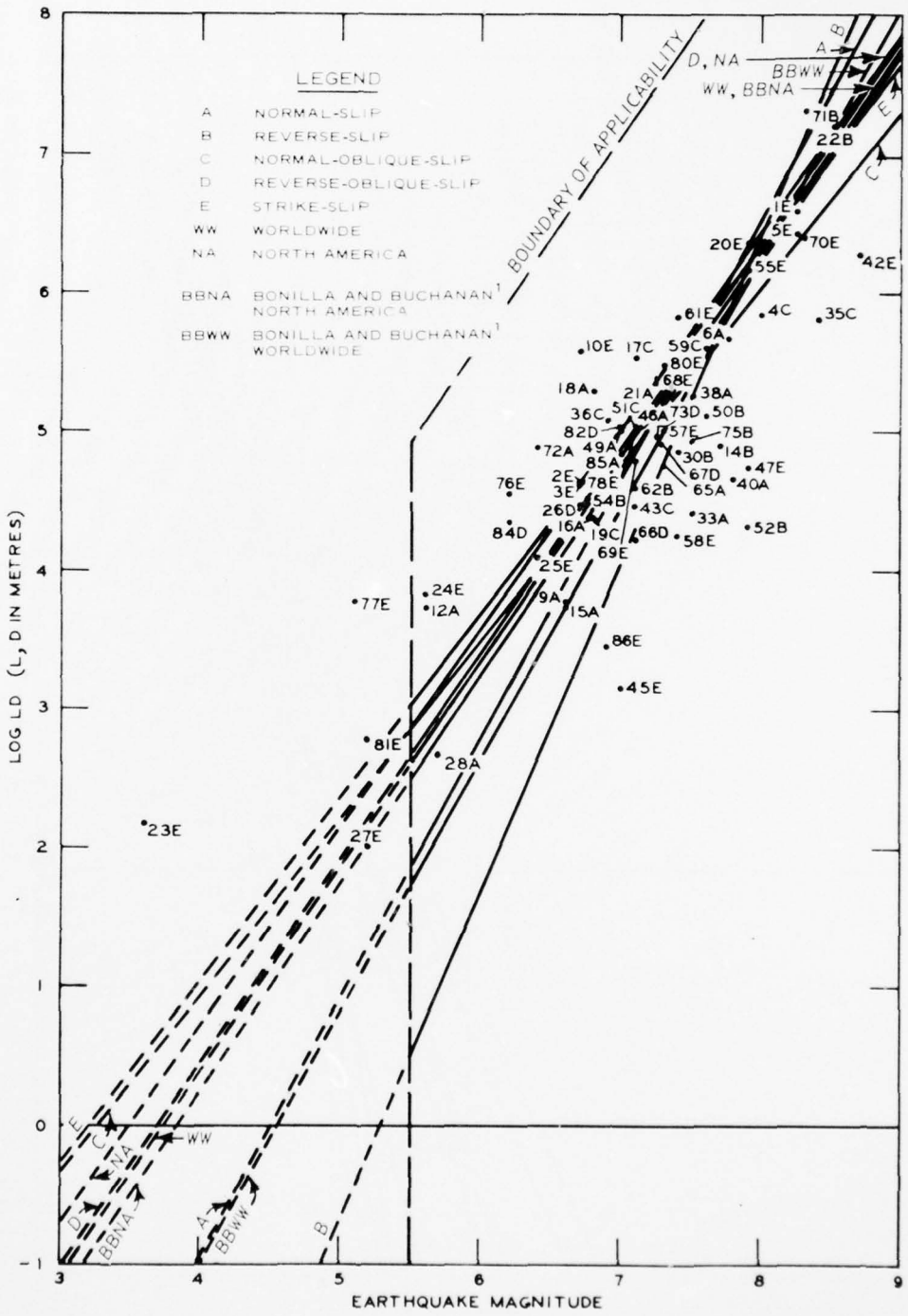


Figure 28. Relation of earthquake magnitude to surface faulting length times maximum surface fault displacement

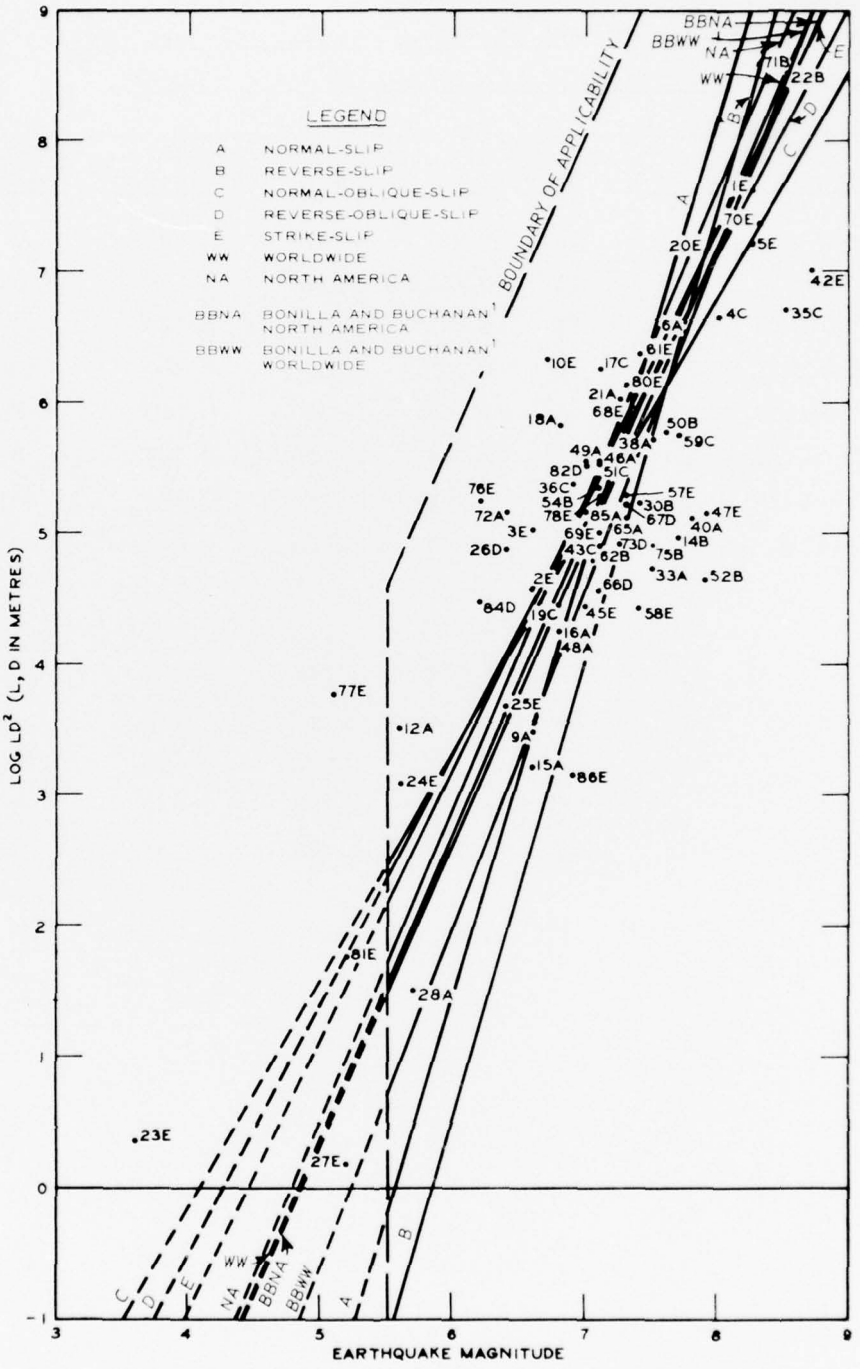


Figure 29. Relation of earthquake magnitude to surface faulting length times square of maximum surface fault displacement

Table 11

Equations of Best Straight-Line Fit for Magnitude Versus Log Displacement: $M = a + b \log D$

Fault	No.	a	b	Standard Deviation	Correlation Coefficient
North America	24	6.745	0.995	0.595	0.840
Rest of world	51	6.821	1.120	0.549	0.643
Worldwide	75	6.750	1.197	0.541	0.791
A normal-slip	20	6.827	1.050	0.449	0.777
B reverse-slip	11	7.002	0.986	0.469	0.744
C normal-oblique-slip	8	6.750	1.260	0.395	0.672
D reverse-oblique-slip	6	6.917	-0.150	0.421	-0.063
E strike-slip	30	6.717	1.214	0.639	0.814
A + C	28	6.757	1.226	0.431	0.774
B + D	17	6.846	1.023	0.506	0.674
C + D + E	44	6.705	1.206	0.586	0.794
C + D	14	6.692	1.165	0.451	0.568
B + E	41	6.767	1.200	0.606	0.811
A + C + E	58	6.737	1.221	0.549	0.806
B + D + E	47	6.742	1.188	0.597	0.795

Table 12

Equations of Best Straight-Line Fit for Log Displacement Versus Log Length: Log D = a + b Log L

Fault	No.	a	b	Standard Deviation	Correlation Coefficient
North America	26	-4.720	1.036	0.632	0.737
Rest of world	48	-1.654	0.444	0.320	0.589
Worldwide	74	-3.185	0.747	0.515	0.645
A normal-slip	20	-4.375	1.014	0.567	0.620
B reverse-slip	9	-2.123	0.568	0.226	0.832
C normal-oblique-slip	8	-0.107	0.128	0.279	0.183
D reverse-oblique-slip	6	1.242	-0.220	0.154	-0.487
E strike-slip	31	-3.571	0.805	0.541	0.703
A + C	28	-2.898	0.705	0.351	0.685
B + D	15	-1.665	0.462	0.276	0.700
C + D + E	45	-2.924	0.684	0.516	0.624
C + D	14	0.033	0.081	0.265	0.130
B + E	40	-3.469	0.797	0.506	0.722
A + C + E	59	-3.239	0.756	0.474	0.680
B + D + E	46	-3.119	0.728	0.501	0.682

Table 13

Equations of Best Straight-Line Fit for Magnitude Versus Log Fault Length: $M = a + b \log L$

Fault	No.	a	b	Standard Deviation	Correlation Coefficient
North America	26	-0.146	1.504	0.628	0.815
Rest of world	49	2.971	0.920	0.500	0.680
Worldwide	75	1.606	1.182	0.603	0.724
A normal-slip	18	1.845	1.151	0.521	0.575
B reverse-slip	9	4.145	0.717	0.167	0.932
C normal-oblique-slip	10	3.117	0.913	0.457	0.604
D reverse-oblique-slip	7	4.398	0.568	0.340	0.522
E strike-slip	31	0.597	1.351	0.694	0.775
A + C	28	2.042	1.121	0.490	0.666
B + D	16	3.355	0.847	0.320	0.833
C + D + E	48	1.149	1.262	0.650	0.737
C + D	17	2.992	0.918	0.437	0.652
B + E	40	1.042	1.277	0.664	0.773
A + C + E	59	1.204	1.260	0.639	0.724
B + D + E	47	1.357	1.217	0.638	0.758

Table 14

Equations of Best Straight-Line Fit for Magnitude Versus Log Length Times Displacement: $M = a + b \log LD$

Fault	No.	a	b	Standard Deviation	Correlation Coefficient
North America	24	3.510	0.701	0.503	0.889
Rest of world	46	4.158	0.610	0.464	0.731
Worldwide	70	3.740	0.680	0.489	0.828
A normal-slip	18	4.551	0.530	0.421	0.750
B reverse-slip	9	5.310	0.423	0.213	0.886
C normal-oblique-slip	8	3.281	0.785	0.325	0.793
D reverse-oblique-slip	6	3.706	0.678	0.353	0.550
E strike-slip	29	3.220	0.759	0.567	0.859
A + C	26	3.691	0.707	0.388	0.792
B + D	15	4.478	0.550	0.327	0.834
C + D + E	43	3.238	0.766	0.510	0.850
C + D	14	3.168	0.802	0.340	0.784
B + E	38	3.424	0.728	0.536	0.859
A + C + E	55	3.393	0.745	0.503	0.837
B + D + E	44	3.441	0.726	0.515	0.853

Table 15

Equations of Best Straight-Line Fit for Magnitude Versus Log Length Times Square of Displacement: $M = a + b \log LD^2$

Fault	No.	a	b	Standard Deviation	Correlation Coefficient
North America	24	4.808	0.420	0.526	0.878
Rest of world	46	4.967	0.417	0.473	0.719
Worldwide	70	4.865	0.427	0.496	0.823
A normal-slip	18	5.568	0.299	0.427	0.742
B reverse-slip	9	5.865	0.289	0.242	0.850
C normal-oblique-slip	8	4.103	0.573	0.309	0.815
D reverse-oblique-slip	6	4.290	0.522	0.373	0.468
E strike-slip	29	4.491	0.480	0.574	0.855
A + C	26	4.752	0.459	0.384	0.796
B + D	15	5.162	0.382	0.350	0.808
C + D + E	43	4.473	0.489	0.513	0.848
C + D	14	3.985	0.590	0.340	0.785
B + E	38	4.597	0.468	0.535	0.859
A + C + E	55	4.582	0.477	0.499	0.840
B + D + E	44	4.587	0.469	0.516	0.852

nucleus of this study, and most of the changes are additions or revisions based on more detailed and recent field observations. In general, with the exception of a shift of the previously anomalous position of some of the relations for reverse-slip faults to one that is closer to that of the other fault types, there are no major differences in position or slope of the new formulations and plots by region or fault type from those of Bonilla and Buchanan. The linear regression analysis shows similar, but somewhat smaller standard deviations on most of the plots, and the improved correlation coefficients indicate increased reliability or closeness of fit for most of the curves. The greatest improvement is represented in reverse-slip and combined reverse-slip and reverse-oblique-slip faults.

Method of Statistical Analysis

111. Examination of standard deviations and correlation coefficients, determined according to conventional procedures, shows the goodness of fit to the straight line, and reflects the importance of the particular parameter shown on determining the magnitude of the resulting earthquake. The displacement parameter shows the best correlation to earthquake magnitude, combined displacement and length parameters show lower correlation coefficients to magnitude, and the fault length parameter provides a moderately good correlation to magnitude.

Data Selected for This Report

112. The data used for this compilation are tabulated in a manner similar to that of Bonilla and Buchanan.[1] Table 16 lists the earthquake reference number, with 28 North American earthquakes and 55 earthquakes from other parts of the world, the type of fault by letter (see Figure 4), the earthquake magnitude, the maximum fault length in metres, the maximum surface fault displacement in metres, date of main earthquake, locality, and main fault(s) activated.

Table 16

Relationships of Earthquake Magnitude, Fault Type, Length of Fault Rupture (in Metres), Maximum Surface Fault Displacement (in Metres), Date of Main Earthquake, Locality, and Name of Fault(s) with Associated Surface Faulting

	Fault Type	Magnitude	Length metres	Maximum Displacement metres	Date	Locality	Fault(s)
1	E	8.20	.3600E 06	.1100E 02	01-09-1857	CA, Ft. Tejon	San Andreas
2	E	6.70	.4830E 05	.9000E 00	10-21-1868	CA, Hayward	Hayward
3	E	6.70	.1770E 05	.2438E 01	12-27-1869	NV, Olinghouse	Olinghouse
4	C	8.00	.1100E 06	.6440E 01	03-26-1872	CA, Owens Valley	Several
5	E	8.25	.4350E 06	.6120E 01	04-18-1906	CA, San Francisco	San Andreas
6	A	7.75	.6200E 05	.5600E 01	10-02-1915	NV, Pleasant Valley	Several
7	C	7.20	.6100E 05		12-20-1932	NV, Cedar Mountain	Several
8	A		.1450E 04	.1220E 00	01-30-1934	NV, Excelsior Mountains	Endowment Mine
9	A	6.60	.1150E 05	.5200E 00	03-12-1934	UT, Hansel Valley	Kosmo
10	E	6.70	.6440E 05	.5790E 01	05-19-1940	CA, Imperial Valley	Imperial
11	E			.7620E-01	04-10-1947	CA, Manix	Manix
12	A	5.60	.8850E 04	.6100E 00	12-14-1950	CA, Ft. Sage Mountain	
13	E	5.60	.3000E 04		01-23-1951	CA, Superstition Hills	
14	B	7.70	.6500E 05	.1220E 01	07-21-1952	CA, Kern County	White Wolf
15	A	6.60	.1770E 05	.3050E 00	07-06-1954	NV, Fallon-Stillwater	Rainbow Mountain
16	A	6.80	.3060E 05	.7620E 00	08-23-1954	NV, Fallon-Stillwater	Rainbow Mountain
17	C	7.10	.5800E 05	.5620E 01	12-16-1954	NV, Fairview Peak	Several
18	A	6.80	.6120E 05	.3250E 01	12-16-1954	NV, Dixie Valley	Several
19	C	6.80	.1931E 05	.1200E 01	02-09-1956	Baja California Norte	San Miguel
20	E	7.90	.3500E 06	.6580E 01	07-10-1958	AK	Fair Weather
21	A	7.25	.2910E 05	.6100E 01	08-17-1959	MT, Hebgen Lake	Several
22	B	8.50	.8000E 06	.2000E 02	04-22-1964	AK	Two or more
23	E	6.60	.1000E 05	.1520E-01	03-04-1966	CA, Imperial	Imperial
24	E	5.60	.3702E 05	.1830E 00	06-28-1966	CA, Parkfield-Cholame	San Andreas
25	E	6.40	.3300E 05	.3800E 00	04-09-1968	CA, Borrego Mountain	Coyote Creek
26	D	6.40	.1200E 05	.2500E 01	02-09-1971	CA, San Fernando	Several
27	E	5.20	.6800E 04	.1500E-01	05-31-1975	CA	Galway Creek
28	A	5.70	.1000E 05	.5500E-01	08-01-1975	CA, Oroville	Cleveland Hill
29	A	0.00	.1287E 06	.9144E 01	06-16-1819	India, Cutch	Allah Bund
30	B	7.40	.3000E 05	.2400E 01	05-08-1847	Japan, Zenkoji	
31	E	7.10	.1000E 06	.6000E 01	10-19-1848	New Zealand	Awatere
32	A	8.00	.1600E 06	.3048E 01	01-23-1855	New Zealand	Wairarapa
33	A	7.50	.1300E 05	.2000E 01	12-26-1861	Greece, Corinth	
34	E	6.70	.5500E 05	.3000E 01	09-01-1888	New Zealand, Amuru	Hope
35	C	8.40	.8000E 05	.8000E 01	10-28-1891	Japan, Mino-Owari or Nobi	Neodani, etc.
36	C	6.90	.5900E 05	.2000E 01	04-27-1894	Greece, Locris	
38	A	7.50	.6000E 05	.3000E 01	08-31-1895	Japan, Riku-U	Senya, Kawafune
39	A	8.70		.1067E 02	06-12-1897	India, Assam	
40	A	7.80	.1500E 05	.3000E 01	02-01-1903	Mongolia, Gurban Saikan	
41	C	8.40	.1150E 06		07-09-1905	Mongolia	Tsetserleg
42	E	8.70	.3500E 06	.5400E 01	07-23-1905	Mongolia	Khangai
43	C	7.10	.1100E 05	.2710E 01	03-17-1906	Taiwan	Meitzukeng
44	E	7.75		.2500E 01	08-09-1912	Turkey	
45	E	7.00	.7000E 04	.2000E 00	05-23-1925	Japan, Tajami	
46	A	7.10	.3200E 05	.3353E 01	01-06-1928	Kenya, Subukai	Gomura
47	E	7.90	.3500E 05	.2700E 01	03-07-1927	Japan, Tango	
48	A	6.80	.4700E 05	.5000E 00	04-14-1928	Bulgaria, Chirpan	
49	A	7.00	.2900E 05	.3500E 01	04-18-1928	Bulgaria, Popovitsa	
50	B	7.60	.3000E 05	.5160E 01	06-17-1929	New Zealand, W. Nelson	White Creek
51	C	7.10	.3200E 05	.3300E 01	11-25-1930	Japan, N-Izu	Tanna, etc.
52	B	7.90	.9700E 05	.3600E 01	02-03-1931	New Zealand, Hawkes Bay	
54	B	7.10	.2500E 05	.3000E 01	04-21-1935	Taiwan	Chihhu
55	E	7.90	.3500E 06	.4200E 01	12-27-1939	Turkey	Anatolia
57	E	7.30	.5000E 05	.2000E 01	12-20-1942	Turkey	Anatolia
58	E	7.40	.3300E 05	.2500E 01	09-10-1943	Japan, Tottori	Shikano, Yoshioka
59	C	7.60	.2650E 06	.1500E 01	11-26-1943	Turkey	Anatolia
60	B	7.60		.6000E 00	01-15-1944	Argentina, San Juan	
61	E	7.40	.1900E 06	.3600E 01	02-01-1944	Turkey	Anatolia
62	B	7.10	.2000E 05	.2000E 01	01-13-1945	Japan, Mikawa	Fukozu, Yokosuka
63	A	7.25		.3500E 01	11-10-1946	Peru, Ancash	
64	E	0.00	.6000E 04	.2000E 01	12-05-1946	Taiwan	Sinhua
65	A	7.30	.2500E 05	.2300E 01	06-28-1948	Japan, Fuqui	
66	D	7.10	.7000E 04	.2300E 01	10-22-1951	Taiwan	Meiluu
67	D	7.30	.4000E 05	.2080E 01	11-25-1951	Taiwan	Yuli
68	E	7.25	.5800E 05	.4300E 01	03-18-1953	Turkey, Yenice-Gonen	
69	E	7.10	.4000E 05	.1600E 01	05-26-1957	Turkey, Abant	Anatolia
70	E	8.30	.2650E 06	.9500E 01	12-04-1957	Mongolia, Gobi-Altai	Bagdu
71	B	8.30	.1000E 07	.2000E 02	05-22-1960	Chile	
72	A	6.40	.4000E 05	.1900E 01	06-02-1961	Ethiopia	
73	D	7.25	.1030E 06	.9000E 00	09-01-1962	Iran, Buyin-Zara	
74	E	6.80	.3000E 05		10-06-1964	Turkey	
75	B	7.50	.1000E 06	.9000E 01	06-16-1964	Japan, Niigata	
76	E	6.20	.7000E 04	.5000E 01	08-03-1966	Japan, Matsushiro	
77	E	5.10	.6000E 04	.1000E 01	10-09-1966	Sudan, Jebel Dumbeir	
78	E	7.10	.5400E 05	.1900E 01	07-22-1967	Turkey, Mudurnu Valley	Anatolia
80	E	7.30	.6900E 05	.4500E 01	08-31-1968	Iran, Dasht-e Bayaz	
81	E	5.20	.6000E 04	.1000E 00	09-24-1968	Turkey	Anatolia
82	D	7.00	.4300E 05	.3030E 01	10-14-1968	Australia, Meckering	
83	B	5.70		.4000E 00	07-24-1969	Peru, Pariahuano	
84	D	6.20	.1600E 05	.1400E 01	10-01-1969		
85	A	7.00	.3100E 05	.2200E 01	03-28-1970	Turkey, Gediz	Several
86	E	6.90	.5500E 04	.5100E 00	05-09-1974	Japan, Izo-Honto-Aki	Irozaki-North
87	E	7.50	.2300E 06	.3400E 01	02-04-1976	Guatemala	

PART VII: FAULT RUPTURE PATTERNS

Introduction

113. Analysis of patterns of faults, folds, and warps along or near active fault zones is essential to determine fault length and type of faulting to be expected. This analysis varies in difficulty from the relatively simple, commonly straight, in places branching patterns of subparallel faults of major strike-slip fault zones, to broad zones of diverse fracture pattern, with distributed, conjugate, en echelon, or complex patterns of many normal-slip and reverse-slip fault zones. All types may be associated with genetically related folds or warps, particularly where distortion by folding or drag provides transitions into monoclinal or other fold types and thereby reduces or eliminates the fault slip component of deformation. In general, the sequence in fault types, from strike-slip, to normal-slip, to reverse-slip, represents increase in complexity of fracture patterns, decrease in fault continuity, and increase in difficulty of analysis and evaluation.

114. The evaluation of each type requires geomorphic, structural, and stratigraphic analysis, with supplemental study by seismologic, geophysical, or geodetic methods. The geomorphic features express the type of fault, and their analysis should consider fracturing at all scales from local to regional as noted in Appendix A.

Types of Distributed and Branching Faults

115. Several types of distributed fracture patterns develop simultaneously from closely related tectonic processes--these include formation of branching faults, antithetic faults, and conjugate fault systems that may combine in the regional deformation by faulting and folding.

116. Branch faults are defined by Bonilla[8] by means of a diagram showing the main fault zone, a branch fault, and two secondary faults (Figure 30). The main fault is the fault with greatest displacement,

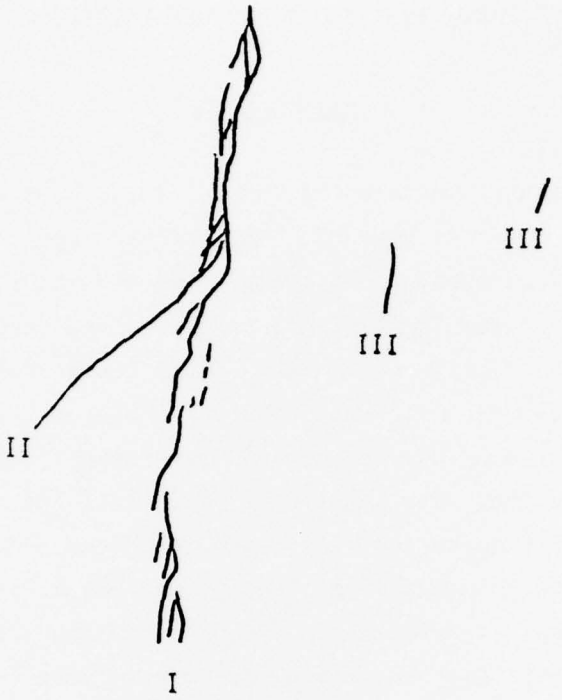


Figure 30. Diagram showing (I) main fault zone; (II) branch fault; and (III) secondary faults (from Bonilla[8])

length, and continuity, and branching faults are those that connect with the main fault, often at an acute angle suggestive of a conjugate relation. The lesser displacements may be easily overlooked in field studies and are, as Bonilla recognized, even more common than the source literature indicates. Bonilla's[9] table of data on displacements indicates 8 examples with branch faults and 10 without branch faults. This writer's unpublished data demonstrate that branch faults are present in three additional cases: the Owens Valley, California, earthquake area of 1872, the Pleasant Valley, Nevada, earthquake area of 1915, and the Dixie Valley, Nevada, earthquake area of 1954. Surface faulting in San Fernando, California, in 1971 provided abundant evidence of branch faulting (Figure 9). The 1954 surface faulting along the Gold King fault on the east side of Dixie Valley has branch faults (Slemmons,[119] and Slemmons et al.[120]), but the sketchy nature of the map of the 1903? faulting precludes recognition of any branching at the time of the 1903? earthquake.

117. Antithetic faults are defined as nearly parallel normal faults with rotation fault-bounded blocks such that the net slip on each fault is greater than it would be without rotation. Such faults appear to be in opposition to the general uplift so that fault scarps tend to face the mountain range. Within the Basin and Range Province of the western United States, an example of this type has been described by Thompson and White[121] in the Mount Rose area near Reno, Nevada (Figure 31). The generally upfaulted and upwarped Mount Rose has Tertiary volcanic rocks and alluvial sediments that dip away from the central axis of the arched area, just east of the crest of the range, and the fault planes of the two flanks of the mountain have many normal faults that dip toward the mountain block and have surface fault scarps that face the uplifted region. This type of faulting may result from the stretching of shallow sediments and volcanic rocks to provide a thin-skin, brittle failure from the extensional forces developed by the upwarp as shown on the cross section of Mount Rose (Figure 31).

118. Other examples of antithetic faulting from the Basin and Range region include the Coyote Uplift, near Bishop, California, and Pilot Mountain, east of Mina, Nevada. No historic examples of antithetic faults slipping are known, but all three of the above examples have fault scarps with Holocene displacement and all are in seismically active regions.

119. Conjugate faults are defined as faults of the same age and tectonic origin, although they have different orientations. The conjugate fracturing can develop simultaneously at all scales from microfractures through small-scale fault trace fractures, through scales represented for most faults encountered in field mapping, to major structures like the San Andreas and Garlock fault zones in California (Tchalenko,[122] Larson,[123] Nakamura and Tsuneishi,[116] and Huzita et al.[69]).

120. The complex interrelations between folding and faulting of a variety of types and orientations are described by Huzita et al.[69] for southwest Japan (Figure 15). The complex conjugate sets include combinations of strike-slip and reverse-slip and provide an especially good example of complex development of conjugate strike-slip and reverse-slip



Figure 31. Antithetic faults of the Carson Range-Truckee Meadows area (after Thompson and White[121])

fault patterns from the horizontal tectonic compression of east-west orientation, as shown in Figure 32. Three types of deformation are developed in this region: Type A, an undulatory warping or folding; Type B, a tear fault due to a boundary between folded and faulted blocks; and Type C, development of conjugate shear planes due to compressive stress in brittle rock units (see Figure 15). Type C is divided into three variants: (a) where the II blocks are separated from I blocks by shear planes that are considered to swell on the free surface by pushing of I blocks; (b) where the strain is released by tilting of I blocks; and (c) where the orthogonal or rhombic fault blocks move like a mosaic combining both types (a) and (b).

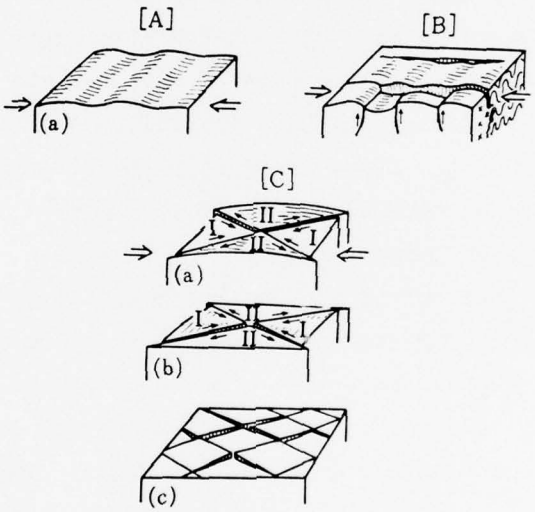


Figure 32. Models of three fundamental structures of basement due to horizontal compression. A: foundation folding predominant in the granitic region. B: tear fault occurring along the boundary between two geologic bodies showing different deformation. C: mosaic movements of the rhombic fault blocks bounded by the conjugate shear planes predominant in the Paleozoic region (Huzita el al.[69])

PART VIII: SIZE AND SHAPE OF AREA TO BE EVALUATED

General Comments

121. The size and shape of the area to be studied vary with the importance of the engineering structure being considered and the distribution and type of faults in the region. Examination of historic examples of surface faulting shows variation in shape of tectonic disturbance that varies from elongate for strike-slip faults to oval, less elongate areas for megathrust fault zones, to equidimensional for most normal-slip and reverse-slip faults. The following examples of each of the four main types provide guidelines for determination of the approximate dimensions and shape of the area required for evaluation. The final selection of the size of the area may be modified to encompass faults with design earthquake magnitudes that would result in potential damage at the site. Generally these examples demonstrate the need for a regional tectonic approach that commonly involves a study area of 150-km or larger radius.

122. The regulations of the Nuclear Regulatory Commission (1973) for reactor siting[23,28] and the recommendations of Sherard et al.[24] for dam siting studies suggest that most studies should include a generally circular study area that has a 150- to 300-km radius (the Nuclear Regulatory Commission requires a 200-mile radius). The detail of the study should be increased near the site.

123. The area of detailed study commonly requires aerial photography and imagery analysis, field mapping, trenching across faults, subsurface drilling and/or geophysical studies, and microearthquake studies. The trenching studies should include application of the special techniques listed in Taylor and Cluff[74] and Krinitzsky.[29]

Megathrust Fault Zones

124. The 1964 Alaska earthquake of 8.5 magnitude disturbed an elongate zone over 800 km in length and between 240 and 500 km in width.

The width of the zones of aftershocks and geodetic changes of megathrust zones may vary according to the dip of the Benioff zone. Seismologists generally predict a maximum length of 800 to 1600 km for an earthquake that would fill a gap or extend the zone of previous earthquake activity. Faults above the megathrust fault plane are capable of generating earthquakes, generally of lower magnitude related to their individual lengths, maximum displacement, and focal depth. There are many active faults above the 1964 Alaska megathrust fault plane that were not activated by the 1964 earthquake (Brogan et al.[63]); their future design events can be individually estimated and their activation may occur independently of future displacements along the megathrust fault plane.

125. The determination of design earthquakes can be accomplished by seismological methods (Fedetov;[124] Kelleher and Savino[65]) for the more frequent larger events on the megathrust fault plane, with some associated branching activity on other active faults of the region. These zones may be marked by some increase in activity prior to large earthquakes of bilateral symmetry, or the faulting may propagate into a historically aseismic segment with unilateral symmetry from an adjoining region. The earthquakes are generally of magnitude 8 or higher, and the zone of faulting is commonly measured in hundreds of kilometres. Other faults of megathrust regions may be strike-slip, normal-slip, or smaller branching or isolated reverse-slip faults above the Benioff zone. These faults can be independently evaluated; their magnitudes may be as great as 8 to 8.5.

Strike-Slip Fault Zones

126. Geodetic movements and aftershock activity associated with the 1906 and more recent strike-slip earthquakes of the San Andreas fault system indicate patterns of activity that are much more elongate than for other fault-slip types. The main zone of 1906 surface faulting exceeded 400 km in length and the main geodetic deformation in the 100-km-wide zone between Farallon Islands and Mt. Diablo was in an even narrower zone near the San Andreas fault (Thatcher[40]). The relatively

narrow widths of surface faulting and geodetic change for strike-slip fault zones may be related to branching or parallel fault domains that limit the width of strain accumulation that is allowed without exciting activity on other faults. The great length and continuity of many strike-slip faults, with lengths measured in hundreds or thousands of kilometres, require that design fault studies be undertaken on a regional basis. The length of the study area should at least be equal to the maximum length likely to be activated during an earthquake, and preferably should include the entire fault system. The width of the study area around the site should at least be equal to the radius of potential damage from earthquakes generated on distant faults. For example, the rock acceleration versus fault distance and earthquake magnitude charts listed in Table 1 indicate that rock accelerations of 0.10 g may be obtained at a distance of 100 km for an earthquake of 8.25 magnitude. For a design value of 0.10 g, the fault study should at least include a region of 100-km radius about the site.

Normal-Slip Fault Zones

127. The 1954 central Nevada earthquakes developed a complex zone of surface faulting in a region about 100 km in north-south length and 50 km in east-west width. The geodetically deformed region was at least 100 km in north-south dimension and was about 100 km in east-west dimension (Savage and Hastie[102]). Although the geodetic changes included a major strike-slip component as well as an east-west extension, the example suggests a crudely circular or oval region of geodetic disturbance for normal-slip faults. This subequal dimension of deformation suggests that for Basin and Range types of faulting, fault studies should include an area of study that is approximately as wide as the longest cases of historic surface faulting, about 120 to 160 km (75 to 100 miles) for the 1872 Owens Valley earthquake, or about 100 km for the better known 1954 earthquake sequence of surface faulting. This is also about the distance from larger earthquakes that would give ground motion of about 10 percent of the acceleration of gravity.

Reverse-Slip Fault Zones

128. Zones characterized by reverse-slip faults provide the most complex types of zones to evaluate (see Figure 9). The geomorphic expression of thrust faults is difficult to identify, the fracture patterns may be complex as shown in Figure 30, and many branch faults may be present in the hanging block above the fault plane. The 1971 San Fernando earthquake produced a broad zone of distributed faulting, and had a somewhat larger, oval area of geodetic change and aftershock activity. The San Fernando faulting activated only a short segment of the longer Santa Susana fault system (Jennings[99]). The branching character of this system would allow possible connections with the Sierra Madre and other reverse-slip and reverse-oblique-slip faults of the Transverse Ranges of southern California. The historic record shows that some of the high-angle reverse-oblique-slip faults of Japan have ruptured from end to end with earthquakes of about 8 magnitude (Matsuda[113]).

129. The oval shape of geodetic change and aftershock activity, and the possibility of high-magnitude events along longer fault zones of this type require regional studies for evaluation of design earthquakes. The size for regional evaluation is similar to that for strike-slip and reverse-slip faults, about 100 to 150 km. The complexity of patterns and the need for determination of fault continuity require careful and detailed studies along the strike and in the hanging wall block of all reverse faults near the site.

Summary

130. The size and shape of the study area are generally determined by the type of faulting and distance to active faults that are capable of producing damaging ground motion at the site. Generally oval or somewhat elongate shaped areas should be studied, with the long axis of the area oriented along the strike of the main faults of the region. Megathrust zones and major strike-slip fault zones should be

evaluated for distances of hundreds to thousands of kilometres as noted by Fedetov[124] and Kelleher and Savino.[65] Shorter reverse-slip and strike-slip faults, and normal-slip faults, including those of complex conjugate patterns, require a more equidimensional study area, with the radius of the study area up to about 100 to 150 km. Consideration should be given to the possiblity of bilateral propagation into aseismic or weakly seismic areas, with lengths of faulting of 50 to 150 km and earthquakes of magnitudes of about 8.

PART IX: DETERMINATION OF FAULT LENGTH AND EARTHQUAKE MAGNITUDE FOR EN ECHELON AND CONJUGATE FAULT SYSTEMS

131. The most important element in assigning design earthquakes from fault length is the proper determination of fault continuity. For major faults of great length and good outcrop exposure, the determination is simple; for more complex faults, or for faults with poor exposures or with concealed segments, many of the techniques described in Part V of this report will be required to resolve continuity. Special studies (listed in Table 8) may be required to resolve continuity or activity of specific fault zones.

132. Bonilla[8,9] described subsidiary faulting--branch faults and secondary faults. He quantitatively showed that the amount of displacement on branch and secondary faults decreased rapidly with distance from the main fault. The independent strain accumulation on the Calaveras and Hayward fault branches relative to the San Andreas fault, shown by recent geodetic deformation (Thatcher[40]), suggests that design earthquakes for sites should include determinations of design earthquakes for each branch or secondary fault, as well as for the main fault in the region.

133. Estimates of maximum magnitude earthquakes for the San Andreas fault and the Hayward and Calaveras branch faults are given in Table 17, with the assumption that one-half of the total fault length would break in a maximum earthquake. The use of one-half of the total fault length, rather than the full fault length, is based on the observation that the surface faulting rarely affects the full fault length. This method of independent selection of design events gives similar results to that discussed below for en echelon and conjugate fault systems.

134. Analysis of en echelon fault systems is illustrated for the complex pattern of faulting on at least four main overlapping fault segments of the 1915 Pleasant Valley fault system as shown in Figure 7, and the 1954 Fairview Peak fault zone between Dixie Valley and Mt. Anna as shown in Figure 8. The Pleasant Valley earthquake developed the pattern shown in Figure 7, with a pattern that affected the western

Table 17

Estimates of Earthquake Magnitude for the San Andreas, Calaveras, and Hayward Fault Zones California (Modified from U. S. Geological Survey Professional Paper 941-A)

Fault Zone	Magnitude of Largest Earthquake	Total Known Fault Half-Length, km	Earthquake Magnitude					
			Tocher[4]	Iida[6]	Bonilla and Buchanan[1]	U.S.G.S. Average (1975)	Bonilla and Buchanan*	Slemmons (This Report)
San Andreas	8.3	600	8.1	8.2	9.9	8.5**	8.4	8.4
Calaveras	6	57.5	7.2	7.4	7.3	7.3	7.2-	7.0
Hayward	6.7†	36	6.7	7.0	6.8	7.0	6.9	6.8-

Tocher:[4] $M = 0.9 \log_{10} L + 5.6$

Iida:[6] $M = 0.76 \log_{10} L + 6.07$

Bonilla and Buchanan:[1] $M = 2.57 \log_{10} L + 2.79$ for strike-slip faults

* Bonilla and Buchanan[1] 1970 data recalculated (see Table 4 herein).

** A value close to the maximum historic earthquake was adopted for this fault.

† Slemmons, new determination; the equations used for determining magnitude are for half-length in kilometres.

edge of four mountain fault blocks to the east of the Sou Hills Scarp, the Pearce Scarp, the Tobin Scarp, and the China Mountain Scarp. A possible fifth scarp of questionable origin may extend the en echelon zone an additional 15 km to the southwest. This set of faults forms a prominent set that can be inferred from the topographic map, with distinct truncations of the pattern at both the northern and southern ends of the zone. These truncations are suggested by microearthquake surveys of the northern end (Wollenberg, personal communication, 1976) and by geophysical anomaly patterns. The 1954 Fairview Peak fault zone has more continuity of faulting, although many en echelon branches are present near the southern part of this zone. The northern and southern truncations are major topographic truncations, and the southern end of the surface faulting abuts against a major tectonic structure, the Walker Lane, and is marked by cross-structure shown in the microearthquake activity (Ryall and Malone[71]) and by coincident strong anomalies in the aeromagnetic map (U. S. Geological Survey[125]).

135. Conjugate fault systems include swarms of subparallel faults, in part with en echelon patterns as noted for the 1915 and 1954 Fairview Peak earthquakes. In addition, faults with two different trends or orientations have been reported for strike-slip and reverse-slip faults. The Tango earthquake (magnitude = 7.5) in Japan activated the 18-km-long northwest-striking Gomura fault with 2.5 m of left-slip displacement and the nearby 7.5-km-long northeast-striking Yamada fault with 0.8 m of right-slip displacement (Matsuda[113]). Other Japanese examples reported by Matsuda include the 1930 N-Izu conjugate faulting on the Tanna fault system and the Himenoyu fault, and the 1943 Tottori earthquake of 7.4 magnitude that activated the Shikano and Yoshioka faults. The Yakutat Bay earthquakes of 1899, of approximately 8.3 and 8.5 magnitudes, apparently activated conjugate faults with large vertical components of displacement along two main northwest-trending fault zones and two northeast-trending fault zones at Yakutat and Disenchantment Bay (Tarr and Martin[126]). This region was not adequately studied but probably combines northwest-striking right-oblique-slip faults and northeast-trending reverse-slip faulting at Disenchantment Bay. Although these

examples have not been thoroughly evaluated with regard to the total length of the faults involved in the above displacements, their total length would yield estimated magnitudes when taken individually that are probably similar to that reported during their historic conjugate faulting (Plafker, personal communication). The zone of conjugate faulting shown by Huzita et al.[69] as shown in Figure 15 and the active fault map of Japan suggest the presence of many faults with full lengths, or of half-lengths that would give earthquakes of the historically observed range of 7 to 8 magnitude for Japan. The Yakutat Bay earthquake is part of a long zone evaluated by Kelleher and Savino.[65] This zone has earthquakes of about 8 to 8.5 magnitude.

PART X: METHODS OF APPLYING FAULT LENGTH TO DETERMINE DESIGN EARTHQUAKE PARAMETERS

136. The following steps are generally used in applying fault length to magnitude relations:

a. Determination of activity. The rationale outlined in Part IV of this report, and summarized in part in Table 7, is applied to determine whether or not the faults near the site are active. Additional studies to resolve the question of activity may be required for faults of uncertain activity as noted in Table 8. Faults that are active, or that are assumed to be active, require a determination of the maximum probable length.

b. Determination of total fault length. The rationale given in Part V of this report is used to determine the total fault length of all active faults within a radius or range of influence as outlined in Part VIII. Faults with an uncertain continuity, due to portions being concealed by recent deposits, lakes, or ocean, may require special geophysical surveys to determine whether interpolation or extrapolation of known segments will yield a true length. Conservative assumptions of continuity between isolated faults are possible, but may lead to very large design earthquakes.

c. Faults of complex regions of en echelon or conjugate fracture systems should be evaluated as noted in Part IX of this report, to give a somewhat larger combined fault area than individual fault segments would indicate. The maximum length of the combined fault pattern is used for plotting the fault length.

d. Fault lengths are plotted on the charts or are solved by the equations for the worldwide, North America, or fault slip-type to obtain estimated earthquake magnitudes. Since the data of Bonilla and Buchanan are improved and expanded from the earlier determinations of Tocher,[4] Iida,[5,6] or Albee and Smith,[7] there is little justification for averaging their determinative charts with those of Bonilla and Buchanan, or of this report. The results by fault type, North America, or worldwide formulations or plots can be averaged, discussed, and the proper type selected. The method of using fault half-length proposed by Wentworth el al.[127] is based on the statement: "Rupture of the whole length of a fault in a single event seems unlikely, and comparison of historic rupture lengths to length of mapped faults in southern California (Allen et al.,[20] Figure 4) suggests that rupture of only half the length or less is a more likely case,

as pointed out by Albee and Smith." This practice involves uncertainties in percent of rupture length as was noted by Wentworth et al.[127] Allen[84] mentions that this practice does not lead to the most conservative results. Allen also mentions the work of Matsuda,[85] who studied the Nobi earthquake of 1891 in Japan, in which during a magnitude 8 earthquake the full length of a fault was ruptured. The method is convenient and the 50% rupture length is the most widely used and appropriate percentage with the present state-of-the-art. This method is applied by many U.S.G.S. researchers and by engineers and for many applications the results lead to results that are compatible with other methods.

e. Comparison of results. The design earthquake obtained from fault length should be compared, if possible, with results from maximum displacement. The results of the several methods should be averaged and compared with the maximum earthquake determined from seismological studies. The final design magnitude can then be converted into the required engineering design parameters by relations indicated in Table 1.

PART XI: METHODS OF DETERMINING OR USING MAXIMUM FAULT DISPLACEMENT

137. The detailed field analysis, based either on geomorphic features or stratigraphic offsets, can give the maximum fault displacements of past faulting events. This value, when plotted directly in Figure 26 or solved by equation in Tables 2 or 11, will determine a design magnitude value. The goodness of fit for this relation is much better than for the value obtained from the fault length, and should be used whenever possible. Use of the relations of magnitude to log LD (Tables 5 and 14, and Figure 28) and magnitude to log LD^2 (Tables 6 and 15, and Figure 29) provides other design earthquake values, but with higher standard deviations for the magnitude value. Where several values are obtained, the results can be averaged for the geological determination, which can then be compared with the seismological determination.

REFERENCES

1. Bonilla, M. G. and Buchanan, J. M., "Interim Report on Worldwide Historic Surface Faulting," Open-File Report, Dec 1970, U. S. Geological Survey, Washington, D. C.

2. Tsuboi, C., "Earthquake Energy, Earthquake Volume, Aftershock Area, and Strength of the Earth's Crust," Physics of the Earth Journal (Tokyo), Vol 4, 1956, pp 63-66.

3. Richter, C. F. Elementary Seismology, Freeman, San Francisco, 1958.

4. Tocher, D., "Earthquake Energy and Ground Breakage," Seismological Society of America Bulletin, Vol 48, No. 2, Apr 1958, pp 147-153.

5. Iida, K., "Earthquake Energy and Earthquake Fault," Nagoya University, Journal, Earth Science, Vol 7, No. 2, 1959, pp 98-107.

6. _____, "Earthquake Magnitude, Earthquake Fault, and Source Dimensions," Nagoya University, Journal, Earth Science, Vol 13, No. 2, 1965, pp 115-132.

7. Albee, A. L. and Smith, J. L., "Earthquake Characteristics and Fault Activity in Southern California," Engineering Geology in Southern California, R. Lung and R. Proctor, eds., Associated Engineering Geologists, Glendale, Calif., 1966, pp 9-33.

8. Bonilla, M. G., "Historic Surface Faulting in Continental United States and Adjacent Parts of Mexico," Open-File Report, 1967, U. S. Geological Survey, Washington, D. C.; also Atomic Energy Commission Report TID-24124.

9. _____, "Surface Faulting and Related Effects in Earthquake Engineering," Earthquake Engineering, Prentice-Hall, Englewood Cliffs, Ch. 3, 1970, pp 47-74.

10. Ambraseys, N. and Tchalenko, J., "Documentation of Faulting Associated with Earthquakes, Part I," Unpublished Manuscript, 1968, Department of Civil Engineering, Imperial College of Science, London.

11. Aki, K., "Scaling Law of Seismic Spectrum," Journal, Geophysical Research, Vol 72, Feb 1967, pp 1217-1231.

12. Brune, J. N., "Seismic Moment, Seismicity and Rate of Slip Along Major Fault Zones," Journal, Geophysical Research, Vol 73, Jan 1968, pp 777-784.

13. Chinnery, M. A., "Earthquake Magnitude and Source Parameters," Seismological Society of America Bulletin, Vol 59, No. 5, Oct 1969, pp 1969-1982.

14. King, C. Y. and Knopoff, L., "Stress Drop in Earthquakes," Seismological Society of America Bulletin, Vol 58, No. 1, Feb 1968, pp 249-257.

15. King, C. Y. and Knopoff, L., "A Magnitude-Energy Relation for Large Earthquakes," Seismological Society of America Bulletin, Vol 59, No. 1, Feb 1969, pp 269-273.

16. Press, F., "Dimensions of the Source Region for Small Shallow Earthquakes," Proceedings, VESIAC Conference on the Source Mechanism of Shallow Seismic Events, VESIAC Report 7885-1-x, 1967, pp 155-164.

17. Wyss, M. and Brune, J. N., "Seismic Moment, Stress, and Source Dimensions for Earthquakes in the California-Nevada Region," Journal, Geophysical Research, Vol 73, No. 14, 1968, pp 4681-4694.

18. Liebermann, R. C. and Pomeroy, P. W., "Source Dimensions of Small Earthquakes as Determined from the Size of the Aftershock Zone," Seismological Society of America Bulletin, Vol 60, No. 3, Jun 1970, pp 879-890.

19. Louderback, G. D., "Faults and Engineering Geology," Application of Geology to Engineering Practice, Geological Society of America, S. Paige, Chmn, Berkey Vol, 1950, pp 125-150.

20. Allen, C. R. et al., "Relationship Between Seismicity and Geologic Structures in the Southern California Region," Seismological Society of America Bulletin, Vol 55, Aug 1965, pp 753-797.

21. Wentworth, C. M., Ziony, J. I., and Buchanan, J. M., "Preliminary Geologic Environmental Map of the Greater Los Angeles Area, Calif.," Report TID-25363, 1970, U. S. Geological Survey, Washington, D. C.

22. International Atomic Energy Agency, "Earthquake Guidelines for Reactor Siting," Technical Report Series No. 139, pp 9-10, 1972, Vienna, Austria.

23. U. S. Atomic Energy Commission, "Nuclear Power Plants; Seismic and Geologic Siting Criteria," Federal Register, Vol 38, No. 218, 13 Nov 1973, pp 31, 281-31, and 282.

24. Sherard, J. L., Cluff, L. S., and Allen, C. R., "Potentially Active Faults in Dam Foundations," Geotechnique, Vol 24, No. 3, 1974, pp 367-428.

25. Willis, B., "A Fault Map of California," Seismological Society of America Bulletin, Vol 13, 1923, pp 1-12 with map.

26. Ambraseys, N. N., "Value of Historical Records of Earthquakes," Nature, Vol 232, Aug 1971, pp 375-379.

27. Sharp, R. P., "Some Physiographic Aspects of Southern California," California Division of Mines Bulletin, Part V, Vol 170, No. 3, 1954, pp 21-28.

28. U. S. Atomic Energy Commission, "Nuclear Power Plants; Seismic and Geologic Siting Criteria," Federal Register, Vol 36, No. 228, 25 Nov 1971, pp 22 and 602.

29. Krinitzsky, E. L., "State-of-the-Art for Assessing Earthquake Hazards in the United States; Fault Assessment in Earthquake

Engineering," Miscellaneous Paper S-73-1, Report 2, May 1974, U. S. Army Engineer Waterways Experiment Station, CE, Vicksburg, Miss.

30. Wallace, R. E., "Earthquake Recurrence Intervals on the San Andreas Fault, California," Geological Society of America Bulletin, Vol 81, 1970, pp 2875-2890.

31. Cluff, L. S., Slemmons, D. B., and Waggoner, E. B., "Active Fault Zone Hazards and Related Problems of Siting Works of Man," Proceedings, Fourth International Symposium on Earthquake Engineering, Roorkee University, Indian Society of Earthquake Technical Bulletin, Vol 1, 1970, pp 401-410.

32. Clark, M. M., "Map Showing Recently Active Breaks Along the Garlock and Associated Faults, California," Miscellaneous Geology Investigation Map I-741, Scale 1:24,000, 1973, U. S. Geological Survey, Washington, D. C.

33. Benioff, H., "Orogenesis and Deep Crustal Structure: Additional Evidence from Seismology," Geological Society of America Bulletin, Vol 65, May 1954, pp 385-400.

34. Oliver, J., "Contributions of Seismology to Plate Tectonics," American Association of Petroleum Geologists Bulletin, Vol 56, No. 2, 1972, pp 214-225.

35. Kasahara, K., "The Nature of Seismic Origins Inferred from Seismological and Geodetic Observations," Earthquake Research Institute, Tokyo University Bulletin, Vol 35, 1957, pp 474-532.

36. Chinnery, M. A., "The Deformation of the Ground Around Surface Faults," Seismological Society of America Bulletin, Vol 51, No. 3, Jul 1961, pp 355-372.

37. Thatcher, W., "Strain Accumulation and Release Mechanism of the 1906 San Francisco Earthquake," Journal, Geophysical Research, Vol 80, No. 35, Dec 1975, pp 4862-4872.

38. Eaton, J. P., O'Neill, M. E., and Murdock, J. N., "Aftershocks of the 1966 Parkfield-Cholame, California, Earthquake: A detailed Study," Seismological Society of America Bulletin, Vol 60, No. 4, Aug 1970, pp 1151-1197.

39. U. S. Department of Commerce, National Ocean Surveys, "Reports on Geodetic Measurements of Crustal Movement, 1906-71," 1973, Government Printing Office, Washington, D. C.

40. Thatcher, W., "Strain Accumulation on the Northern San Andreas Fault Zone Since 1906," Journal, Geophysical Research, Vol 80, No. 35, 1975, pp 4873-4880.

41. Hofmann, R. B., "State-of-the-Art for Assessing Earthquake Hazards in the United States; Factors in the Specification of Ground Motions for Design Earthquakes in California," Miscellaneous Paper S-73-1, Report 3, June 1974, U. S. Army Engineer Waterways Experiment Station, CE, Vicksburg, Miss.

42. Krinitzsky, E. L. and Chang, F. K., "State-of-the-Art for Assessing Earthquake Hazards in the United States; Earthquake Intensity and the Selection of Ground Motions for Seismic Design," Miscellaneous Paper S-73-1, Report 4, Sep 1975, U. S. Army Engineer Waterways Experiment Station, CE, Vicksburg, Miss.

43. Gutenberg, B. and Richter, C. F., "Earthquake Magnitude, Intensity, Energy, and Acceleration," Seismological Society of America Bulletin, Vol 46, Apr 1956, pp 105-145.

44. Schnabel, P. B. and Seed, H. B., "Acceleration in Rock for Earthquakes in the Western United States," Seismological Society of America Bulletin, Vol 63, No. 2, Apr 1973, pp 501-516.

45. Benioff, H., "Ground Movement in the Vicinity of the Fault," 1962, Unpublished report to Chief Engineer, California Department of Water Resources, Sacramento, Calif.

46. Seed, H. B., "The Response of Earth Dams During Earthquakes," Proceedings, Seismic Instrumentation Conference on Earth and Concrete Dams, 1970, U. S. Army Engineer Waterways Experiment Station, CE, Vicksburg, Miss.

47. Housner, G. W., "Intensity of Earthquake Ground Shaking near the Causative Fault," Proceedings, Third World Conference on Earthquake Engineering, New Zealand, Vol 1, 1965.

48. Krishna, J., "Seismic Data for the Design of Structures," Proceedings, Second World Conference on Earthquake Engineering, Japan, Vol 3, 1960.

49. Boore, D. M. and Page, R. A., "Accelerations near Moderate Sized Earthquakes," Manuscript approved for publication, 1972, U. S. Geological Survey, Washington, D. C.

50. Figueroa, J. A., "Some Considerations About the Effect of Mexican Earthquakes," Proceedings, Second World Conference on Earthquake Engineering, Japan, Vol 3, 1960, pp 1553-1561.

51. Jenschke, V. A., Clough, R. W., and Penzien, J., "Characteristics of Strong Ground Motions," Proceedings, Third World Conference on Earthquake Engineering, Vol 1, 1965, pp 125-142.

52. Neumann, F., Earthquake Intensity and Related Ground Motion, University of Washington Press, Seattle, 1954.

53. Coulter, H. W., Waldron, H. H., and Devine, J. F., "Seismic and Geologic Siting Considerations for Nuclear Facilities," Proceedings, Fifth World Conference on Earthquake Engineering, Rome, Paper 302, 1973.

54. Hershberger, J., "A Comparison of Earthquake Accelerations with Intensity Ratings," Seismological Society of America Bulletin, Vol 46, No. 4, Oct 1956, pp 317-320.

55. Trifunac, M. D. and Brady, A. G., "On the Correlation of Seismic Intensity Scales with the Peaks of Recorded Strong Ground Motion,"

Seismological Society of America Bulletin, Vol 65, Feb 1975, pp 139-162.

56. Brune, J. N. and Allen, R. C., "A Low-Stress-Drop, Low-Magnitude Earthquake with Surface Faulting--the Imperial, California, Earthquake of March 4, 1966," Seismological Society of America Bulletin, Vol 57, No. 3, Jun 1967, pp 501-514.

57. Matsuda, T., "Magnitude and Recurrence Interval of Earthquakes from a Fault (in Japanese)," Earthquake, Series 2, Vol 28, 1975, pp 269-283.

58. Isacks, B., Oliver, J., and Sykes, L. R., "Seismology and the New Global Tectonics," Journal, Geophysical Research, Vol 73, Sep 1968, pp 5855-5899.

59. Le Pichon, X., "Sea-Floor Spreading and Continental Drift," Journal, Geophysical Research, Vol 73, Jun 1968, pp 3661-3697.

60. Dewey, J. F. and Bird, J. M., "Mountain Belts and the New Global Tectonics," Journal, Geophysical Research, Vol 75, May 1970, pp 2625-2647.

61. Morgan, W. J., "Deep Mantle Convection Plumes and Plate Motions," American Association of Petroleum Geologists Bulletin, Vol 56, 1972, pp 203-213.

62. Smith, R. B. and Sbar, M. L., "Contemporary Tectonics and Seismicity of the Western United States with Emphasis on the Intermountain Seismic Belt," Geological Society of America Bulletin, Vol 85, Aug 1974, pp 1205-1218.

63. Brogan, G. E. et al., "Active Faults of Alaska," Tectonophysics, Vol 29, 1975, pp 73-85.

64. Plafker, G., "Alaska Earthquake of 1964 and Chilean Earthquake of 1960," Journal, Geophysical Research, Vol 77, No. 5, Feb 1972, pp 901-925.

65. Kelleher, J. and Savino, J., "Distribution of Seismicity Before Large Strike-Slip and Thrust-Type Earthquakes," Journal, Geophysical Research, Vol 80, No. 2, Jan 1975, pp 260-271.

66. Savage, J. C. and Hastie, L. M., "Surface Deformation Associated with Dip-Slip Faulting," Journal, Geophysical Research, Vol 71, Oct 1966, pp 4897-4904.

67. Plafker, G., "Tectonic Deformation Associated with the 1964 Alaska Earthquake," Science, Vol 148 (3678), 1965, pp 1675-1687.

68. _____, "Tectonics of the March 27, 1964 Alaska Earthquake," Professional Paper 543-I, pp I1-I74, 1969, U. S. Geological Survey, Washington, D. C.

69. Huzita, K., Kishimoto, Y., and Shiono, K., "Neotectonics and Seismicity in the Kinki Area, Southwest Japan," Osaka City University Journal of Geoscience, Vol 16, 1973, pp 93-124.

70. Oakeshott, G. B., "Patterns of Ground Ruptures in Fault Zones Coincident with Earthquakes: Some Case Histories," Geology, Seismicity, and Environmental Impact, Special Publication, pp 287-312, 1973, Association of Engineering Geologists, Los Angeles, Calif.

71. Ryall, A. S., Slemmons, D. B., and Gedney, L. D., "Seismicity, Tectonism, and Surface Faulting in the Western United States," Seismological Society of America Bulletin, Vol 56, No. 5, 1966, pp 1105-1135.

72. Cluff, L. S. et al., "Site Evaluation in Seismically Active Regions--an Interdisciplinary Team Approach," International Conference on Microzonation, 1972.

73. Hamilton, R. M., "Aftershocks of the Borrego Mountain Earthquake from April 12 to June 12, 1968," The Borrego Mountain Earthquake of April 9, 1968, Professional Paper 787, pp 31-54, 1972, U. S. Geological Survey, Washington, D. C.

74. Taylor, C. L. and Cluff, L. S., "Fault Activity and Its Significance Assessed by Exploratory Excavation," Proceedings, Conference on Tectonic Problems of the San Andreas Fault System, R. L. Kovach and A. Nur, eds., Stanford University Publications, Geological Sciences, Publisher, Stanford, Calif., Vol 13, 1973, pp 239-247.

75. Clark, M. M., Grantz, A., and Rubin, M., "Holocene Activity of the Coyote Creek Fault as Recorded in Sediments of Lake Cahuilla," Professional Paper 787, pp 112-130, 1972, U. S. Geological Survey, Washington, D. C.

76. Dickinson, W. R. and Grantz, A., "Indicated Cumulative Offsets Along the San Andreas Fault in the California Coast Ranges," Proceedings, Conference on Geological Problems of San Andreas Fault System, Stanford University Publications, Geological Sciences, Publisher, Stanford, Calif., Vol 11, 1968, pp 117-119.

77. Slemmons, D. B., "Pliocene and Quaternary Crustal Movements of the Basin-and-Range Province, U. S. A.," Osaka City University Journal of Geoscience, Vol 10, 1967, pp 91-103.

78. Sugimura, A. and Matsuda, T., "Atera Fault and Its Displacement Vectors," Geological Society of America Bulletin, Vol 76, 1965, pp 509-522.

79. Sugimura, A., "Uniform Rates and Duration Period of Quaternary Earth Movements in Japan," Osaka City University Journal of Geoscience, Vol 10, 1967, pp 23-25.

80. Lamar, D. L., Merifield, P. M., and Proctor, R. J., "Earthquake Recurrence Intervals on Major Faults in Southern California," Geology, Seismicity, and Environmental Impact, Association of Engineering Geologists, Special Publication, University Publishers, Los Angeles, 1973, pp 265-276.

81. Wentworth, C. M. and Yerkes, R. F., "Geologic Setting and Activity of Faults in the San Fernando Area, California," San Fernando,

California, Earthquake of February 9, 1971, Professional Paper 733, pp 6-16, 1971, U. S. Geological Survey, Washington, D. C.

82. Wahrhaftig, C. et al., "Nature and Timing of Movement on Hines Creek Strand of Denali Fault System, Alaska," Geology, Vol 3, No. 8, 1975, pp 463-466.

83. Ambraseys, N. N., "Maximum Intensity of Ground Movements Caused by Faulting, Santiago, Chile," Proceedings, Fourth World Conference on Earthquake Engineering, Vol 1, 1969, pp 705-740.

84. Allen, C. R., "Geological Criteria for Evaluating Seismicity," Geological Society of America Bulletin, Vol 86, Nov 1975, pp 1041-1057.

85. Matsuda, T., "Surface Faults Associated with the Nobi (Mino-Owari) Earthquake of 1891, Japan" (in Japanese), Special Bulletin No. 13, pp 85-126, 1974, Earthquake Research Institute, Tokyo University, Japan.

86. Matsuda, T. and Okada, A., "Studies of Active Faults in Japan" (in Japanese), Quaternary Research, Vol 7, 1968, pp 188-199.

87. Slemmons, D. B., "New Methods of Studying Regional Seismicity and Surface Faulting," American Geophysical Union Transactions, EOS, Vol 50, 1969, pp 397-398.

88. Clark, M. M., "Solar Position Diagrams - Solar Altitude, Azimuth, and Time at Different Latitudes, Geological Survey Research 1971," Professional Paper 750-D, pp D145-148, 1971, U. S. Geological Survey, Washington, D. C.

89. Cluff, L. S. and Slemmons, D. B., "Wasatch Fault Zone - Features Defined by Low-Sun-Angle Photography," Publication 1, pp 61-69, 1972, Utah Geological Association, Salt Lake City, Utah.

90. Slemmons, D. B., "Microzonation for Surface Faulting," Proceedings, International Conference on Microzonation, Vol 1, 1972, pp 347-361.

91. Gay, S. P., Jr., "Prevasive Orthogonal Fracturing in the Earth's Continental Crust," 1973, American Stereo Map Company, Salt Lake City, Utah.

92. Hileman, J. A., Allen, C. R., and Nordquist, J. M., "Seismicity of the Southern California Region, 1 Jan 1932 to 31 Dec 1972," 1973, Seismological Laboratory, California Institute of Technology, Pasadena, Calif.

93. Thatcher, W., Hileman, J. A., and Hanks, T. C., "Seismic Slip Distribution Along the San Jacinto Fault Zone, Southern California, and Its Implications," Geological Society of America Bulletin, Vol 86, No. 8, Aug 1975, pp 1140-1146.

94. Gimlett, J. I., "Gravity Study of Warm Springs Valley, Washoe County, Nevada," Report 15, 1967, Nevada Bureau of Mines, University of Nevada, Reno, Nevada.

95. Andreasen, G. E. at al., "Geologic Interpretation of Magnetic and Gravity Data in the Copper River Basin, Alaska," Professional Paper 316-H, pp 135-153, 1964, U. S. Geological Survey, Washington, D. C.

96. Smith, T. E., "Aeromagnetic Measurements in Dixie Valley, Nevada: Implications Regarding Basin-Range Structure," Geophysical Study of Dixie Valley Region, Nevada, G. A. Thompson et al., Final Science Report AFCRL-66-848, Part III, 1967, U. S. Air Force Cambridge Research Laboratories, Bedford, Mass.; and Journal, Geophysical Research, Vol 73, pp 1321-1331.

97. Greene, H. G. et al., "Faults and Earthquakes in the Monterey Bay Region, California," Survey Map MF-518, 1973, U. S. Geological Survey, Washington, D. C.

98. Curray, J. R. and Nason, S. D., "San Andreas Fault North of Point Arena, California," Geological Society of America Bulletin, Vol 78, No. 3, Mar 1967, pp 413-418.

99. Jennings, C. W., "Fault Map of California," Geologic Data Map No. 1, Scale 1:750,000, 1975, California Division of Mines and Geology, Sacramento, Calif.

100. Reid, H. F., "The Mechanics of the Earthquake, The California Earthquake of April 18, 1906," Report of the State Investigation Commission, pp 16-28, Vol 2, 1910, Carnegie Institute of Washington, Washington, D. C.

101. Hastie, L. M. and Savage, J. C., "A Dislocation Model for the Alaska Earthquake," Seismological Society of America Bulletin, Vol 60, Aug 1970, p 1389.

102. Savage, J. C. and Hastie, L. M., "A Dislocation Model for the Fairview Peak, Nevada, Earthquake," Seismological Society of America Bulletin, Vol 59, No. 5, 1969, pp 1937-1948.

103. Ambraseys, N. N., "Some Characteristic Features of the Anatolian Fault Zone," Tectonophysics, Vol 9, 1970, pp 143-165.

104. Plafker, G., "Surface Faults on Montague Island Associated with the 1964 Alaska Earthquake," Professional Paper 543-D, pp 1-42, 1967, U. S. Geological Survey, Washington, D. C.

105. Gutenberg, B. and Richter, C. F., Seismicity of the Earth and Associated Phenomena, Princeton University Press, Princeton, N. J., 1954.

106. Duda, S. J., "Secular Seismic Energy Release in the Circum-Pacific Belt," Tectonophysics, Vol 2, No. 5, 1965, pp 409-452.

107. Matsuzawa, T., Study of Earthquakes, Uno Shoten, Tokyo, 1964.

108. Karnik, V., Seismicity of the European Area, 1 and 2, Reidel, Dordrecht, 1971.

109. Rothe, J. P., Seismicity of the Earth, 1953-1965, UNESCO, Canderman Cournai Publishers, Belgium, 1969.

110. Toppozada, T. R., "Earthquake Magnitude as a Function of Intensity Data in California and Western Nevada," Seismological Society of America Bulletin, Vol 65, No. 5, 1976, pp 1223-1238.

111. Hill, R. L. and Beeby, D. J., "Surface Faulting Associated with the 5.2 Magnitude Galway Lake Earthquake of May 31, 1975 - Mojave Desert, San Bernardino County, California," Geological Society of America Abstracts with Programs, Vol 8, No. 3, 1976, p 381.

112. Kamb, B. et al., "Pattern of Faulting and Nature of Fault Movement in the San Fernando Earthquake," Professional Paper 733, 1971, U. S. Geological Survey, Washington, D. C.

113. Matsuda, T., "Active Fault Assessment for Irozaki Fault System, Izu Peninsula," Earthquake, 1975, pp 121-125.

114. Meade, B. K. and Miller, R. W., "Horizontal Crustal Movements Determined from Surveys After San Fernando Earthquake," San Fernando, California, Earthquake of February 9, 1971, Vol III, Geological and Geophysical Studies, N. A. Benfer, J. L. Coffman, and J. R. Bernick, eds., 1973; Vertical and Horizontal Geodesy, pp 243-293, 1973, U. S. Department of Commerce, National Oceanic & Atmospheric Administration, Environmental Research Laboratory, Washington, D. C.

115. Morrison, N. L. "Vertical Crustal Movements Determined from Surveys Before and After San Fernando Earthquake," San Fernando, California, Earthquake of February 9, 1971, Vol III, Geological and Geophysical Studies, N. A. Benfer, J. L. Coffman, and J. R. Bernick, eds., 1973; Vertical and Horizontal Geodesy, pp 295-334, 1973, U. S. Department of Commerce, National Oceanic & Atmospheric Administration, Environmental Research Laboratory, Washington, D. C.

116. Nakamura, K. and Tsuneishi, Y., "Ground Cracks at Matsushiro Probably of Underlying Strike-Slip Fault Origin, I--Preliminary Report," Bulletin, Earthquake Research Institute, Vol 44, 1967, pp 1371-1384.

117. Seih, K. E. and Jahns, R. H., "1857 Displacements Along the San Andreas Fault Between Cholame and Cajon Pass," Geological Society of America Abstracts with Programs, Vol 8, No. 3, 1976, pp 409-410.

118. Tasdemiroglu, M., "The Gediz Earthquake in Western Anatolia, Turkey," Seismological Society of America Bulletin, Vol 61, No. 6, Mar 1971, pp 1507-1528.

119. Slemmons, D. B., "Geological Effects of the Dixie Valley-Fairview Peak, Nevada, Earthquakes of December 16, 1954," Seismological Society of America Bulletin, Vol 47, No. 4, Oct 1957, pp 353-375.

120. Slemmons, D. B. et al., "Wonder, Nevada, Earthquake of 1903," Seismological Society of America Bulletin, Vol 49, No. 3, Jul 1959, pp 251-265.

121. Thompson, G. A. and White, D. E., "Regional Geology of the

Steamboat Springs Area, Washoe County, Nevada," Professional Paper 458-A, 1964, U. S. Geological Survey, Washington, D. C.

122. Tchalenko, J. S., "Similarities Between Shear Zones of Different Magnitude," Geological Society of America Bulletin, Vol 81, 1970, pp 1625-1640.

123. Larson, E. R., "Minor Features of the Fairview Fault, Nevada," Seismological Society of America Bulletin, Vol 47, No. 4, Oct 1957, pp 377-386.

124. Fedetov, S. A., "On the Seismic Cycle, Possibility of Collective Seismic Regionalization, and Longterm Seismic Prediction," Seismicheskoe Reionirovanie SSR, Moscow, 1968, pp 121-150.

125. U. S. Geological Survey, "Aeromagnetic Map of the Luning Quadrangle, Nevada," Open-File Map, 1967, Washington, D. C.

126. Tarr, R. S. and Martin, L. "The Earthquakes at Yakutat Bay, Alaska, in September 1899," Professional Paper 69, 1912, U. S. Geological Survey, Washington, D. C.

127. Wentworth, C. M., Bonilla, M. G., and Buchanan, J. M., "Seismic Environment of the Sodium Pump Test Facility at Burro Flats, Ventura County, California," Open-File Report, 1969, U. S. Geological Survey, Washington, D. C.

128. Gilbert, G. K., "The California Earthquake of April 18, 1906," Report of the State Earthquake Investigation Commission; Record of Observations, A. C. Lawson, Carnegie Institute of Washington, Publication 87, Vol 1, 1908.

129. Tchalenko, J. S. and Ambraseys, N. N., "Structural Analysis of the Dasht-e Bayaz (Iran) Earthquake Fractures," Geological Society of America Bulletin, Vol 81, 1970, pp 41-60.

130. Brown, R. D., Jr., and Vedder, J. G., "Surface Tectonic Fractures Along the San Andreas Fault, California," The Parkfield-Cholame, California, Earthquakes of June-August 1966--Surface Geologic Effects, Water-Resources Aspects, and Preliminary Seismic Data, R. D. Brown, Jr., et al., ed., Professional Paper 579, pp 2-23, 1967, U. S. Geological Survey, Washington, D. C.

131. Wallace, R., "Earthquake of August 19, 1966, Varto Area, Eastern Turkey," Seismological Society of America Bulletin, Vol 58, Feb 1968, pp 11-46.

132. Lawson, A. C. et al., "The California Earthquake of April 18, 1906," Report of the State Earthquake Investigation Commission, Vol 1, Part 1, pp 1-254, Part 2, pp 255-451, 1908, Carnegie Institute of Washington, Washington, D. C.

133. Radbruch, D. H., "New Evidence of Historic Fault Activity in Alameda, Contra Costa and Santa Clara Counties, California," Proceedings, Conference on Geologic Problems of the San Andreas Fault System, September 14-16, 1967, W. R. Dickinson and

A. Grantz, eds., Stanford University Press, Stanford, Calif., 1968, pp 46-54.

134. Hope, R. A., "Map Showing Recently Active Breaks Along the San Andreas Fault Between Cajon Pass and Salton Sea, California," Open-File Report, Scale 1:24,000, 1969, U. S. Geological Survey, Washington, D. C.

135. Ross, D. C., "Map Showing Recently Active Breaks Along the San Andreas Fault Between Tejon Pass and Cajon Pass, Southern California," Miscellaneous Geologic Investigation Map I-553, Scale 1:24,000, 1969, U. S. Geological Survey, Washington, D. C.

136. Vedder, J. G. and Wallace, R. E., "Map Showing Recently Active Breaks Along the San Andreas and Related Faults Between Cholame Valley and Tejon Pass, California," Miscellaneous Geologic Investigation Map I-574, Scale 1:24,000, 1970, U. S. Geological Survey, Washington, D. C.

137. Brown, R. D., Jr., and Wolfe, E. W., Jr., "Map Showing Recently Active Breaks Along the San Andreas Fault Between Point Delgada and Bolinas Bay, California," Miscellaneous Geologic Investigation Map I-692, Scale 1:24,000, 1972, U. S. Geological Survey, Washington, D. C.

138. Sharp, R. V., "Map Showing Recently Active Breaks Along the San Jacinto Fault Zone Between the San Bernardino Area and Borrego Valley, California," Miscellaneous Geologic Investigation Map I-675, Scale 1:24,000, 1972, U. S. Geological Survey, Washington, D. C.

139. Lensen, G. J., "Earth Deformation in Relation to Town Planning in New Zealand," unpublished report, 1976, New Zealand Geological Survey.

140. Slemmons, D. B., "Cenozoic Deformation Along the Sierra Nevada Province and the Basin and Range Province Boundary," California Geology, Vol 28, No. 5, May 1975, pp 100-103.

141. Gilbert, G. K., "Lake Bonneville," Monograph 1, 1890, U. S. Geological Survey, Washington, D. C.

142. Ambraseys, N. N. and Tchalenko, J. S., "Seismotectonic Aspects of the Gediz, Turkey, Earthquake of March 1970," Geophysical Journal, Royal Astronomical Society, Vol 30, 1972, pp 229-252.

143. Jones, J. C., "The Pleasant Valley, Nevada, Earthquake of October 2, 1915," Seismological Society of America Bulletin, Vol 5, No. 4, 1915, pp 190-205.

144. Johnson, D., "Fault Scarps and Fault-Line Scarps," Journal, Geomorphology, Vol 2, 1939, pp 174-177.

145. California Division of Mines and Geology, "Earthquake in Kern County, California, During 1952," Bulletin 171, 1955, Sacramento, Calif.

146. U. S. Geological Survey, "Surface Faulting in the San Fernando, California, Earthquake of February 9, 1971," Professional Paper 733, pp 55-76, 1971, Washington, D. C.

147. Friedman, M. et al., "Experimental Folding of Rocks Under Confining Pressure; Part III. Faulted Drape Folds in Multilithologic Layered Specimens," Geological Society of America Bulletin, Vol 87, Jul 1976, pp 1049-1066.

APPENDIX A: GEOMORPHIC FEATURES OF ACTIVE FAULT ZONES

Introduction

1. The geomorphic features of the three main types of fault zones, strike-slip, normal-slip, and reverse-slip, provide the main means of identifying active faults, tracing their length, and characterizing the type of slip movement to be expected during future events. The morphology varies from small-scale features that develop at the time of surface faulting to large-scale geomorphic forms that form their main topographic expression. Faults may be along boundaries between mountains and valleys or have less conspicuous topographic expression within mountainous or more moderate terrains.

Minor Geomorphic Features of Active Strike-Slip Faults

2. The geomorphology of strike-slip faults is the simplest of the three main slip types of faults, but even with strike-slip faults of vertical dip, the detailed pattern of surface rupture may be complex. This complexity may be preserved by major, long-term geomorphological features or by minor, rapidly healed surface ruptures. The discussion of geomorphic features of strike-slip fault zones can be considered both from the morphology of the fractures developed during a surface faulting event, and from the long-term cumulative effects which appear as major landforms along the fault zone. Typical patterns of rupture are illustrated to assist in future correlation studies for other fault zones.

3. Gilbert[128*] recognized four types of fault traces along the 1906 breaks of the San Andreas fault zone between Tomales Bay and Bolinas Lagoon. These he named the ridge phase, trench phase, and echelon phase; he also noted that a few places were marked by a simple, narrow and straight break that was parallel to the main fault zone.

---

* Raised numerals refer to similarly numbered items in the References at the end of the main text.

During the 1960's and 1970's there have been a number of strike-slip active fault zones carefully studied and mapped. This led to recognition and naming of minor types of features. These features include minor pressure mounds, pressure ridges, and linear or elongate "mole-tracks." In addition to raised areas, there are fissures, depressions, and, especially, patterns of en echelon fissuring. The main types of surface breakage or morphological features include the following.

Ridge traces, pressure ridges,
mole tracks, and pressure mounds

4. Ridge traces (Gilbert[128]) are low ridgelets developed by loosening of turf and soil from strike-slip displacements along active faults (Figure A1). The 1906 surface faulting along the San Andreas fault zone developed ridgelets that varied in width from 1 to 3 m and in height from a few centimetres to 0.5 m. The ridging results from increased soil volume by fragmentation and loosening of soil and turf to increase in voids and develop features similar to a giant "mole track." Similar features are shown in Figure 15 in Tchalenko and Ambraseys.[129]

5. The cracking and loosening of the surficial materials were described by Gilbert[128] to vary from irregular into regular en echelon patterns similar to that described by Tchalenko[122] from laboratory microscopic and intermediate Riedel experiment scales to a regional scale as shown by surface faulting during the 1968 Dasht-e Bayaz (Iran) earthquake. Tchalenko's experimental work demonstrates the development of en echelon fractures that initially form sets of conjugate shears (Figure A2) and with continuous shears parallel to the main fault (Figure A2B). The post-peak and residual-peak structures form through a wide range of dimensions, including the scale of major strike-slip faults (Figure A3).

6. The en echelon patterns provide a pattern that is diagnostic as to whether the displacement is of the right-slip or left-slip type:

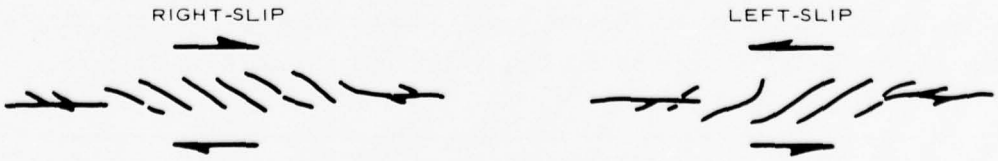
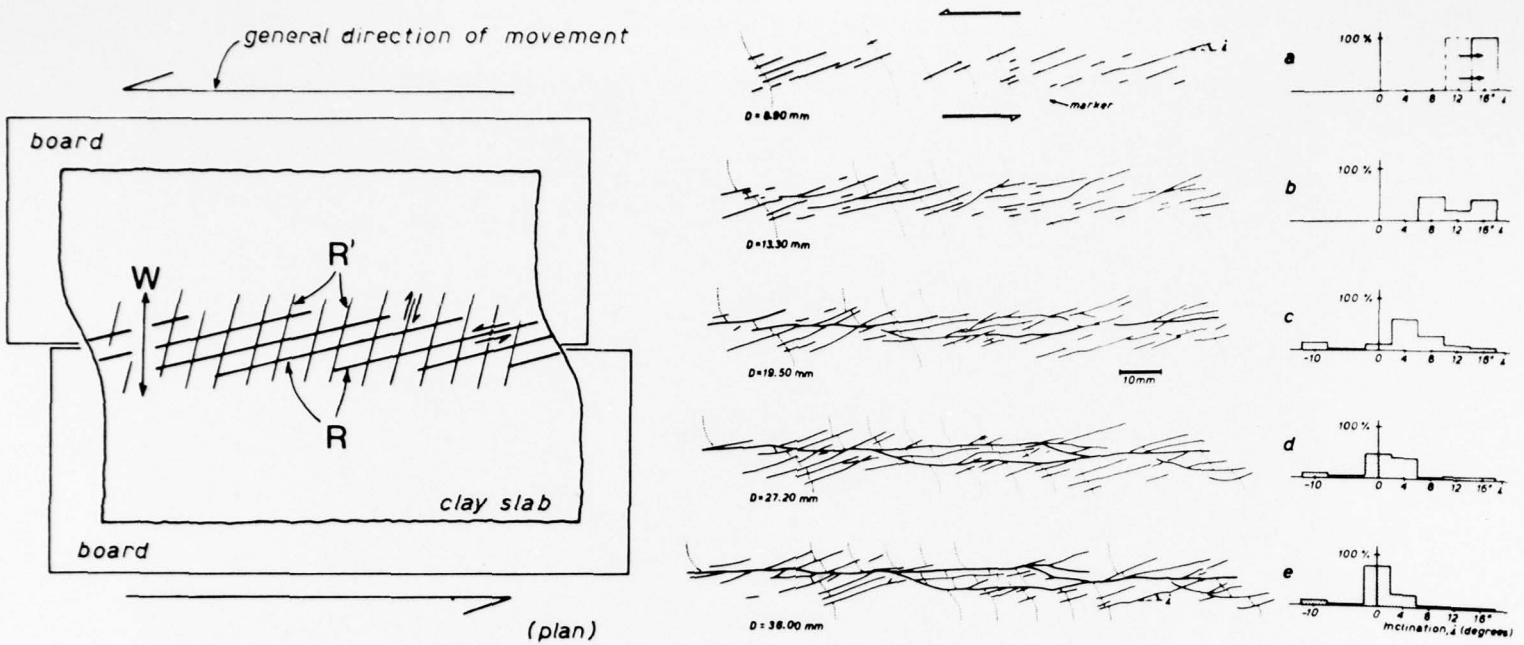




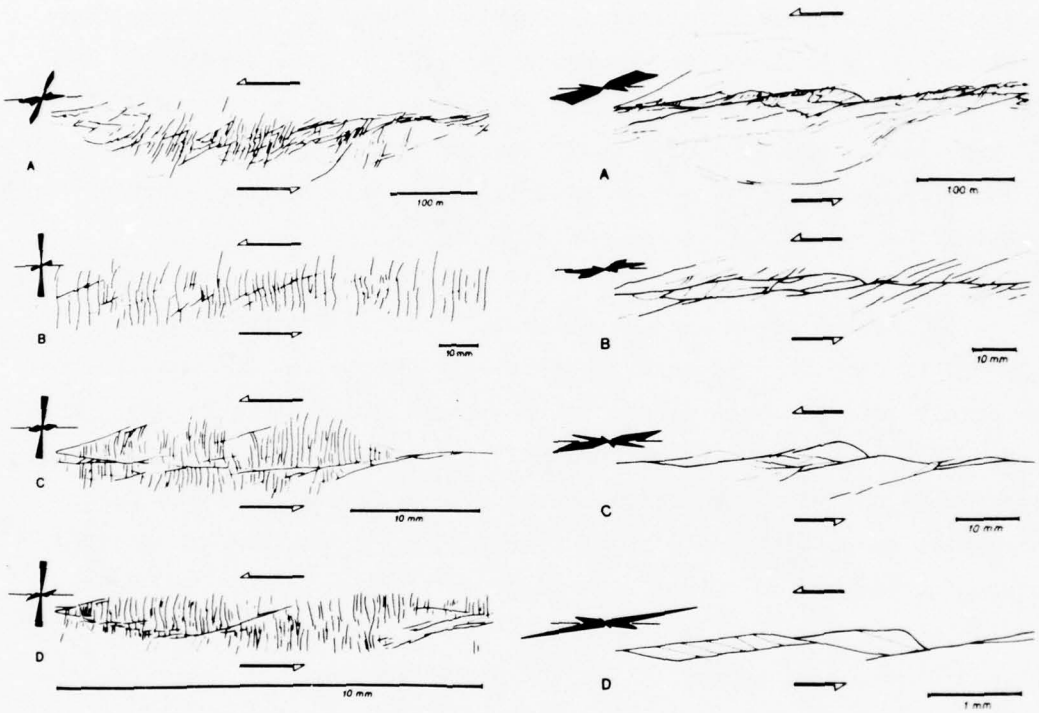
Figure A1. Ridge trace on the 1906 San Andreas fault zone 1 mile northwest of Bolinas Lagoon; view to southwest (photograph from Gilbert[128])



a. Diagram of Riedel experiment. R = Riedel shear. R' = conjugate Riedel shear. W = width of the shear zone.

b. Sequence of structures in Riedel experiment. D = total board movement. Shears are inclined at angle i at each stage of movement. Stage a appears just before peak strength is reached with an average angle of inclination of 12°. Stage b is postpeak shear strength with some 8° shears. Stage c includes some shears at -10° and some Riedel shears connect. Stage d is preresidual structure with the first continuous shears at angles of 0 to 4°. Stage e, residual structure with nearly all displacements along a single principal displacement shear.

Figure A2. Diagram of, and sequence of structures in, the Riedel experiment (Tchalenko[122])



a. Peak structure

b. Postpeak structure
(A) Dasht-e Bayaz earthquake fault
(B) Riedel experiment
(C) entire shear box
(D) detail of shear box sample
Dotted lines indicate less prominent shears. The structures plotted in the form of rose diagrams show Riedel and conjugate Riedel directions.

Figure A3. Comparisons of peak and postpeak structures in shear zones of different magnitudes (from Tchalenko[122])

7. The terms ridge, mole track, buckle, bulge, and pressure ridge denote ridgelike features along the fault trace. The term pressure mound or termination bulge is appropriate for a tumulus or mound produced by pressure rather than loosening; mound is the more general term that includes features resulting from increase in volume from fissuring as well as pressure effects. Detailed features of this type have been mapped by Wallace (in Brown and Vedder[130]) for a segment of the Parkfield-Cholame surface faulting of 1966 on the San Andreas fault zone (Figure A4). This type of ground breakage was the most common type of surface expression of the 1906 faulting along the San Andreas fault in the Tomales Bay to Bolinas Lagoon segment.

Trench trace scarps

8. Trench trace scarps (Gilbert,[128] pp 66-76) are shallow trenchlets developed by settlement of soil and shallow unconsolidated materials into fissures along active surface faults (Figure A5). This type of feature marked short segments of the 1906 faulting on the San Andreas fault zone. The settlement may be accompanied by irregular blocky or en echelon patterns of fracture, or by settled or uplifted branching blocks, in places with wedge or rhombic forms. The pattern indicates whether the displacement is right- or left-strike-slip. Microtrench traces were mapped by Wallace along the trace of the Parkfield-Cholame fault segment of the San Andreas fault, see Figure A4.

En echelon or echelon traces

9. These are unconnected short, parallel fissures along active fault zones with individual, unconnected segments that diverge at angles of about 45° to the strike of the main fault, with a pattern that is indicative of right- or left-slip faulting. The mechanics of this type of fracture pattern is discussed in detail by Tchalenko.[122] Gilbert noted that this type of pattern was developed chiefly in wet alluvium. This type of fissuring is commonly developed along faults with rapid creep, and the careful study of the dilation along individual segments can provide useful data on the amount of offset (Figure A6). The pattern can also be extremely complex as shown in Figure A7 from the Parkfield-Cholame earthquake area.

BEST AVAILABLE COPY

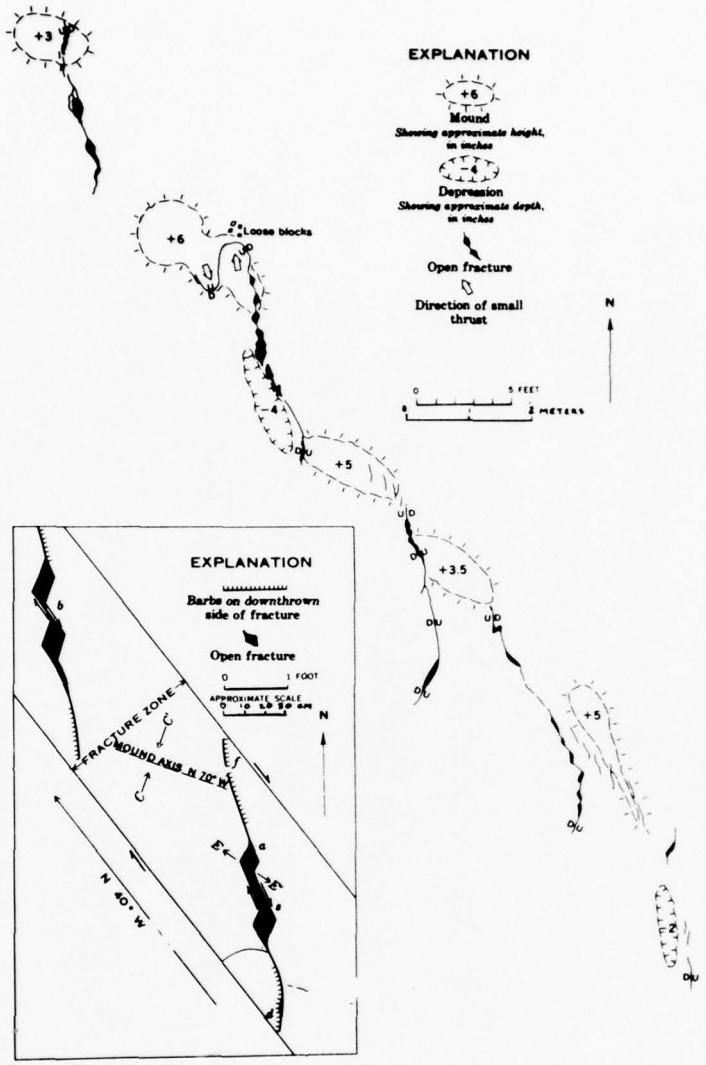


Figure A4. Sketch map of the detailed relations between right-slip en echelon fractures, accompanying mounds or pressure ridges, which together make up mole tracks on the San Andreas fault zone and depressions or trench traces, Parkfield-Cholame earthquake area of June-August 1966. Fractures mapped by R. E. Wallace on July 21, 1966. U, upthrown; D, downthrown. Inset is a diagram of the fracture system and related pressure ridges where individual fractures result from a composite of shear and extension movement, alternating in a steplike arrangement as at a, s, and b. Note the backward or reverse sigmoid pattern formed by the bowed ends at d and f. Mound relief is compensated by vertical displacement indicated at d and f. Greatest extension E-E' nearly parallel to the mound axes or normal to the shortening direction C-C'. The maximum fracture wall separation is about 14 cm and the right-separation is about 5 cm (from Brown and Vedder[130])



Figure A5. Trench trace or trench phase trace of Gilbert.[128] The photograph is of the San Andreas fault trace of 1906, 1 mile northwest of Bolinas Lagoon

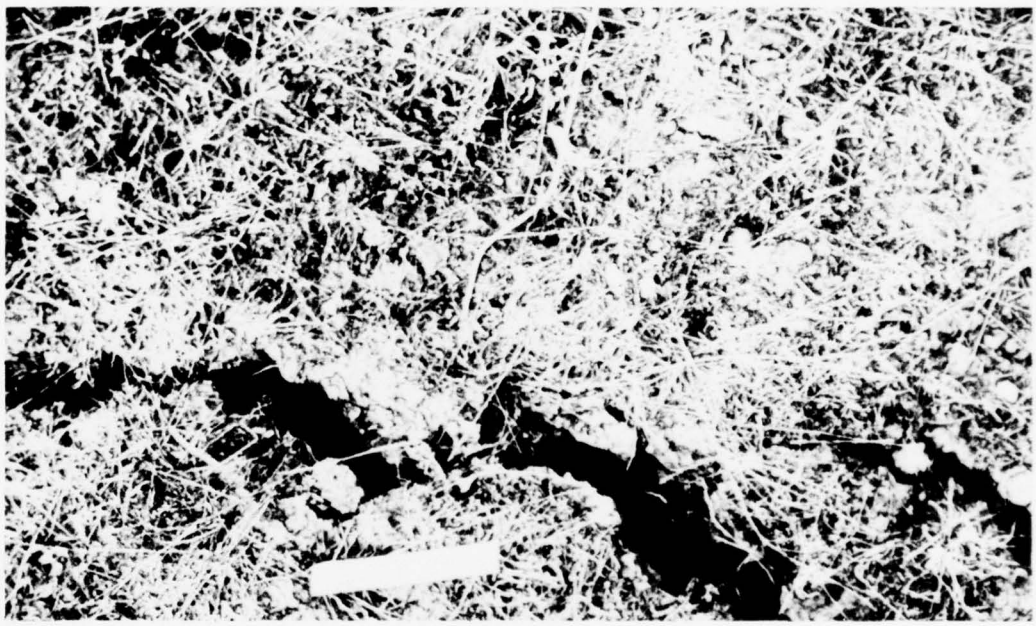


Figure A6. Fracture with en echelon appearance on the Anatolian fault zone near the Varto, Turkey, earthquake area of 1966. The pattern is characteristic of right slip. Scale length is 15 cm (after Wallace[131])

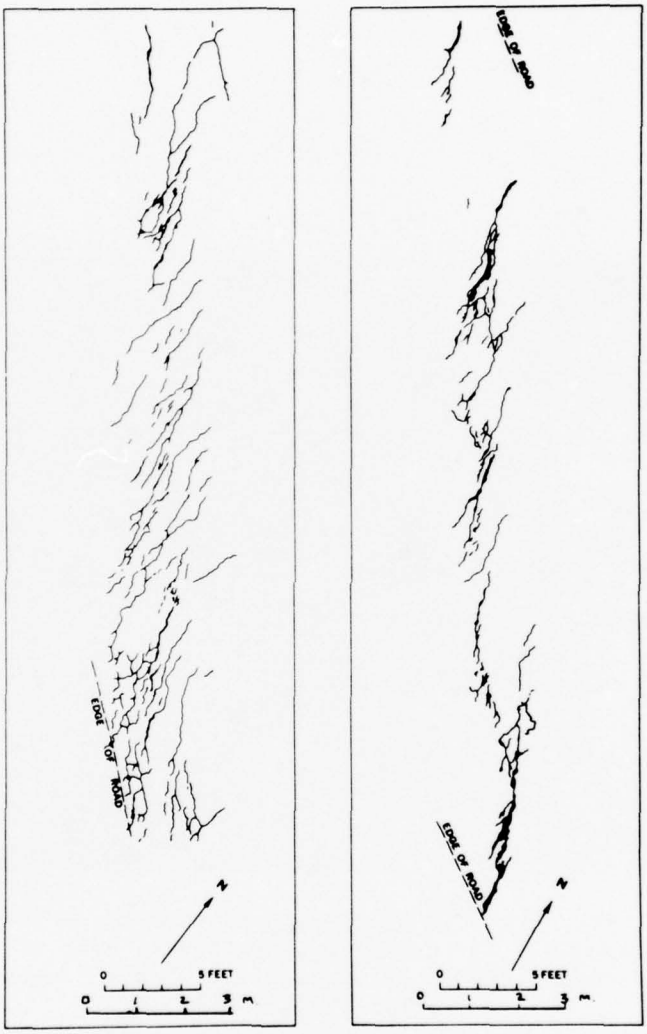


Figure A7. En echelon fractures in asphalt from the 1966 Parkfield-Cholame area.
A. Across Parkfield road 1.4 miles southeast of Turkey Flat road intersection.
B. Across Meng road, 0.6 mile southeast of Highway 46 (from Brown and Vedder[130])

10. This type of pattern, along with various oblique-slip combinations with reverse-slip and normal-slip faulting, is present along extensive segments of many historic zones of faulting.

Path traces

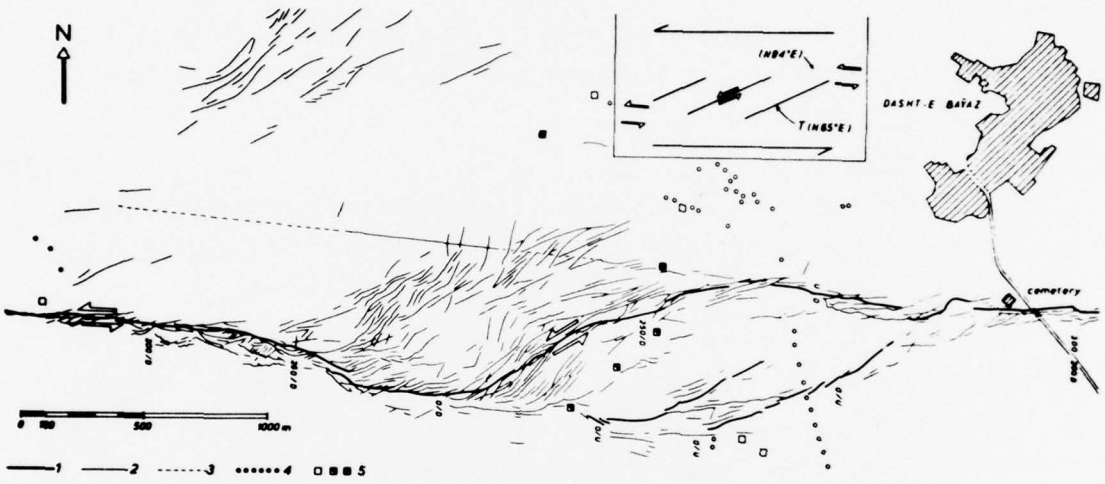
11. Malcolm Clark has described a pathlike appearance at the surface of fault traces along strike-slip faults. This pattern may involve a decrease or change in sorting of rock fragments along the fault trace, and the paths along parts of the Garlock fault in California are developed in low topographic settings and are noted by Clark[32] as "pebbly paths."

Linear fault traces

12. These are the straight to slightly arcuate fractures caused by simple breakage along active faults. This type of breakage is less common than the previously mentioned types. Gilbert[128] described a segment of the 1906 San Andreas fault with the statement: "There are a few spots where for short distances the surface expression is a simple straight fracture along which horizontal motion took place." Brown and Vedder[130] describe this type of fault expression along the 1966 Parkfield-Cholame segment of the San Andreas fault zone as less common than the en echelon type, and it connects segments with en echelon fracturing. Linear fault traces can grade into slightly en echelon types. In the Parkfield-Cholame area, the average length of segments of this type was 6.1 m with a width of 2.5 cm, and the maximum length was about 18.3 m with a width of about 9 cm. Small vertical offsets were noted in some places and may represent differential compaction of the surficial materials at the fault, or offsets of topographic slope. Experiments by Tchalenko[122] indicate that linear traces are more common during advanced stages of strike-slip deformation (see Figure A3).

Sigmoid fault traces

13. For many fractures, these include open S-forms with an arcuate termination. Suggestions of sigmoidal fault traces are shown in Figures A7 and A8. The sigmoidal patterns are as follows:



LEGEND

1. FRACTURE SHOWING GREATEST AMOUNT OF RELATIVE DISPLACEMENT.
2. SMALL FRACTURE.
3. PREEARTHQUAKE FAULT LINEAMENT.
4. QANAT LINE.
5. ISOLATED MUD HOUSES RESPECTIVELY UNDAMAGED, DAMAGED, AND DESTROYED. RELATIVE DISPLACEMENTS IN CENTIMETRES, FIRST FIGURE LEFT-LATERAL MOVEMENT–SECOND FIGURE VERTICAL MOVEMENT.

Figure A8. Fault map of a section of the Dasht-e Bāyaz earthquake zone, Iran, of 1966 (from Tchalenko and Ambraseys[129]). Note sigmoidal or open S-shapes of en echelon fractures



Major Geomorphic Features of Strike-Slip Faults

14. The main geomorphological features developed along strike-slip faults are described in a number of specific fault studies. The first classic major study is the report by Lawson et al.,[132] of the surface faulting and related effects accompanying the 1906 San Francisco earthquake. This report described in detail the surface faulting along the northern part of the San Andreas fault zone. A number of recent studies have mapped in detail a number of historic and prehistoric surface breaks along strike-slip zones. These reports provide an excellent basis for study of other zones of this type. They include: Tchalenko and Ambraseys[129] and the U. S. Geological Survey Series of Miscellaneous Geological Information and Open-Filed Maps that include: Radbruch,[133] Hope,[134] Ross,[135] Vedder and Wallace,[136] Brown and Wolfe,[137] Sharp,[138] and Clark.[32]

15. The typical landforms of strike-slip zones are shown by block diagrams in Figures A9 and A10. Figure A9 is representative of segments of the San Andreas and Garlock fault zones in mountainous regions with extensive alluvial valleys at or near the fault. Figure A10 is more representative of those sections of strike-slip faults in broader, rift valleys or more hilly terrain like the San Andreas fault in the Carrizo Plain area (Vedder and Wallace[136]) and north of Bolinas Bay (Brown and Wolfe[137]). The surface appearance of surface strike-slip faulting is shown in Figure A11.

16. No standard terminology for major geomorphological features of strike-slip fault zones has been adopted. Many of the terms in current use are given in geomorphology texts and glossaries. Sharp[27] reviews geomorphic features of active faults and methods of

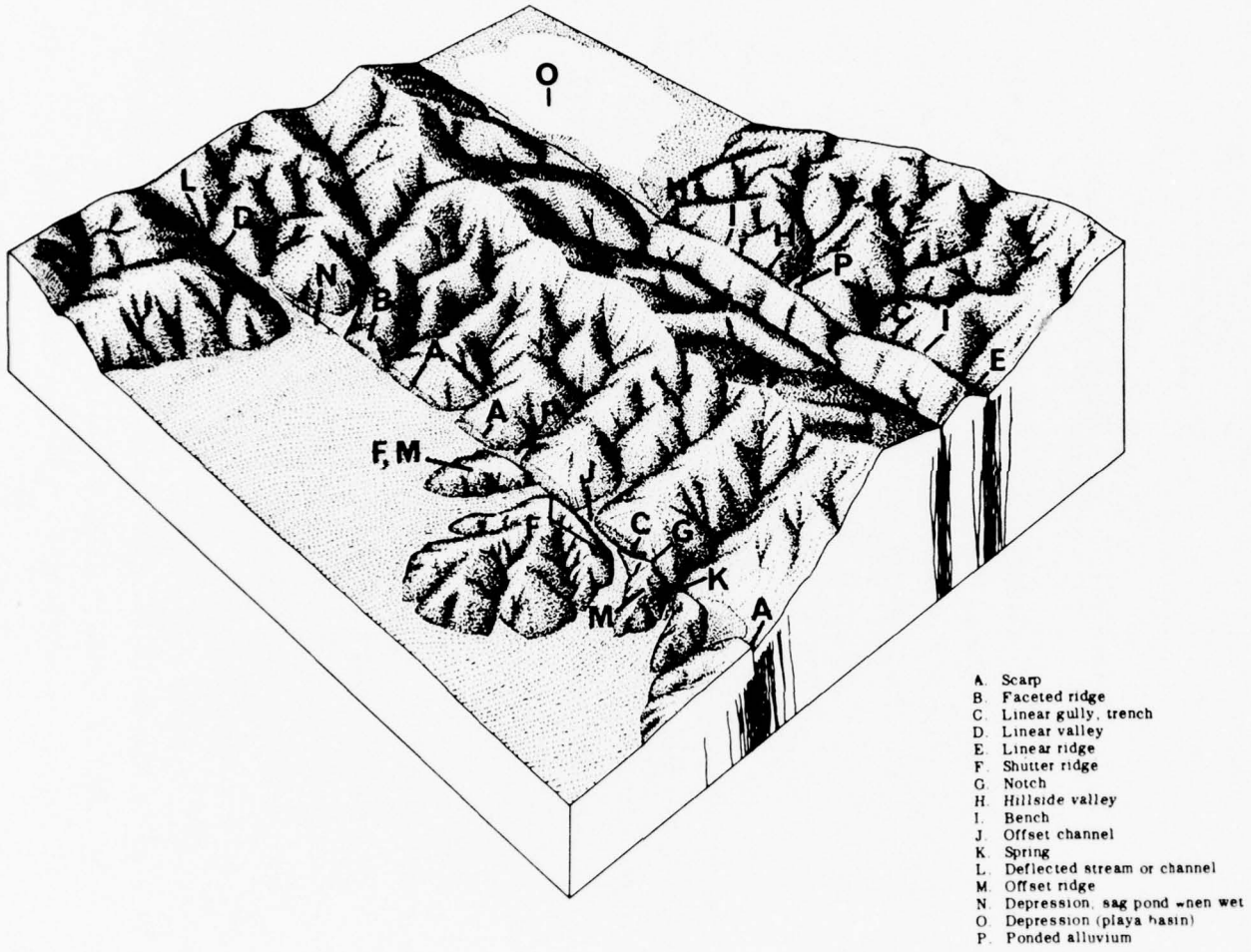


Figure A9. Block diagram showing landforms produced along active strike-slip faults in areas with steep topography (after Clark[32])

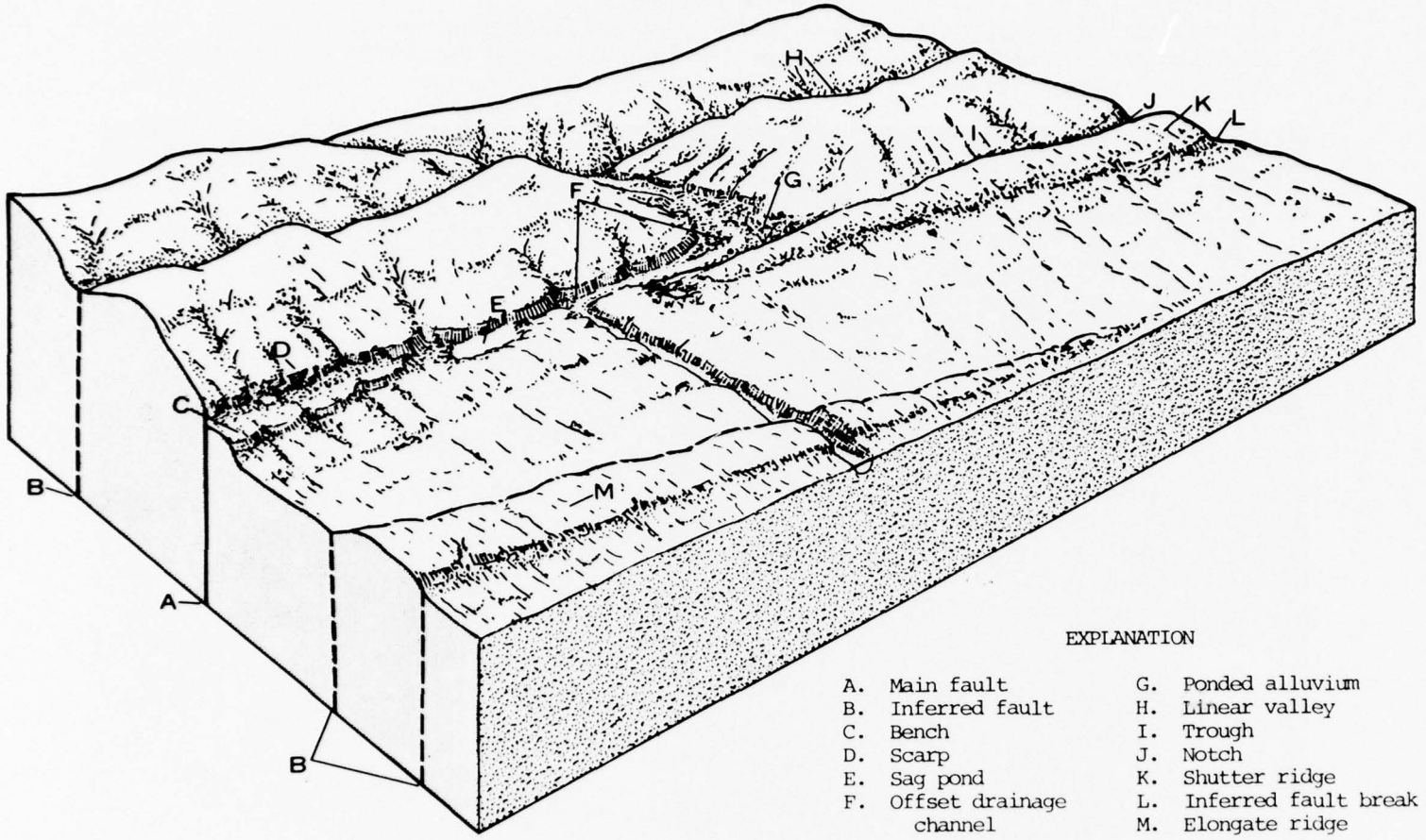


Figure A10. Block diagram showing geomorphic features developed along active strike-slip faults in area with moderately steep topography (Brown and Wolfe[137])



Figure All. Oblique aerial view of the San Andreas fault, Carrizo Plains, California. The fault is characterized by sidehill ridges and trenches, benches, offset drainage lines, elongate ridges, shutter ridges, deflected and diverted drainages, and ponded alluvium

distinguishing between active and inactive faults. Lensen[139] has described many other geomorphic landforms associated with strike-slip fault zones in New Zealand.

17. Typical geomorphic landforms that have been noted along active strike-slip faults in a variety of climatic zones in California are listed in Table A1 and summarized as: (1) scarp or eroded scarp; (2) bench; (3) linear canyon, gully, gulch, swale, trench, trough, stream, or valley; (4) pond, depression, swampy depression, sag, playa, sag pond, swampy trench, etc; (5) offset drainage channel or stream; (6) fault gap, notch, or saddle; (7) trench; (8) offset ridgeline or hill; (9) deflected or diverted drainage channel, gully, gulch, stream, or valley axis; (10) linear or elongate ridge; (11) trough; (12) ponded alluvium; (13) alined notches and swales; (14) shutter ridge; (15) scarplet; (16) swale; (17) alined vegetation or linear boundary; (18) alined gullies, gulches, valleys, and streams; (19) side-hill (or hillside) trench or trough; (20) spring, elongate spring, marsh, or groundwater barrier; (21) lineament (lithologic, topographic, altered, mineralized, soil contrast, en echelon or Riedel, etc.); (22) fault valley or graben; (23) fault trace; (24) fault path or pebbly path; (25) open crack or fissure; (26) faceted ridge or spur, triangular facets; (27) alinement of springs or a very elongate spring. Additional features are listed by Lensen[139] for strike-slip fault zones. They include: beheaded drainages, wedges, tilted wedges, transcurrent buckles, and bulges.

Geomorphic Features of Normal-Slip Faults

18. Surface expression of faulting associated with normal-slip faults generally includes more complex relations than have been noted for strike-slip faults. The fault plains generally have dips that vary from 50° to 90°, with most dips clustered at about 60° or at 90°, to give fault traces in mountainous terrains that are less linear than is characteristic of strike-slip faults. Percent of regional extension varies with the dip of the fault plane. For 60° dips the extensional component is 50% of the dip-slip component. The large vertical

Table A1

Relative Abundance of Geomorphological Features Observed Along Strike-Slip Faults in California

Feature	San Andreas Tejon-Cajon Sector (Ross[135])	San Andreas Cholame-Tejon Sector (Vedder and Wallace[136])	San Jacinto (Sharp[138])	San Andreas Delgada-Bolinas Sector (Brown and Wolfe[137])	Garlock (Clark[32])	Overall Rank in Abundance
Scarp or eroded scarp	1	1	1	3	5	1
Bench	Present	3	4	5	1	2
Linear canyon, gully, gulch, swale, trench, trough, stream, or valley	Common	Common	2	Common	3	3
Pond, depression, swampy depression, sag, playa, sag pond, swampy trench, etc.	3	4	8	2	10	4
Offset drainage channel or stream	Present	6	--	Present	2	5
Fault gap, notch, or saddle	Present	8	5	Present	6	6
Trench	6	Common	6	1	Present	7
Offset ridgeline or hill	--	Common	Present	--	4	8
Deflected or diverted drainage channel, gully, gulch, stream, or valley axis	5	5	10	Present	Present	9
Linear or elongate ridge	7	Present	9	Common	9	10
Trough	Present	2	--	Present	Present	11
Ponded alluvium	--	7	3	--	Present	12

(Continued)

Note: Other possible features include (Lensen[139]): (a) beheaded drainage; (b) wedges; (c) tilted wedges; (d) transcurrent buckles; and (e) bulges.

Table A1 (Concluded)

Feature	San Andreas Tejon-Cajon Sector (Ross[135])	San Andreas Cholame-Tejon Sector (Vedder and Wallace[136])	San Jacinto (Sharp[138])	San Andreas Delgada-Bolinas Sector (Brown and Wolfe[137])	Garlock (Clark[32])	Overall Rank in Abundance
Alined notches and swales	Common	Common	Present	Present	9	13
Shutter ridge	Present	Present	Present	Present	8	14
Scarplet	Present	9	Present	4	Common	15
Swale	Present	10	Present	Present	Present	16
Alined vegetation or linear boundary	2	Present	Present	Present	Present	17
Alined gullies, gulches, valleys, and streams	Common	Common	7	Present	Present	18
Side-hill (or hillside) trench or trough	Present	Present	Present	Present	Present	19
Spring, elongate spring, marsh, groundwater barrier	8	Present	Present	Present	Present	20
Lineament (lithologic, topographic, altered, mineralized, soil contrast, etc.)	--	Present	--	--	Present	21
Fault valley or graben	Present	Present	--	--	Present	22
Fault trace	Present	Present	Present	6	Common	23
Fault path or pebbly path	--	--	--	--	Present	24
Open crack or fissure	--	Present	--	--	Present	25
Faceted ridge or spur, triangular facets	--	--	Present	--	Present	26
Alinement of springs or very elongate spring	Present	--	Present?	--	Present	27

component develops steep and high scarps which may be preserved for long periods of geologic time. Branch faults are common and tend to transfer displacements to more than one fault to give zigzag patterns with marked and abrupt differences in the strike of faults from one segment of a fault zone to another, or may have hinged displacements with reversed direction of movement on different segments of the fault; such faults may have much greater length than first inspection may suggest. In addition, the inclined nature of many fault planes provides the possibility of faulting and secondary failures in surficial materials with a higher angle dip, often 90°, with branching fractures. The overall result is shown diagramatically in Figure A12.[140]

19. Most normal faults break through surficial unconsolidated materials with a nearly vertical dip. This change in dip near the earth's surface leads to the development of features that characterize the geomorphology of associated normal faults. In general, the extension of the earth's surface with normal faulting and the change in dip of the fault plane lead to the development of an open fissure near the earth's surface. Various types of soil or ground failure in combination with branching of the tectonic fault plane can lead to a variety of fault planes first noted by Gilbert.[141] More recently, Slemmons[119,140] has suggested terms for these fault features. Since the landforms are developed at all scales from the details of small displacements along a fault trace, to wide structures, distributed over a zone of a kilometre or more in width, the terminology for fault traces is similar to that of major geomorphic landforms. The following discussion divides the landforms into features developed by the actual fault trace or scarp, and the longer term, eroded features along the scarp.

20. The main landforms developed along normal-slip faults are described by Gilbert,[141] Ambraseys and Tchalenko,[142] and Slemmons.[119,140] The minor features also include those described by Larson.[123] The details of fault scarp morphology, varying from initial free faces to debris slopes to more gentle slopes with aging and time, have been studied in detail by Wallace (in press). The main types of surface

breakage or morphological features include the following.

Simple fault scarps

21. Figure A12A illustrates the surface rupturing along a single break which extends to the earth's surface with little or no change in

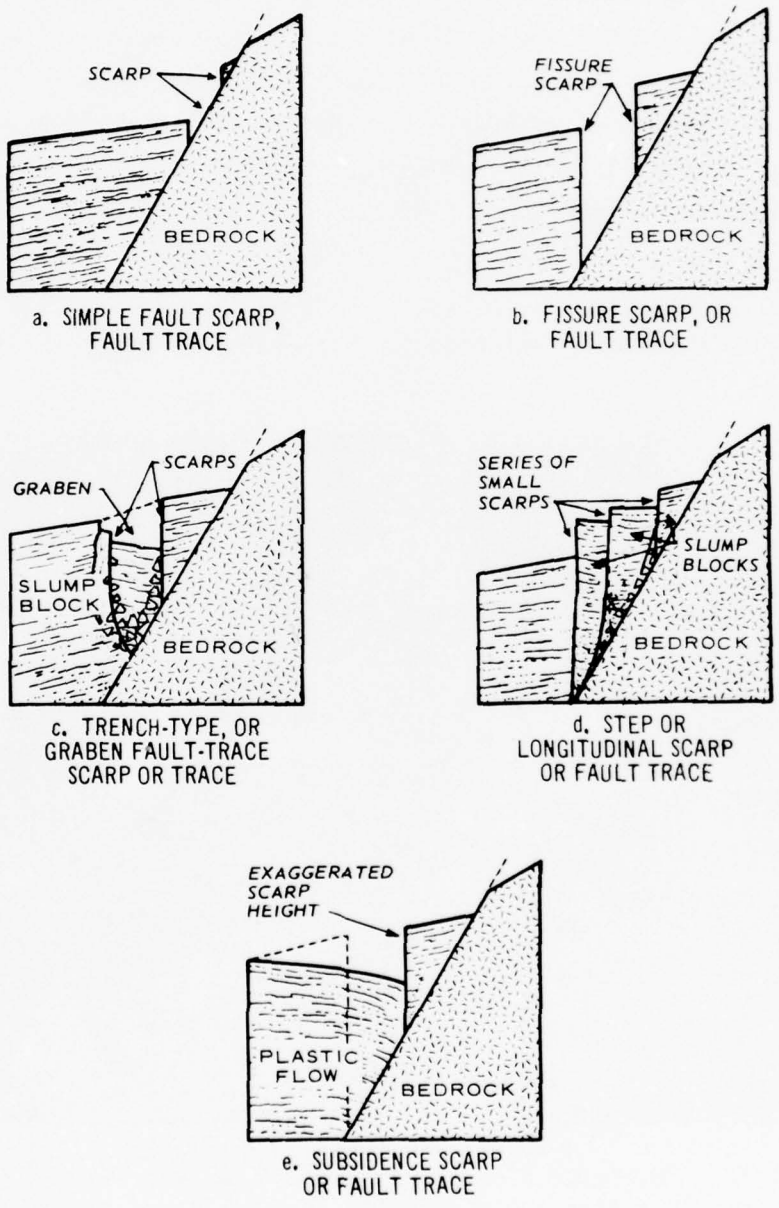


Figure A12. Types of fault scarps and fault traces for normal-slip faults (modified from Slemmons[119,140])

the fault dip so that the fault scarp is closely alined along the bedrock-alluvium boundary. The fault plane is thereby exposed on the earth's surface, sometimes showing striations or slickensides that express the detailed path of the fault slip (Figure A13). For such examples the exposed fault plane is the scarp and the strike, dip, and slip direction and net amount of slip can all be measured directly. This type of example probably develops most readily with well-consolidated surficial materials that are above the water table. Examples are expecially well shown along the 1915 Pleasant Valley fault zone, Nevada (Figures A14 and A15).

Fault fissure
scarps or fissure traces

22. Figure A12B indicates the common tendency for the fault trace

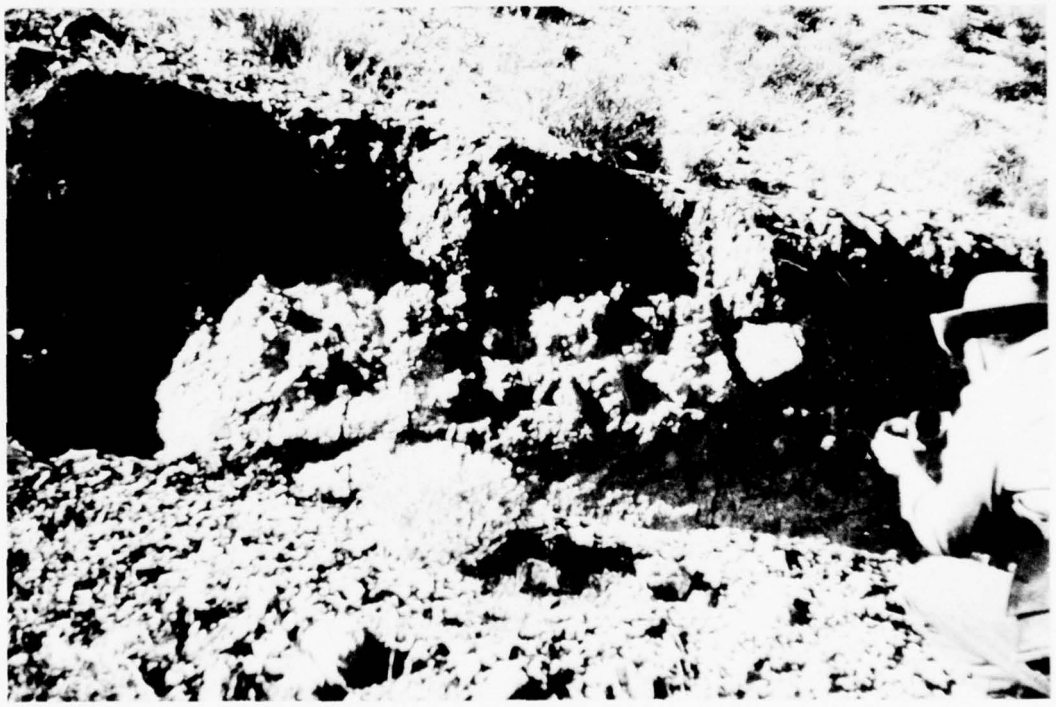


Figure A13. Striations on the 1954 Fairview Peak fault. The offset measured from stream and right-slip is 2 to 3 m of right-slip separation and a vertical-slip component of 1 m. This is in agreement with the 20° slip direction of the striations



Figure A14. The 1915 Pleasant Valley, Nevada, fault scarp with an irregular trace at or near the bedrock-alluvium contact. Scarp height is 3 to 5 m



Figure A15. The 1915 Pleasant Valley, Nevada, fault scarp with a "zigzag" trace at the bedrock-alluvium contact

at the earth's surface to develop at the instant of offset a simple fissure or zone of surface extension. The unstable nature of the unconsolidated surficial materials, probably accompanied by the very strong earthquake motion at the fault, generally results in gravitational failure by slumping of one or more blocks or slices as shown by the dashed lines in Figure A12B. The slump blocks or plastic deformation of the surficial materials normally results in the development of one of the fault trace types shown in Figure A12. For western conterminous United States only two examples have been described: one in the 1915 Pleasant Valley, Nevada, earthquake area by Jones[143] as shown in Figure A16, the other in the 1954 Fairview Peak earthquake area by Slemmons.[119] Soil erosion and deposition have already concealed the exposed dipping fault planes of these two examples.

Trench-trace scarps or
graben fault-trace scarps

23. These scarps (Figure A12C) result from the gravitational failure of slump blocks. This type of landform is the direct result of the extensional nature of normal-slip faults with a dipping fault plane that breaks at a high angle through surficial materials and the trenchlike feature commonly extends long distances along active fault scarps usually a short distance out into the valley from the bedrock outcrops along the fault zone. Excellent examples are developed along the 1954 Dixie Valley fault zone (Figure A17). The slump blocks may develop in either the hanging or foot wall block of the fault; in either case the slump blocks may rotate to give a more nearly horizontal or back-tilted slope in the trench block. The width of the graben is related to the dip of the primary fault plane in bedrock, the fracture direction in the surficial material, and the thickness of the surficial material as given by Ambraseys and Tchalenko.[142]

Longitudinal-trace
or step-trace scarps

24. These scarps (Figure A12D) develop when one or more slump blocks on the uphill side of the fault trace slide into the fissure trace to develop a stairstep arrangement of blocks that is similar to

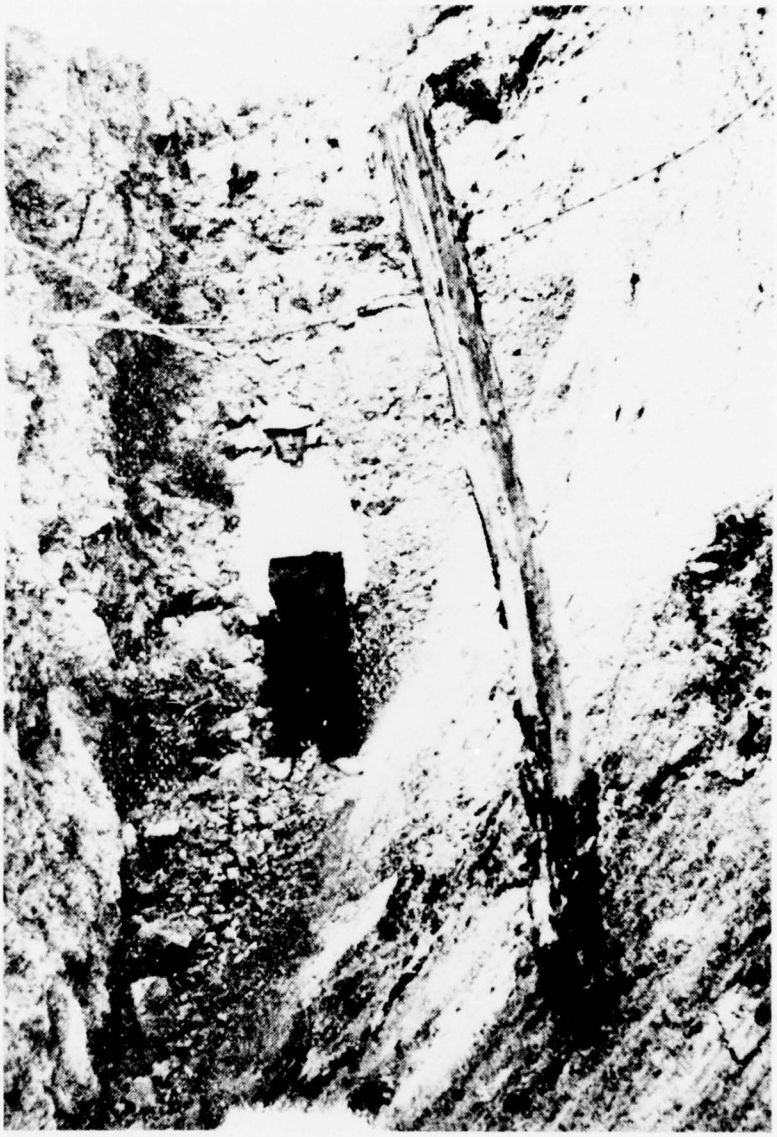
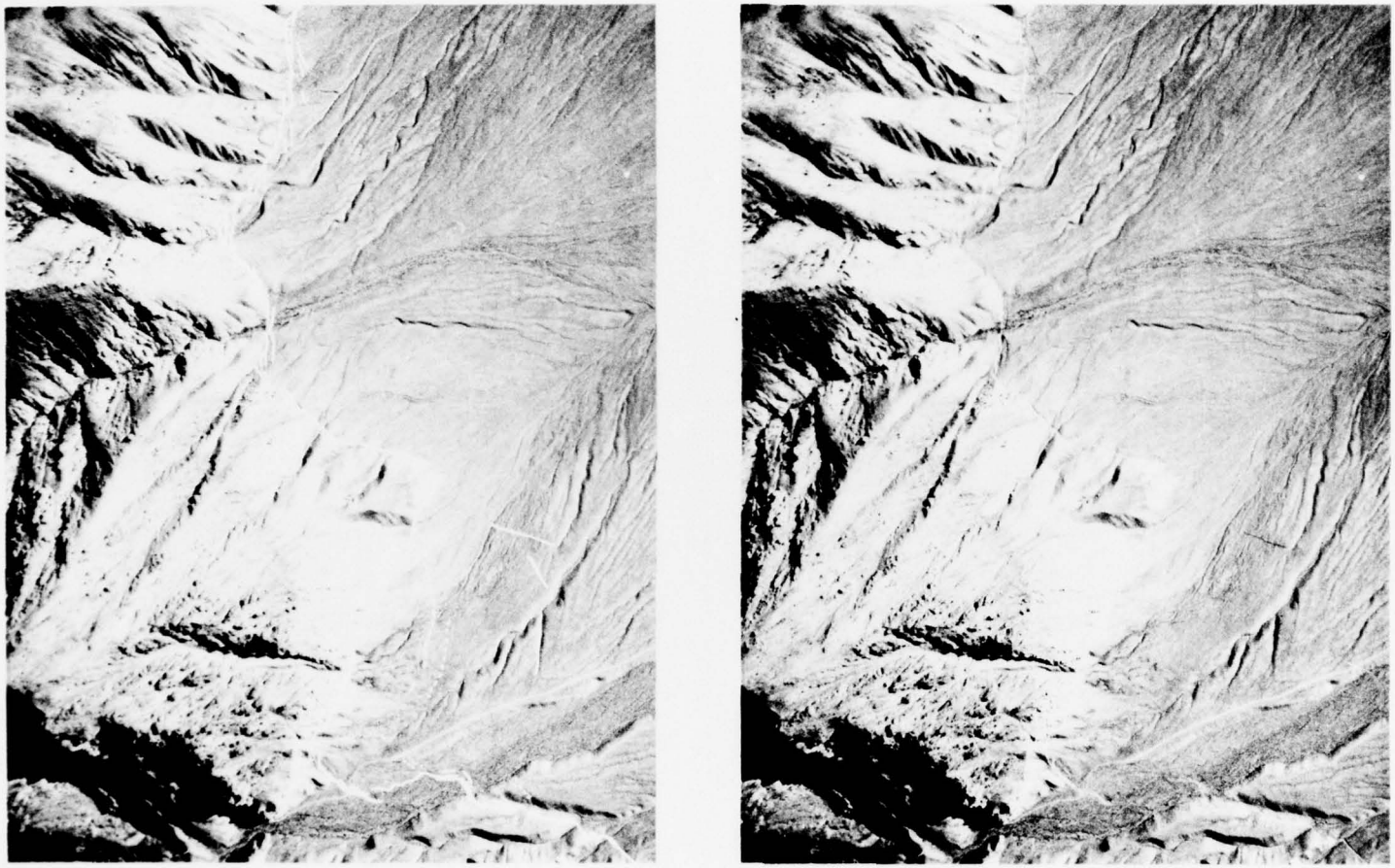


Figure A16. Fault-trace fissure on the 1915 Pleasant Valley fault which exposed the bedrock fault with vertical component of offset of 3.78 m on a fault plane of 54° W dip; the striations have an angle of pitch of 85° N, indicating a right-slip of about 30 cm



a. Fault traces marked

b. Fault traces unmarked

Figure A17. Graben trace along 1954 Dixie Valley fault zone along west side of Dixie Valley. Early morning sun illumination

that found in many landslides. The slump blocks generally have a back-rotation to give treads with a more nearly horizontal slope than the original surface. This type of trace is fairly common along normal-slip fault scarps.

Subsidence trace faults or scarps

25. These (Figure A12E) form where the hanging wall block fills the incipient fissure trace by semiplastic flow into the zone of extension. This type of fault scarp normally develops on fault traces crossing areas of unconsolidated alluvial sediments with a shallow water table. This effect produces a sag in the unconsolidated deposits that is in the opposite direction from that produced by fault drag. This may explain at least some cases of apparent "reverse drag."

26. Normal faults commonly are controlled by preexisting rectilinear or orthogonal fracture systems that have conjugate displacements on two sets to give zigzag fault traces with little or no oblique-slip component, or have minor right- and left-slip components due to the extension component. Normal-slip faults are the most common type of fault over most of the western United States and typically develop a Basin and Range type topography that varies in appearance from youthful (northern Basin and Range Province) with rapid tectonic activity, to old age (southern Basin and Range Province-Sonora Desert) with geologically long periods of erosion following an ancient period of tectonic activity. Faults of the youthful terrain are active; those of the old terrain are generally dead.

27. Wallace (unpublished manuscript) has shown that fault scarps in unconsolidated materials of north-central Nevada have initial, free-face slopes of 50 to 90°, erode, and are covered by slope wash to give slopes of about 35° in a few thousand years and become more gentle in slope with age, to 20-30° in about 12,000 years. The break in slope also broadens with age. Scarps in fractured bedrock commonly have slopes of 30 to 35° and are believed to be up to a million or more years in age. Mountain slopes believed to be about 10,000,000 years old have slopes of approximately 15°.

28. Rejuvenation of fault scarps by recurrent displacements

develops compound fault scarps. The recently formed scarps are conspicuous by their freshness, degree of scarp dissection, formation of terraces upstream on drainages crossing the fault, and character of faceted bedrock spurs, and by the presence of "wine-glass" shaped rejuvenated valleys in bedrock above the scarp.

29. The normal-slip fault geomorphology is generally much more complex than that of strike-slip faults as the result of several factors:

a. Normal-slip faults more commonly have lower angle dips than strike-slip faults to give more irregular surface traces, as seen in plan view, particularly in mountainous terrain.

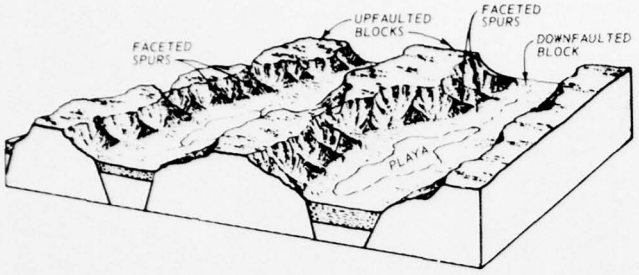
b. The intermediate angle of dip, generally between 50 and 70° and averaging 60° in bedrock, often breaks with a higher angle in unconsolidated, near-surface materials to create a variety of complex gravitational collapse features.

c. Normal faults are often controlled by rectilinear or orthogonal fracture systems that tend to give zigzag fault traces with little or no oblique-slip component to the overall fault zone, but can develop alternating oblique-slip directions on the alternate "zigs" and "zags" (see Figures A14, -15, -17, and -18). These types, with change of strike, can become conjugate strike-slip or normal-oblique-slip faults. The normal-slip faults are one of the most widespread types of active faults in conterminous United States and are found in nearly all parts of the western United States and especially in the Basin and Range Province. Their main development is typically either by patterns of alternating mountain and basin (horst and graben) topography from crustal extension, or by tilted or rotated fault blocks with erosion of fault scarps and deposition in adjoining downtilted blocks to form a terrain consisting of alternating mountains and valleys. The appearance of typical faulted mountain fronts generally is affected by the average rate of uplift and faulting, or long-term cyclic changes in rate of uplift. The overall effect is shown by the three stages shown in Figure A19.

30. The first stage is the result of rapid rates of faulting with short recurrence intervals. The steep mountain fronts, commonly with frontal slopes of 30° or higher, have faceted or triangular-fronted



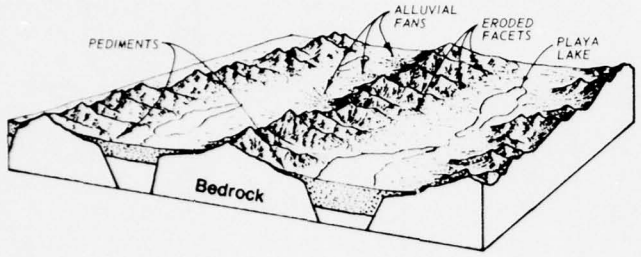
Figure A18. Simple fault scarp near Genoa, Carson Valley, Nevada. Note irregular or zigzag fault trace which closely follows the irregular mountain front. The uplift of this part of the mountain is in two stages with the moderately rugged, but broader terrain in the upper half of the photograph--representing an earlier stage of faulting and erosion--and a steepened lower slope due to rejuvenation by a recent increase in rate of faulting. Note the eroded or battered faceted spurs with the best formed facet to the right of center stream. The fault scarp is 13.4 m in height and is the result of 10.4 m of vertical-slip component at the quarry. The change in base level from the faulting has given 5 sets of terraces in the lower part of the center canyon, which indicates that the fresh fault scarp was probably formed by five faulting events, averaging about 2.2 m each. The fault plane exposed in the quarry has a dip of 58° NE and the scarp has been eroded to a slope of 38°. The uniformly oversteepened base of the mountain defined by the fault scarp is diagnostic of the faulting. Note also the stream terraces in several valleys cut by the fault



a. EARLY STAGE

EARLY STAGE

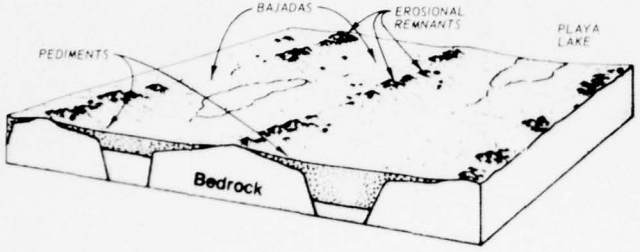
1. MAXIMUM RELIEF OCCURS IN THE INITIAL STAGE DUE TO BLOCK FAULTING OR FOLDING, AND, IF RECURRENT MOVEMENT ALONG THE FAULTS DOES NOT OCCUR, RELIEF WILL DIMINISH THROUGH SUCCESSIVE STAGES.
2. ALLUVIAL FANS BUILD OUTWARD FROM THE MOUNTAIN FRONT AND BASINS BECOME FILLED WITH EROSIONAL DEBRIS.
3. SHALLOW, TEMPORARY LAKES (PLAYAS) MAY FORM IN THE CENTRAL PART OF THE BASIN AND EXPAND OR CONTRACT WITH FLUCTUATIONS IN CLIMATE.
4. INTERIOR DRAINAGE COMMON.



b. MIDDLE STAGE

MIDDLE STAGE

1. MOUNTAIN MASS IS DISSECTED INTO AN INTRICATE SET OF CANYONS, DIVIDES, AND PEAKS. MOUNTAIN FRONT HAS RETREATED FROM ORIGINAL POSITION.
2. PEDIMENTS DEVELOP ALONG THE MOUNTAIN FRONT.
3. LOCAL RELIEF DIMINISHES.
4. ALLUVIAL FANS MERGE TO FORM AN ALLUVIAL SLOPE CALLED A BAJADA.
5. INTERIOR OR EXTERIOR DRAINAGE.



c. LATE STAGE

LATE STAGE

1. CONTINUED FILLING OF THE INTERMONTANE BASINS BY DEBRIS OCCURS.
2. PEDIMENTS REPLACE MORE OF THE MOUNTAIN MASS AS THE MOUNTAINS BECOME SMALLER.
3. ULTIMATELY ONLY SMALL, ISLANDLIKE REMNANTS (INSELBERGS) OF THE MOUNTAINS REMAIN, AND ALMOST THE TOTAL AREA IS COVERED BY DEBRIS.
4. EXTERIOR DRAINAGE COMMON.

Figure A19. Three stages of mountain and valley development by block faulting

ridges or spurs due to truncation by faulting and rapid uplift along the frontal fault scarp. The valleys emerging from the range are steep and narrow and generally have trends that are at high angles with the main fault. The profiles of the rivers and streams emerging from these valleys may have knick-points separating sections of different gradient as the result of faulting episodes or changes in rate of uplift. Such streams may also have terraces as the result of renewed faulting and rejuvenation of the streams by the temporary change of base level at the mountain front.

31. Block-faulted regions, with tilted or rotated blocks, like Basin and Range topography can form valley and mountain terrain, but the pattern is commonly more irregular or blocky as shown in Figure A20. Faults may develop an orthogonal pattern. During earthquakes the faulting may simultaneously offset several bordering faults to develop a complex pattern of faulting.

32. The second stage represents a more mature, less active stage of fault activity at the mountain frontal faults. This stage has more extensive lateral corrosion by the rivers and streams; the erosion is more directly controlled by differential erosion due to lithologic differences in the bedrock to give a more irregular mountain front, with alluvial aprons extending well up into the valleys draining the mountain block.

33. The third stage consists of an old-age stage of erosion with little or no contemporaneous faulting, so that pediments extend well into the mountain blocks, the main faults have little or no surface

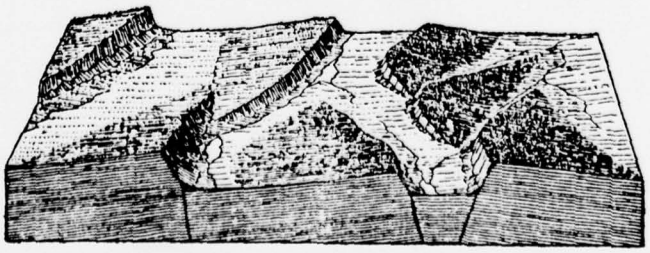


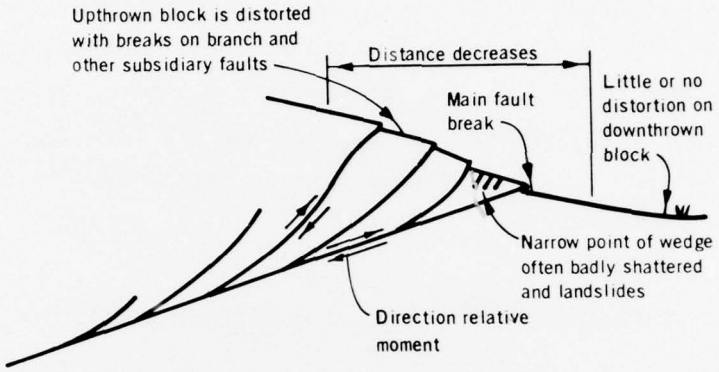
Figure A20. Block-fault mountain and valley terrain with rotated and tilted fault blocks

expression, and much of the mountain block has been eroded to a gently sloping surface, or pediment, that is covered by a thin veneer of alluvial deposits. In the southwestern part of the United States, the time of last displacement on the main faults along many of the mountain ranges may date back to the early Quaternary, the Pliocene, or even to the Miocene. Such landforms, with extensive development of pediments, form large areas of Arizona and New Mexico, and may also form smaller subprovinces in less active or inactive parts within the Basin and Range Province to the north.

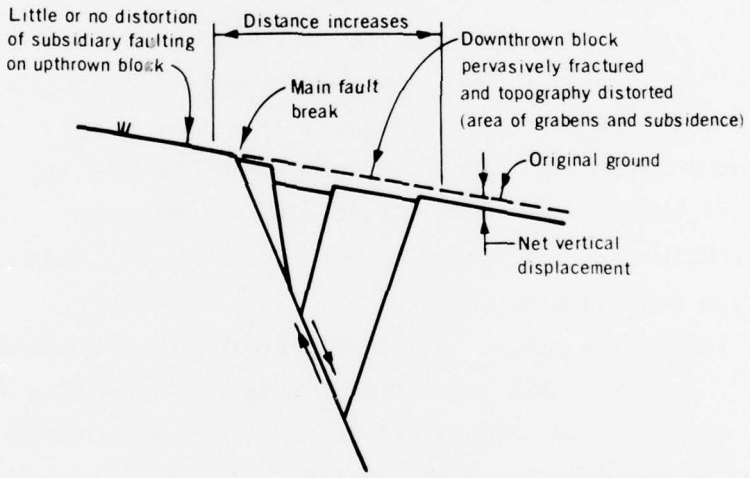
Geomorphic Features of Reverse-Slip Faults

34. The geomorphic features of reverse-slip faults generally are more subtle and difficult to distinguish than those of strike-slip and normal-slip faults. Scarps may have complex patterns with even lower angles of dip than for normal-slip faults, and have more irregular traces that make them much less conspicuous and more difficult to trace than strike-slip and normal-slip fault zones. The relatively low angle of dip of many reverse-slip faults, commonly below 45°, may result in branching fracture systems that "short cut" to the surface, to give complexly shattered surface displacements with greatly reduced scarp height of the individual strands.

35. The general geomorphic features have been summarized by Johnson.[144] He noted that the overthrusting of the hanging wall block develops a sharpened or overstepped block that is frequently covered by landslides and gravity slips that obscure the true compressional character of the fault. The historic scarps of this type commonly result in a "bulldozed" or "mole track" appearance of the scarp. The branching aspect of the scarp compared to normal-slip faults is shown in Figure A21, from Sherard et al.[24] Historic examples illustrating the general aspects are described for the 1964 earthquake on Montague Island (Figure A22, from Plafker[104]), the White Wolf fault zone of 1952 (California Division of Mines,[145]), the San Fernando faulting of 1971 (U. S. Geological Survey[146]), and the Meckering, West Australia, earthquake of



a. Reverse-slip fault



b. Normal-slip fault

Figure A21. Distributed fault pattern for reverse-slip and normal-slip faults (Sherard et al.[24])

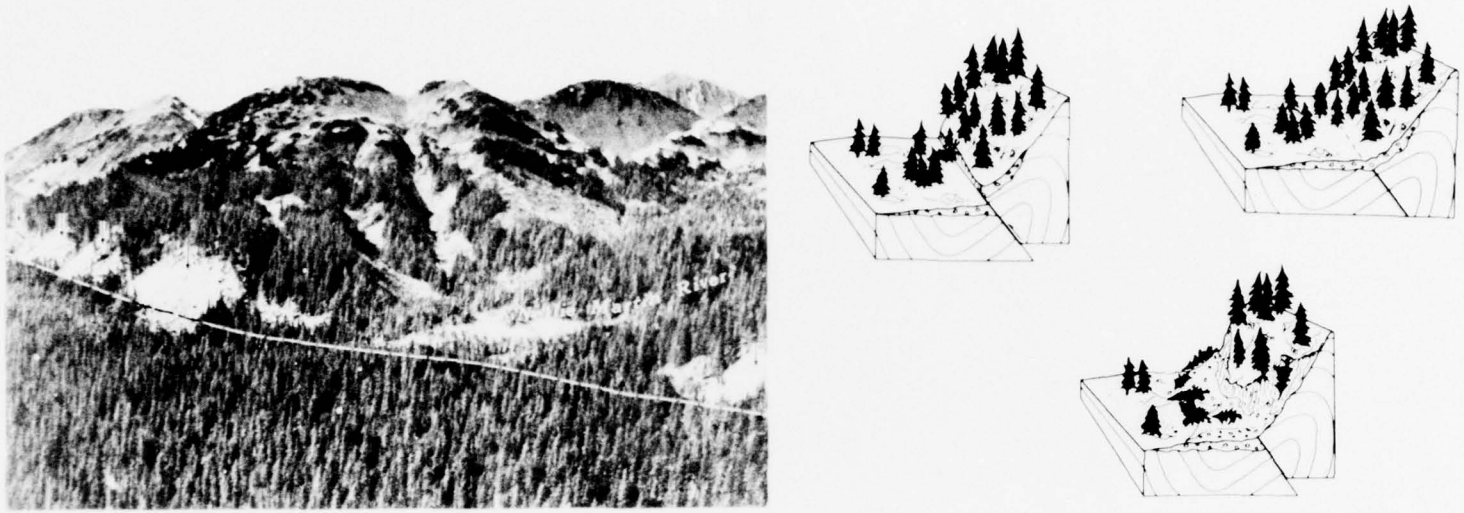


Figure A22. Patton Bay reverse-slip fault, Montague Island, from the 1964 Alaska earthquake. The photograph shows the steepened front of the mountain block, with landslide scars as high as 60 m (arrows) across the face of the upthrown block. The fault exposed near Nellie Martin River has a dip of about 50° and at least 15 m of vertical displacement. The sequential diagram shows the preearthquake eroded fault scarp at the upper right, the overhanging scarp during the earthquake at the upper left, and the collapsed talus and slide following the collapse of the loosened and unstable slope above the scarp (from Plafker[104]).

1968 (see Figure 14, Krinitzsky[29]). The complex pattern of shattering is well demonstrated, particularly for the alluvial plains, by surface faulting in the San Fernando earthquake area of 1971.

36. The origin of the complex fractures near the surface, including the seemingly anomalous prevalence of extensional fracturing and presence of grabens and drape folds, was studied experimentally by Friedman et al.[147] Their experimental studies developed many structural features expressed in the topographic and shallow stratigraphic expression of reverse faults--downward-curving concave reverse fault planes, drape folds, bedding plane slip, layer thickness changes, fold hinges, and extensional fractures, including graben zones and low-angle normal faults that are conjugate to the reverse faults. Representative cross-section relations are shown in Figure A23.

BEST AVAILABLE COPY

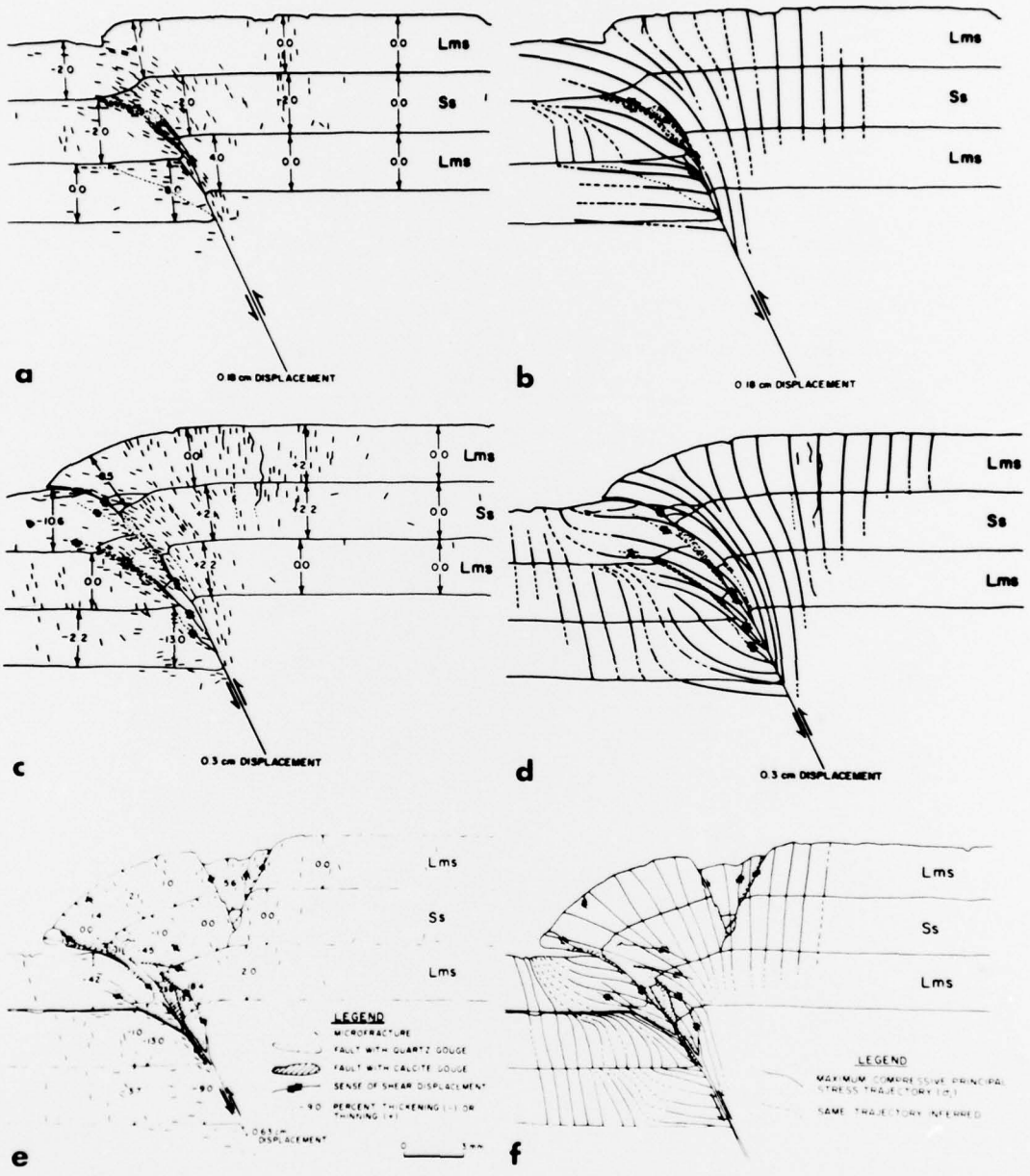


Figure A23. Examples of microscopically deformed rock with faulted drape folds. Diagrams a, c, and e show deformation features in thin section. Microfractures are shown with proper position and orientation. Arrows perpendicular to bedding indicate strain calculated from bedding-thickness changes (thinning is shown positive). Diagrams b, d, and f show stress trajectories inferred from all microscopic data from a, c, and e (from Friedman et al.[147])

In accordance with ER 70-2-3, paragraph 6c(1)(b), dated 15 February 1973, a facsimile catalog card in Library of Congress format is reproduced below.

Slemmons, David B
State-of-the-art for assessing earthquake hazards in the United States; Report 6: Faults and earthquake magnitude, by David B. Slemmons, Mackay School of Mines, University of Nevada, Reno, Nevada. Vicksburg, U. S. Army Engineer Waterways Experiment Station, 1977.
1 v. (various pagings) illus. 27 cm. (U. S. Waterways Experiment Station. Miscellaneous paper S-73-1, Report 6)
Prepared for Office, Chief of Engineers, U. S. Army, Washington, D. C., under Contract No. DACW 39-76-C-0009.
Includes bibliography.

1. Earthquake engineering. 2. Earthquake hazards. 3. Earthquake resistant structures. 4. Earthquakes. 5. Faults and faulting (Geology). 6. Fractures and fracturing (Geology). 7. State-of-the-art studies. I. Nevada. University. Mackay School of Mines. II. U. S. Army. Corps of Engineers. (Series: U. S. Waterways Experiment Station, Vicksburg, Miss. Miscellaneous paper S-73-1, Report 6)
TA7.W34m no.S-73-1 Report 6